Aus dem Institut für Physiologie der Universität Tübingen

Abteilung für Vegetative und Klinische Physiologie

Effect of Anoctamin 6 and γ-secretase inhibitor DAPT on platelet activation and apoptosis

Inaugural-Dissertation

zur Erlangung des Doktorgrades

der Humanwissenschaften

der Medizinischen Fakultät

der Eberhard Karls Universität

zu Tübingen

vorgelegt von

Liu, Guoxing

2018

Dekan:	Professor. Dr. I. B. Autenrieth
1. Berichterstatter:	Professor. Dr. F. Lang
2. Berichterstatter:	Professor. Dr. A. J. García-Sáez

Tag der Disputation: 19.06.2018

Table of contents

List of figures

List of table

Abbreviations

ACD:	Acid citrate dextrose
ADP:	Adenosine diphosphate
AD:	Alzheimer's disease
APP:	Amyloid precursor protein
Aβ:	amyloid-β
Ano 6:	Anoctamine 6
BSA:	Bovine serum albumin
CaCC:	Ca^{2+} activated Cl^- channel
Caspase:	Cysteine-aspartic proteases
CalDAG-GEFI:	Calcium and diacylglycerol-regulated guanine nucleotide exchange factor I
CD62:	P-selectin
CRAC:	Ca^{2+} release activated Ca^{2+}
CRP:	Collagen related peptide
CXCL16:	Chemokine CXC motif ligand 16
CytC:	Cytochrome c
DAG:	Diacylglycerol
DCFDA:	2',7'- dichlorodihydrofluorescein diacetate
DIT:	Drug-induced thrombocytopenia
DTS:	Dense tubular system
ER:	Endoplasmic reticulum
FACS:	Fluorescence activated cell sorting
FITC:	Fluorescein isothyocyanate
FSC:	Forward scatter
H_2O_2:	Hydrogen peroxide
i-CLiPs:	intramembrane-Cleaving proteases
ITAM:	Immunoreceptor tyrosine-based activation motif

MARCKS:	Myristoylated alanine-rich C kinase substrate
MIF:	Macrophage migration inhibitory factor
MKs:	Megakaryocytes
MLCK:	Myosin light-chain kinase
MPTP:	Mitochondria permeability transition pore
mRNA:	messenger RNA
Δψm:	Mitochondrial membrane potential
NAADP:	Nicotinic acid adenine dinucleotide phosphate
NCX:	Na^{+}/Ca^{2+} exchanger
OCS:	Open canalicular system
PAR:	Protease-activated receptor
PE:	Phycoerythrin
PI3K:	Phosphoinositide 3 Kinase
PIP2:	Phosphatidylinositol 4,5-trisphosphate
PKC:	Protein kinase C
PRP:	Platelet rich plasma
PS:	Phosphatidylserine
PSGL-1:	P-selectin glycoprotein ligand 1
PSL:	Platelet storage lesion
ROS:	Reactive oxygen specie
SGK1:	Serum- and glucocorticoid-inducible kinase 1
SNAREs:	Soluble N-ethylmaleimide sensitive factor attachment protein receptors
SOCs:	Store-operated Ca^{2+} channels
SOCE:	Store-operated Ca^{2+} entry
STIM:	Stromal interaction molecule
TF:	Tissue factor
TRPC:	Transient receptor potential cation channel
vWF:	von Willebrand factor

1. Introduction

The discovery of human platelets takes a long time. It is not until 1880s that Bizzozero fulfilled a detailed description of it for the first time, following a more comprehensive study conducted with microscope (Brewer 2006), (De Gaetano 2001). Platelets are small anucleate blood cells derived from megakaryocytes (MKs). They are formed from MKs' cytoplasm fragments with the auxiliary of shear forces of circulating blood (George 2000). They lack genomic DNA since they are non-nucleated. However, platelet cytoplasm retains a large number of messenger RNA (mRNA), which is carried over from megakaryocytes, and maintain the survival and perform physiological functions of platelets (Harrison and Goodall 2008), (Rowley et al. 2012). The normal circulating human platelets are discoid in shape, with the average diameter of only 2.0 ~5.0 μm and the mean volume of 7 ~11 femtoliters (*fl*) (Gremmel et al. 2016), (Harrison 2005). Nevertheless, activated platelets change their shape to a sphere, and protrude their dendritic pseudopodia with the constriction of the microtubular ring and cytoskeletal reorganization (George 2000). Normally, an adult human produces 100 billion platelets per day, and maintains the level of 150 to 350 × 10^9/L platelets in circulating blood. The production number can increase under some special circumstances, such as bleeding caused by vascular wall damage (George 2000), (Italiano 2008), (Kaushansky 2008).

1.1 The physiological functions of platelets

Undoubtedly, platelets participating in hemostasis following vascular injuries is considered to be their most important function (Broos et al. 2011). Under the physiological circumstances, platelets can survive for 10 days, and are decomposed and removed in spleen after senescence. They can flow freely in the lumen of blood vessel, and do not bond to each other or intact with blood

vessel wall (Aster 1966), (Gehrmann et al. 1972). However, injured vascular triggers platelet activation through a series of signalling cascades. Then activated platelets aggregate and adhere to the extracellular matrix until platelet plug formed at the injured site, (Broos et al. 2011), (Ni and Freedman 2003). Defective platelets can lead to a lot of diseases. For example, gray platelet syndrome and scott syndrome. In addition, activated platelets may also cause thrombus formation during the hemostasis, which plays a key role in stroke (Hou et al. 2015). Besides, platelets also contribute to coronary artery disease, peripheral vascular disease, host defense, Inflammation, tumor metastasis, and so on. (Sabrkhany et al. 2011), (Smyth et al. 2009), (Xu et al. 2016), (Yeaman 2014).

1.2 Platelet granules and bio-marker glycoproteins

Platelets secretory granules are critical for such anucleate cells to perform physiological functions. There are three types of secretory granules in platelet cytoplasm: α-granules, dense granules and lysosomes. The first two types are more important and in larger number (George 2000). Platelet α-granules are derived from MKs. In matured α-granules, there are two types of predominant contents - membrane bound proteins and soluble proteins, such as P-selectin (CD62), fibrinogen, von Willebrand factor (vWF), some of chemokine and so on. Majority of them are from MKs, and then stored in granules vesicles. In addition, plasma-derived proteins are taken up by α-granules through the mechanism of endocytosis (Rendu and Brohard-Bohn 2001), (Blair and Flaumenhaft 2009). Platelet dense granules mainly contain some small molecules, such as calcium, ADP, ATP, serotonin and so on (King and Reed 2002). Although less is known about dense granules compare with α-granules, it is clear that these small molecules play important roles in platelet activation, aggregation and vascular remodeling. Upon the stimulation of injured vessels, rapidly elevated cytosolic

Ca^{2+} trigger release of dense granules contents by exocytosis. During this process, ADP can also further stimulate and activate platelets as an effective agonist (Morimoto et al. 1990), (Reed 2004), (Jones et al. 2011).

With the development of electrophoresis technology, many platelet glycoproteins, such as GPIIb-IIIa, GPIa-IIa, GPIb-IX-V, GPVI and so on, have been reported over the past few decades. They play a key role in platelet interaction and combination with endothelial matrix during hemostasis (Nurden 2014). αIIbβ3, also known as GPIIb/IIIa, is the most important member of integrin glycoproteins family. They can be found in platelet α-granules, and are largely expressed and located at the surface of platelets after platelet activation. Moreover, this kind of glycoprotein account for about one-sixth of the total platelet membrane protein mass, and can be easily detected as a marker of platelet activation in vitro (Gremmel et al. 2016).

Integrin αIIbβ3 contributes to platelet activation and aggregation as the receptor of fibrinogen and vWF. However, they have a low affinity for ligands in the resting platelets. When platelets are activated, the concentration level of intracellular Ca^{2+} rapidly elevate and thus triggers inside-out signalling cascades of integrin αIIbβ3, which changes the conformation of integrin protein binding site and results in the improvement of receptor-ligand affinity.(Broos et al. 2011). At the same time, extracellular ligands binding also activate the outside-in signalling of integrin. With the addition of more intermediate proteins and adapters, such as Rac, Rho GTPases, paxillin, Nck and so on, platelet cytoskeletal reorganization is promoted, which is important for platelet spreading, the stability of aggregation and clot retraction (Coller and Shattil 2008), (Ginsberg et al. 2005).

Furthermore, glycoprotein P-selectin, another marker of platelet activation, is found in α-granule of resting platelets, which translocate rapidly to surface of platelets upon platelet activation(Garcia-Martinez et al. 2004). P-selectin

glycoprotein ligand 1 (PSGL-1) is the main ligand of P-selectin, which is expressed on the surface of endothelial cells and leukocytes. Besides, binding of ligand-receptor can subsequently lead to platelet aggregation and adhesion in hemostasis (Andre 2004), (Merten and Thiagarajan 2004).

1.3 The mechanism of coagulation

The paramount physiological function of platelets is contributing to cessation of bleeding by developing a hemostatic plug on the site of vascular injury. The coagulation mechanism is rather complicated. In early times, it is summarized as a cascade model that involves both extrinsic and intrinsic pathways. However, the cascade model cannot well explain hemostasis in vivo because of separate coagulation pathways. Later on, a cell-based model that describes the process of coagulating on three types (or states) of cell surfaces is presented and widely accepted, which contributes to a better understanding hemophilia (Monroe 2002), (Hoffman and Monroe 2001).

In this model, the whole process is divided into three overlapping steps: initiation, amplification and propagation (Fig.1.1). Briefly, the coagulation cascades starts with tissue factor (TF), which is released by TF-bearing cells on site of the injured blood vessel. In the initiation phase, cascades reaction generates small amount of thrombin (FIIa) as clotting factor Xa (FXa) binding to prothrombin (FII). This phase occurs on the surfaces of TF-bearing cells. During the amplification phase, thrombin further stimulates the feedback mechanism, while the platelet state conversion from resting to activation takes place. At the same time, many factors are activated at the surface of platelets, such as FIXa, FVIIIa, FVa. These activated factors lead to the formation of FXa/FVa complex at surface of activated platelets, which then combine with FII to produce a large number of thrombin. High concentration of thrombin can cleave fibrinogen into fibrin monomer, which eventually results in a stable fibrin clot on injured blood vessel

wall (Monroe 2002), (Eyre and Gamlin 2010), (Hoffman and Monroe 2007).

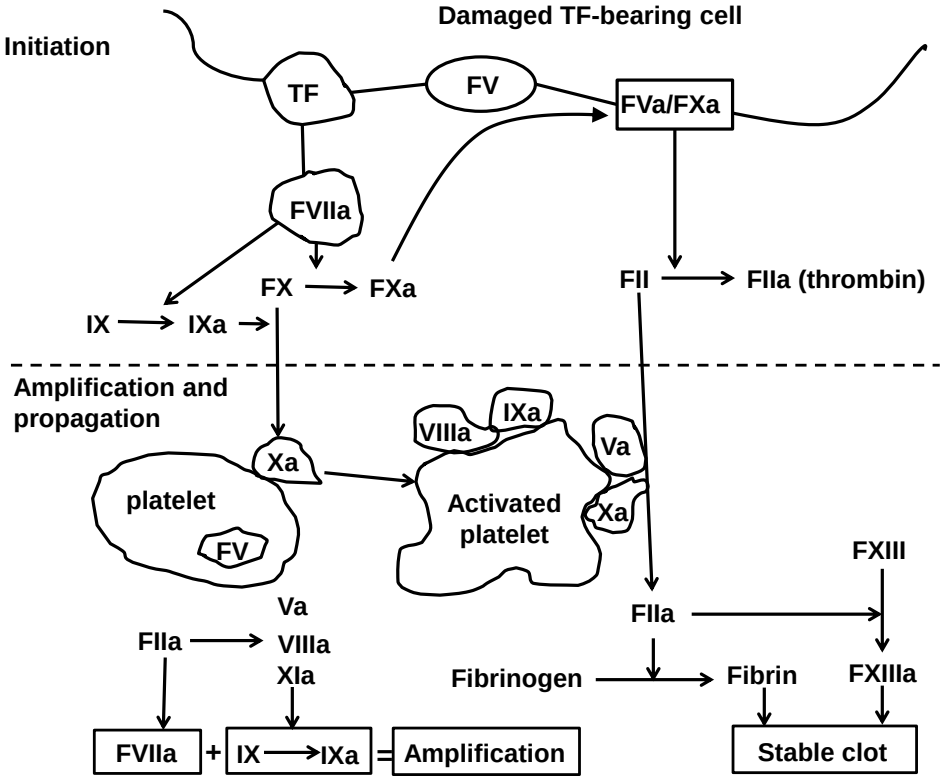

Fig.1.1. Cell-based model of coagulation (Eyre and Gamlin 2010)

1.4 The mechanism of platelet activation

1.4.1 Platelet agonists and receptor pathways

The activation of platelets starts with the binding of some agonists with specific receptors, which triggers downstream cascades of outside-in signalling as well as platelet activation (Goggs and Poole 2012). There are two major types of signalling pathways in platelets. The first is tyrosine kinase pathway, in which platelet activation relies on phosphorylation of tyrosine in common immunoreceptor tyrosine-based activation motif (ITAM) or hem-ITAM. Generally, this pathway can influence platelet adhesion and aggregation by regulating downstream signalling (Stegner and Nieswandt 2011), (Bergmeier and Stefanini 2013).

A Typical example is GPVI, a collagen receptor, which forms a complex with FcR-γ chain to perform functions. The cascade reaction begins with phosphorylation of ITAM as well as Syk. Upon phospholipase Cγ2 (PLCγ2) activation, downstream PI3 kinase is further activated, which ultimately triggers Ca^{2+} mobilization, integrin αIIbβ3 activation and platelet aggregation (Stegner and Nieswandt 2011), (Watson et al. 2010). Besides, integrin αIIbβ3 and GPIb-V-IX also rely on tyrosine kinase pathway to activate platelets. The former can bind to fibrinogen, while the latter can bind to vWF (Watson et al. 2005), (Jackson et al. 2003).

Moreover, most soluble agonists, such as ADP, thrombin, TxA_2 and so on, mainly activate platelets through G-protein coupled receptor pathway. The ligand-receptor interaction trigger different downstream cascades by coupling different types of G protein, and further regulate platelet Ca^{2+} mobilization, shape change, and aggregation (Offermanns 2006).

1.4.2 The effect of Ca^{2+} on platelet aggregation

Cytosolic Ca^{2+} plays a key role in platelets as the second messenger. Agonists-induced cascades lead to rapid increase of cytosolic Ca^{2+} levels. High level of Ca^{2+} concentration can activate downstream mediator protein, which ultimately influences platelet full activation, aggregation, spreading and so on (Li et al. 2010), (Bergmeier and Stefanini 2009).

Ca^{2+} and diacylglycerol (DAG)-regulated guanine nucleotide exchange factor I (CalDAG-GEFI) is one of the important Ca^{2+} binding proteins in platelets, which consists of two Ca^{2+}-binding EF hand, one Ras exchange motif and one DAG-binding C1 domain. However, it only has a weak affinity with DAG (Guidetti et al. 2013). DAG is derived from phosphatidylinositol 4,5-trisphosphate (PIP_2), which is hydrolyzed by PLCβ isoforms following agonist stimulation (Lian et al. 2005). High concentration of cytosolic Ca^{2+} and DAG bind to CalDAG-GEFI

together, which further activate the small GTPase Rap1b. This process can be stopped by PKA-mediated inhibition mechanism (Subramanian et al. 2013) (Crittenden et al. 2004). Activated Rap1b is an important mediator for integrin activation of inside-out cascades signalling, which mediate αIIbβ3 activation by regulating protein complex of integrin β subunits tail (Zhang et al. 2011), (Guidetti and Torti 2012). The complex contains many kinds of proteins, such as Talin-1, Kindlin-3, RIAM and so on. It enhances affinity of integrin to ligand by disrupting the salt bridge between the two tails of αIIbβ3 subunits (Banno and Ginsberg 2008), (Lefort et al. 2012).

Protein kinase C (PKC) is another important regulator of integrin activation via Ca^{2+} dependent approach. Typically, PKCα, an isoform of PKC family that also contains DAG and Ca^{2+} binding domain, can effectively regulate integrin αIIbβ3 activation via interaction with Rap1 upon intracellular Ca^{2+} increase (Cifuni et al. 2008), (Harper and Poole 2010), (Han et al. 2006). It is already well known that activated integrin promotes the binding of fibrinogen in circulating blood and leads to the platelet aggregation and adhesion under different shear conditions (Jackson 2007).

1.4.3 The effect of Ca^{2+} on platelet secretion

High concentration of intracellular Ca^{2+} regulates not only platelet aggregation but also secretion of platelet granules. Platelets release granule contents to respond to stimulation through Ca^{2+}-induced exocytosis, which is a complex and unique process. Although a large number of researches have been reported, the mechanism of platelet exocytosis remains indistinct (Blair and Flaumenhaft 2009).

According to current studies, soluble N-ethylmaleimide sensitive factor attachment protein receptors (SNAREs), which are membrane-associated proteins, can be divided into two categories - target membranes (tSNAREs) and

vesicles associated proteins (vSNAREs). They mediate the release of platelet granule contents by fusing granule membrane with plasma membrane or open canalicular system (OCS) (Flaumenhaft 2017), (Huang and Whiteheart 2015). The increased intracellular Ca^{2+} can induce platelet shape change through the assembly of cytoskeletal F-actin, which subsequently enrich α-granules to membrane vesicles and membrane fragments (Woronowicz et al. 2010), (Ge et al. 2012). At the same time, the adaptor protein of F-actin, VARP, binds to related vSNAREs of α-granules (VAMP-7), and guide granules to contact and fuse with plasma membrane (Koseoglu et al. 2015).

As is described above, PKC is activated following intracellular Ca^{2+} increase, which can phosphorylate many kinds of tSNAREs proteins and SNAREs-related regulators, such as SNAP-23, syntaxin 4, Munc-18, myristoylated alanine-rich C kinase substrate (MARCKS) and so on (Polgar et al. 2003), (Chung et al. 2000), (Schraw et al. 2003), (Elzagallaai et al. 2000). The phosphorylation of these proteins can directly or indirectly affect the formation of SNAREs complex during the fusion of membranes. In addition, Ca^{2+} activated PKC also regulate platelet secretion by interacting with downstream effector protein PKD2. However, this pathway only selectively regulates dense granule secretion according to Konopatskaya's report (Konopatskaya et al. 2011).

Munc13-4 is another story in platelet exocytosis. Generally, Munc13-4 regulates tSNAREs protein via Ca^{2+}-dependent PKC pathway. However, it is possible to affect the fusion of membranes by binding and clustering phospholipid PS in response to direct interaction with Ca^{2+}. Moreover, Ca^{2+}-dependent Munc13-4-phospholipid helps stabilize dense granule in resting and activated platelets (Chicka et al. 2016). At the same time, Munc13-4 can also bind to the small GTPase Rab27 on granule surface. Such two-way combination could be another factor contributing to the stability of membrane fusion (Shirakawa et al. 2004).

1.4.4 The effect of Ca^{2+} on platelet shape change

Upon agonists stimulation, the contractile and reorganization of cytoskeletal systems can lead to platelet shape change via Ca^{2+}-dependent and -independent signalling (Aslan 2017). Rapidly elevated intracellular Ca^{2+} binds to calmodulin firstly. Then the complex further activates myosin light-chain kinase (MLCK), which can initiate the mechanism of actin-myosin interaction of platelet shape change via the phosphorylation of myosin light-chain (Bauer et al. 1999). Furthermore, Ca^{2+} regulates cytoskeletal reorganization by binding activated actin to related proteins, such as gelsolin and calpain, which play a critical role in platelet spreading (Calaminus et al. 2008), (Kuchay et al. 2012), (Falet et al. 2000). Ca^{2+}-dependent actin cytoskeletal reorganization also contributes to the activation of integrin and platelet granules secretion according to the reports (Ge et al. 2012), (Falet 2017).

1.4.5 Ca^{2+} stores and releases in platelets

As is mentioned above, platelets rely on the increase of intracellular Ca^{2+} concentration ($[Ca^{2+}]_i$) in response to agonists stimulation, and the elevation of $[Ca^{2+}]_i$ mainly results from the release of endogenous stores and influx of extracellular Ca^{2+}. There are two independent intracellular stores in platelet cytoplasm. The first one is the dense tubular system (DTS), an endoplasmic reticulum (ER)-like membrane system, which is the major Ca^{2+} store (Gerrard et al. 1978). Sarco-ER Ca^{2+}-ATPase (SERCA), an important member of the Ca^{2+} pump family on platelet DTS surface, can transport cytosolic Ca^{2+} into DTS compartments in ATP consumption-dependent manner (Flaumenhaft 2016). However, this process can be stopped by thapsigargin, a non-competitive inhibitor of SERCA (Hakii et al. 1986). Furthermore, the release of Ca^{2+} by DTS relies on the binding of inositol 1,4,5-trisphosphate (IP_3) to IP_3 receptor on DTS surface upon the stimulation of agonists, such as thrombin, ADP and so on,

which subsequently activate related Ca^{2+} channel to complete the process. (Jardin et al. 2008).

The second Ca^{2+} store in platelets is lysosome related acidic organelles, including mitochondria and secretory granules (Jardin et al. 2008). Similarly, Ca^{2+} enter organelles via different SERCA isoforms, and can be blocked by high concentration of thapsigargin or 2,5-di-(t-butyl)-1,4-hydroquinone (TBHQ) (Rosado 2011). However, the release of intracellular Ca^{2+} of acidic organelles to cytosol relies on nicotinic acid adenine dinucleotide phosphate (NAADP) and membrane related receptors. This mechanism remains to be developed.(Coxon et al. 2012).

1.4.6 Extracellular Ca^{2+} entry pathway

The release of intracellular Ca^{2+} plays an important in the initial stage of platelet response to stimulation. However, the sustainable and stable functioning of platelets relies on the influx of a large amount of extracellular Ca^{2+} that rapidly refills the store depletion. Exogenous Ca^{2+} can enter cytosol across the platelet plasma membrane via a variety of pathways, such as the family of transient receptor potential cation channels (TRPCs), Na^{+}/Ca^{2+} exchanger (NCX), ATP-gated P2X1 receptor (Sage et al. 2002), (Harper and Sage 2007), (Mahaut-Smith et al. 2011). These pathways are important to maintain Ca^{2+} balance in resting platelets and induce procoagulant activity upon the activation of platelets (Mahaut-Smith 2013). Yet, much attention to Ca^{2+} entry pathway was focused on store-operated Ca^{2+} entry (SOCE) in recent years, which can support massive of Ca^{2+} influx across the plasma membrane in platelets as well as many other cells (Prakriya and Lewis 2015).

1.4.7 Store-operated Ca^{2+} channels of platelets

The agonist-receptor interaction leads to the activation of phospholipase C via G proteins or tyrosine kinase signalling pathway. When PIP_2 are hydrolyzed by

phospholipase C, IP_3 is produced, which can bind to the receptors of DTS surface and ultimately empty Ca^{2+} stores. The depletion of Ca^{2+} pool results in the entry of extracellular Ca^{2+} through plasma membrane channels to refill the stores. This process was known as SOCE and reported by Putney in 1986 (Putney 1986). However, it was not until 1992 that the existence of SOCE in platelets was proved for the first time (Sargeant et al. 1992).

Extracellular Ca^{2+} refilling the stores via SOCE rely on store-operated Ca^{2+} channels (SOCs) of platelet plasma membrane. Researchers firstly focused on the TRPC family, which can contribute to SOCE in many other kinds of cells (Cheng et al. 2013). TRPC1 also express in human platelets, and involve in the regulation of platelet SOCE according to the report of Rosado *et al* (Rosado et al. 2002). However, further experiments have demonstrated that TRPC1 is not the major SOC in platelets, as TRPC1 deficient mice still display fully intact SOCE (Varga-Szabo et al. 2008). TRPC1 and TRPC6 may indirectly regulate extracellular Ca^{2+} entry via interaction with stromal interaction molecule1 (STIM1) or Orai1. But the role of TRPC in platelet SOCE remains controversial until now (Jardin et al. 2008), (Jardin et al. 2009).

In addition, Ca^{2+} release-activated Ca^{2+} (CRAC) channel is considered as the most important SOC for platelet SOCE in recent years (Lang et al. 2013). CRAC channel can rapidly regulate the entry of extracellular Ca^{2+} to refill the stores, thus plays a critical role in performing platelet Ca^{2+}-dependent functions.

1.4.8 CRAC channel of platelets

Current studies show that the most attractive SOC channel is CRAC channel, which can regulate platelet SOCE via the interaction between the pore forming CRAC moiety (CRACM1) Orai1 and Ca^{2+} sensor STIM1 of platelet ER membrane (Fig.1.2) (Lang et al. 2013), (Braun et al. 2009). Orai protein family is divided into three kinds of isoforms, respectively termed as Orai1, Orai2 and

Orai3, all of which are found in human platelets utilizing real time PCR and Western blotting. However, the four transmembrane helices protein Orai1 has been identified as the most important CRAC channel protein in platelets (Lang et al. 2013), (Berna-Erro et al. 2012). Similarly, the STIM1 and STIM2 are also found in human platelet ER. Especially, STIM1 is the major isoform during STIM-induced SOCE (Berna-Erro et al. 2012).

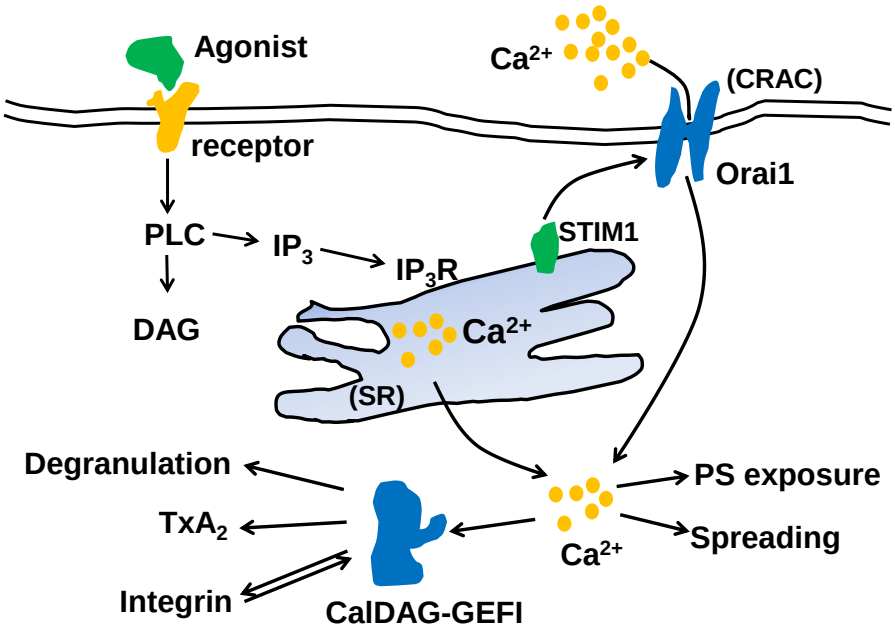

Fig.1.2. Orai1/STIM1 mediated SOCE and Ca^{2+} signaling in platelets (Bergmeier and Stefanini 2009)

Following platelet activation and further depletion of ER Ca^{2+}, Ca^{2+} sensitive-STIM1 can couple Orai1 of plasma membrane by changing its molecular conformational, which ultimately results in extracellular Ca^{2+} influx (Frischauf et al. 2008), (Braun et al. 2009). Platelets from Orai1^{R93W} (partial mutation of Orai1) mice display reduced Ca^{2+} influx. At the same time, R93W mutation also causes impaired activation and phosphatidylserine (PS) exposure in response to agonists' stimulation. However, this mutation did not effectively influence the platelets aggregation and adhesion in comparison with wild type mice (Bergmeier et al. 2009). The effect of STIM1/Orai1 on platelet SOCE was

further demonstrated in STIM1 and Orai1 deficient mice respectively. But the deficiency in Orai1 cannot entirely block the PS exposure and thrombus formation (Gilio et al. 2010).

2-aminoethoxydiphenyl borate, a soluble inhibitor of Orai1, can effectively blunts platelet SOCE, and suppress Ca^{2+}-dependent thrombus formation (van Kruchten et al. 2012), (Lang et al. 2015). In addition, STIM1/Orai1 mediated SOCE can also be blunted in platelets by their antibodies (Galan et al. 2009), or nonsteroidal estrogens after incubation (Dobrydneva et al. 2010).

1.4.9 The regulation of STIM1/Orai1-dependent Ca^{2+} signalling in platelets

The couple of STIM1/Orai1 plays a crucial role in platelet SOCE. However, the regulation mechanisms of them, as well as related Ca^{2+} signalling remain to be clarified. It was reported many years ago that Phosphoinositide 3-Kinase (PI_3K) involves in the regulation of platelet functions. Gilio reports that it can strongly regulate GPVI-dependent $[Ca^{2+}]_i$ elevation (Gilio et al. 2009). Orai1 protein abundance in human platelets increases significantly within a short time upon thrombin stimulation. At the same time, this process can also be effectively blunted by the inhibitor of PI_3K (Munzer et al. 2013). PI_3K signalling regulates multiple downstream signalling molecules in different cells, such as Akt (Protein kinase B, PKB) and serum- and glucocorticoid-inducible kinase 1 (SGK1) (Lang and Shumilina 2013).

SGK1 is expressed in both platelets and megakaryocytes. The elevation of $[Ca^{2+}]_i$, and thus platelet activation as well as thrombus formation in vitro are significantly attenuates in the platelets from SGK1 deficient mice (Borst et al. 2012). Besides, the expression of Orai1 protein remarkably decreases in SGK1 knocked out platelets or inhibitor treated megakaryocytic cell line, although STIM1 expression in such cells is not affected. (Borst et al. 2012). Along with this line, more regulators of SGK1 signalling are attractive in the regulation of

STIM1/Orai1 mediated SOCE, such as NF-κB, IKKβ, IκBα and so on. However, the roles of all of them in platelets need more experiments to confirm (Lang et al. 2015).

The Akt family protein is another signalling molecule of PI_3K signalling, and all three isoforms express in platelets (Lang et al. 2015). The absence of Akt1 leads to attenuated elevation of $[Ca^{2+}]_i$ and platelet aggregation in response to thrombin and vWF treatment respectively. (Chen et al. 2004), (Yin et al. 2008). Moreover, the Akt also contributes to chemokine CXC motif ligand 16 (CXCL16) mediated platelet activation (Borst et al. 2012), and can regulate Orai1 expression upon PDGF stimulation in human arterial smooth muscle cells (Ogawa et al. 2012). However, there was no direct evidence proving that Akt can affect the STIM1/Orai1 signalling in platelets. The hypothesis is that it only plays a supplement role when SGK1 are absent (Lang et al. 2015).

Reactive oxygen species (ROSs) generate in platelets upon the stimulation of agonists through multiple mechanisms, such as xanthine oxidase and NADPH oxidase. (Wachowicz et al. 2002). The ROSs derived from NADPH oxidase not only contribute to platelet apoptosis, but also affect platelet activation, aggregation and thrombus formation (Girish et al. 2013), (Begonja et al. 2005). In addition, $[Ca^{2+}]_i$ in ROS-treated human platelets slightly increase via the release of agonist-sensitive intracellular stores. But the regulation mechanism of ROS is still unclear (Redondo et al. 2004), (Loiko et al. 2003). The ROS regulated $[Ca^{2+}]_i$ via release of intracellular stores and inhibition of SOCE in lymphocytes has been reported by Bogeski. The study also showed that the inhibited CRAC channel protein was Orai1, but not Orai3 (Bogeski et al. 2010). Further experiments indicated that ROS-regulated inhibition of CRAC channel in HEKS1 cells was accomplished by specific sites oxidation of Orai1 protein, which reduced the formation of Orai1 cluster (Alansary et al. 2016). However, the regulator role of ROSs to platelet STIM1/Orai1 needs further study.

1.5 Platelet apoptosis

Normally, the average life of human platelets in the blood is about 10 days. Similar to nucleated cells, senescent platelets can start a process of programmed cell death (also called apoptosis), and finally be removed from the blood circulation (George 2000). In addition, the stored platelets in vitro, even those isolated from healthy human blood, sometimes undergo apoptosis-like events, which influence on platelet physiological functions. This is known as platelet storage lesion (PSL), which was induced by multiple factors, such as storage temperature, storage agitation and so on (Shrivastava 2009), (Mittal and Kaur 2015), (Wang et al. 2013).

The extrinsic factors for platelet apoptosis have been reported in some researches. Many kinds of drugs or chemical compounds, such as Vancomycin, Thymoquinone and so on, are toxic to human platelets and can induce platelet apoptosis in a dose-dependent manner (Towhid et al. 2013) (Towhid et al. 2011). Clinically, the use of some drugs may lead to the excessive suicidal death or apoptosis of platelets, thus resulting in the significant decrease of platelets in circulating blood. This is termed as drug-induced thrombocytopenia (DIT), which will result in bleeding disorders (Williamson et al. 2014). Moreover, some agonists also induce platelet apoptosis events via interaction with related receptors of platelet membrane surface (Li et al. 2010).

1.5.1 The mechanisms of platelet apoptosis

Different factors induce platelet apoptosis via different mechanisms. Like the nucleated cells, the apoptotic pathways of platelets can also be classified to intrinsic and extrinsic pathways (Kile 2014). Generally, the apoptotic process of senescent platelets is accomplished through the intrinsic pathway. Kile BT has already reviewed and built a molecular model based on previous researches (Kile 2009). Briefly, Bcl-2 family proteins make platelets survive by controlling the

pro-apoptotic Bak/Bax protein upon the stimulation of apoptotic signalling. For example, as an apoptotic signalling, DNA injury can activate the BH3-only proteins. The activated BH3-only protein further binds to Bcl-2 family proteins and release the Bak/Bax protein at the same time. Bak/Bax complex can form a pore in the mitochondrial membrane and discharge cytochrome c (CytC), which ultimately lead to caspase-3 activation, phosphatidylserine exposure and platelet disassembly (Vogler et al. 2011).

Although the intrinsic pathway of platelet apoptosis is clear, the extrinsic pathway still lacks enough studies. According to previous researches, mitochondria might play a key role in platelet apoptosis induced by extrinsic stimulation (Gyulkhandanyan et al. 2017). Towhid's study showed that the mitochondrial membrane potential ($\Delta\psi_m$) significantly decreased with ceramide formation upon the thymoquinone treatment in human platelets, which activate the caspase cascades and lead to platelet apoptosis. Concomitantly, $[Ca^{2+}]_i$ also increase significantly, which could be induced by thymoquinone via PI_3k/Akt signalling pathway (Towhid et al. 2011). High level of $[Ca^{2+}]_i$ can directly lead to $\Delta\psi_m$ loss by opening the mitochondria permeability transition pore (MPTP) (Sveshnikova et al. 2015). $\Delta\psi_{m.}$ loss might also be caused by the binding of high level of $[Ca^{2+}]_l$ to potential mediator calpain, which can induce platelet apoptosis in Ca^{2+}-dependent manner (Zhang et al. 2011). In addition, ROS, like hydrogen peroxide (H_2O_2), can regulate SOCE and $[Ca^{2+}]_i$ (Rosado et al. 2004), the release of cytochrome c, as well as the activation of caspase-3 (Lopez et al. 2007). Besides, further experiments show that ROS treatment can also lead to the activation of Bid and Bax, thus resulting in platelet apoptotic (Fig.1.3) (Lopez et al. 2008).

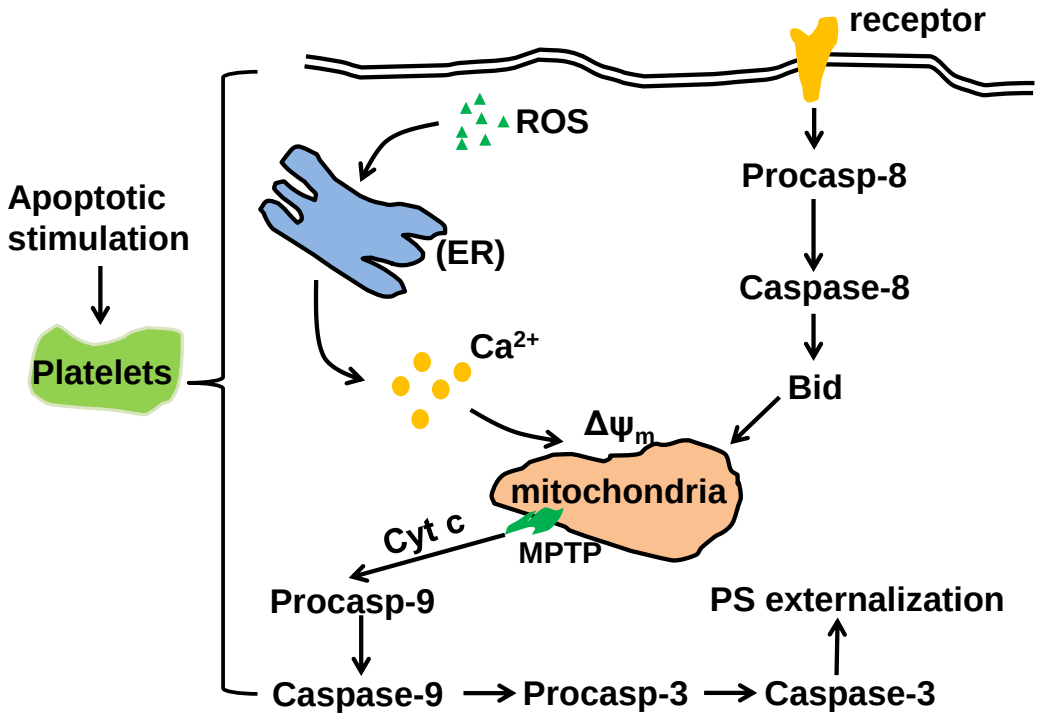

Fig.1.3. General mechanism of platelet apoptosis (Thushara et al. 2015)

1.5.2 Agonists-induced platelet apoptosis

As is described earlier, platelets perform the hemostatic function depending on the stimulation of agonists. Yet many kinds of agonists can also induce platelet apoptotic events according to the reports (Leytin 2012).

Low concentration of thrombin evokes high level expression of platelet P-selectin in vitro. However, thrombin-induced caspase-3 expression of platelets, PS exposure and $\Delta\psi_m$ loss were in a dose-dependent manner (Leytin et al. 2007). Furthermore, ROS play an important role in thrombin-induced platelet apoptotic events, because they can directly or indirectly trigger $\Delta\psi_m$ loss, thus leading to the activation of caspase cascades (Lopez et al. 2007). Carrim's research showed that thrombin mediated ROS production was through its binding to protease-activated receptor 4 (PAR4), but not PAR1. At the same time, GPIbα also contributed to this process. GPIbα/PAR4 together activated downstream effector protein FAK and NOX1, thus inducing ROS formation (Carrim et al. 2015). In addition, thrombin triggered platelet apoptotic events in

vitro were also associated with the temperature and time of treatment. Besides, it could selectively cause platelet activation or apoptosis by different mechanisms under different conditions (Gyulkhandanyan et al. 2013).

Like thrombin, collagen, another potent agonist, can also induce platelet apoptotic events. Although the $\Delta\psi_m$ only changes slightly, the caspase-3 and caspase-9 increase significantly following the treatment of collagen (Lin et al. 2009). Moreover, some weak agonists, such as ADP and U46619, can also cause apoptosis events in human platelets (Tonon et al. 2002).

1.5.3 Apoptotic markers of anucleate platelets

Similar to nucleated cells, the apoptosis of anucleate platelets exhibit a variety of characteristics in protein level and morphological change. The detection methods and applications of these characteristics have been reviewed by Gyulkhandanyan *et al* (Gyulkhandanyan et al. 2012). Depolarization of $\Delta\psi_m$ is considered as one of the important characteristics of platelet apoptosis induced by both intrinsic and extrinsic pathways (Jackson and Schoenwaelder 2010). In addition, PS exposure is a key characteristic of the nucleated cells apoptosis. However, PS exposure is increased during both platelet activation and apoptosis, which could be induced by different mechanisms (Kile 2014), (Arachiche et al. 2009). Moreover, platelet apoptosis can lead to morphological changes, such as cell shrinkage, blebbing, shedding of microparticles and so on (Leytin et al. 2004).

1.5.4 The effects of PS exposure on platelets

PS is one of the phospholipids in plasma membranes of most mammalian cells. Normally, they are located in the inner leaflet of the phospholipid bilayer, and form an asymmetric distribution with other phospholipids, such as phosphatidylcholine and sphingomyelin (Zwaal 1978). The asymmetry of membrane phospholipids depends on the regulation of flippases, floppases and

scramblases (Hankins et al. 2015). Upon the stimulation of apoptotic signalling, large quantities of PS are transported from inner leaflet to outer leaflet. Afterward, exposed PS can bind to PS receptor Tim4 of macrophages surface, which can clear the senescent platelets with the combined action of various proteins, such as MFG-E8, Gas6 and protein S (Toda et al. 2012), (Dransfield et al. 2015). Xkr8 plays a key role in caspase-related PS exposure during FasL-induced nucleated apoptosis (Suzuki et al. 2013). It can be activated by caspase-3 cleavage, and execute phospholipid scrambling by forming a complex with basigin (BSG) or neuroplastin (NPTN) (Suzuki et al. 2016).

The PS exposure of platelets also contributes to blood coagulation (Lentz 2003). As is described above, some coagulation factors, such as FVII, FIX and FII, can assemble with some protein cofactors and form a complex at the surface of phospholipid membrane during blood coagulation. This is accomplished by the binding of PS to N-terminal γ-carboxyglutamic acid (Gla) residues of these Vitamin K-dependent enzymes only, which can only take place when Ca^{2+} exist. (Ohkubo and Tajkhorshid 2008). However, some proteins, such as nonenzymatic cofactors FVIIIa and FVa, require the attendance of PS rather than Ca^{2+} to bind to the plasma membrane. They may bind to phospholipid of plasma membrane via C2 domain (Ngo et al. 2008).

1.6 Anoctamin 6 (Ano 6)

1.6.1 Anoctamin protein family

Anoctamin (Ano, also known as Tmem16) protein family was first identified and characterized through sequence analysis by Katoh et al. in 2004 (Katoh 2004a). It contains 10 members in mammalian cells, which are termed from Ano 1 (Tmem16A) to Ano 10 (Tmem16K) successively (Duran and Hartzell 2011). All Anoctamin family proteins contain a 8- transmembrane domains, and C- and N-termini that insert into cytosol (Pedemonte and Galietta 2014). In addition, the

first two members of Anoctamin family were reported respectively as the typical Ca^{2+}-activated Cl^- channel (CaCC) in 2008 by three different laboratories (Caputo et al. 2008), (Yang et al. 2008), (Schroeder et al. 2008). Further studies show that the physiological role of each member is different, yet none is completely clear until now.

1.6.2 Defective Ano 6 underlies the Scott syndrome

The Scott syndrome was reported many years ago as a rare inherited bleeding disorder (Weiss et al. 1979), (Satta et al. 1997). The platelets from Scott patients display defective Ca^{2+} -dependent PS exposure, which further results in low consumption of serum prothrombin and thus decreased generation of thrombin (Lhermusier et al. 2011). As is described above, the platelet PS exposure is regulated by scramblase. This mechanism in Scott platelets remains obscure, though early studies showed that the platelets from Scott patients displayed strong scrambling of membrane phospholipids upon agonists stimulation. (Rosing et al. 1985).

According to Suzuki's report, the knock down of Ano 6 (Tmem16F) significantly decreased Ca^{2+} -dependent PS exposure in Ba/F3 cell line (Suzuki et al. 2010). Later on, Yang and his colleagues further reported that compared with wild type mice, Ano 6 knockout mice exhibited prolonged bleeding, reduced thrombin production in PRP, and decreased PS exposure (Yang et al. 2012). All of these phenomena were analogous to the characteristics of Scott syndrome. Moreover, two novel mutation sites were found in the Tmem16F gene through the sequence analysis of the platelet DNA from a Scott patient (Castoldi et al. 2011). Recently, different mutation sites of Tmem16F gene were reported in another two Scott patients (Boisseau et al. 2016). These reports indicate that Ano 6 involves in platelet scramblase activity and is strongly associated with Scott syndrome.

1.6.3 The effect of Ano 6 on platelets

Yang *et al* reported that Ano 6 was a Ca^{2+} dependent cation channel with Ca^{2+} permeability, which regulated thrombin generation and procoagulant activity through its regulation of platelet lipid scrambling. (Yang et al. 2012). When treated with thrombin/collagen, Scott platelets exhibited reduced PS exposure and Δψm depolarization compared with normal platelets. However, in both the Soctt platelets and control groups, $[Ca^{2+}]_i$ increased similarly with the agonists stimulation (van Kruchten et al. 2013). Moreover, upon the treatment of A23187, platelets from Tmem16Ffl/fl;Pf4-CRE mice, a platelet-specific Ano 6 deficient mice, displayed suppressed microparticle shedding in vitro; upon the treatment of laser, they showed decreased thrombus formation in vivo. (Fujii et al. 2015). According to Baig's report, the platelets from conditional Ano 6 knockout mice also exhibited prolonged bleeding and fibrin formation (Baig et al. 2016).

Despite the aforementioned reports on the effect of Ano 6 on platelets, the role of Ano 6 in platelets remains less known. Therefore, this study further explores whether Ano 6 participates in the regulation of platelet $[Ca^{2+}]_i$, oxidative stress, activation and agonists induced apoptosis by using a Ano 6 deficient mice model.

1.7 γ-secretase and DAPT

γ-secretase, a member of intramembrane-cleaving proteases (i-CLiPs) family, consist of nicastrin, presenilin, anterior pharynx defective 1 and presenilin enhancer 2 (Sun et al. 2015). Presenilin, divided into presenilin-1 and presenilin-2, are indispensable among all the components and play a crucial role in catalyzing the hydrolysis of substrate (Kimberly et al. 2003). Most of the currently identified genetic mutations causing Alzheimer's disease (AD) occur in the genes encoding presenilin-1 protein (De Strooper et al. 2012). In platelets, presenilin-1 are extensively expressed as the catalytic subunits of γ-secretase

and mainly located in the membrane of α-granules (Mirinics et al. 2002).

DAPT, N-[N-(3,5-Difluorophenacetyl)-L-alanyl]-S-phenylglycine t-butyl ester, potently inhibit activity of γ-secretase complex as a specific inhibitor through binding with C-terminal fragment of presenilin (Fig.1.4) (Morohashi et al. 2006). DAPT was wildly used in the related researches of functions and signaling of γ-secretase and its target proteins, such as Notch, CD44 and APP (Androutsellis-Theotokis et al. 2006), (Roberts et al. 2017), (Johansson et al. 2017).

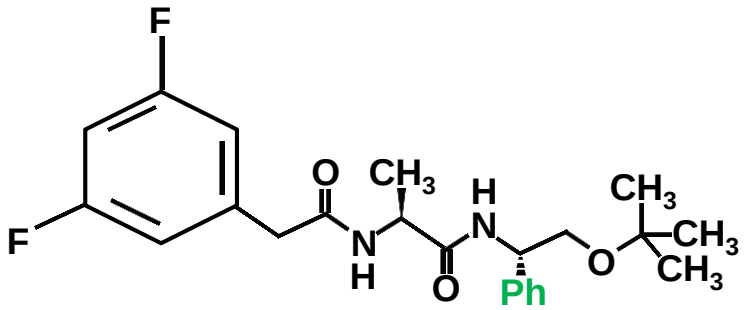

Fig.1.4 Chemical structure of γ-secretase inhibitor DAPT (Sigma-Aldrich PubChem Substance ID 24893987)

1.7.1 The functions of γ-secretase

It was reported that γ-secretase and the related components can perform proteolytic and non-proteolytic functions in different cells (Zhang et al. 2014). First of all, as an i-CLiPs, γ-secretase mainly catalyze and cleave type I membrane proteins, such as amyloid precursor protein (APP), CD44, Notch-1–4 and so on (Kopan and Ilagan 2004). APP is firstly cleaved by β-secretase. Then carboxyl-terminal fragments of APP (APP-βCTF or C99) are further cleaved by γ-secretase to successively produce amyloid-β (Aβ) peptide of different lengths (Haass et al. 2012). It is well known that the mass aggregation of Aβ in brain results in AD. Besides, platelets expressed a variety of isoforms of APP and released Aβ upon agonists stimulation (Evin and Li 2012). Gowert et al. reported that at different concentrations, Aβ could enhance the ADP-induced platelet

activation, and also cause PS exposure, ROS generation and caspase-3 activation (Gowert et al. 2014).

Secondly, the non-proteolytic role of γ-secretase and the related components have attracted some attention. In rat neurons, the expression of mutated presenilin-1 not only inhibited γ-secretase activity, but also displayed prolonged SOCE upon the stimulation of cyclopiazonic acid. Further experiments showed that the γ-secretase inhibitor treated neurons also displayed slightly prolonged SOCE (Shideman et al. 2009). The death of B103 cells, induced by A23187 in Ca^{2+}-dependent manner, significantly reduces following its co-incubation with γ-secretase inhibitors. However, these inhibitors cannot block the effect of staurosporin, which induce the apoptosis of B103 cells in a caspase-dependent manner (Choi et al. 2010).

1.7.2 The proteolysis of CD44 depend on γ-secretase activity

CD44, a multifunctional transmembrane glycoprotein and (co)receptor widely expressed in many cells, contribute to the regulation of cell migration, growth, wound healing and so on (Liu et al. 2016). Similar to APP, they were also cleaved by γ-secretase to generate and release two fragments- intracellular domain (CD44-ICD) and soluble CD44 (Fig.1.5) (Nagano and Saya 2004). The former translocated to nucleus and regulated the transcription of target genes (including CD44 itself) through binding to TPA-responsive elements (Okamoto et al. 2001). The ectodomain cleavage of CD44 involved in the regulation of cell migration (Sugahara et al. 2003).

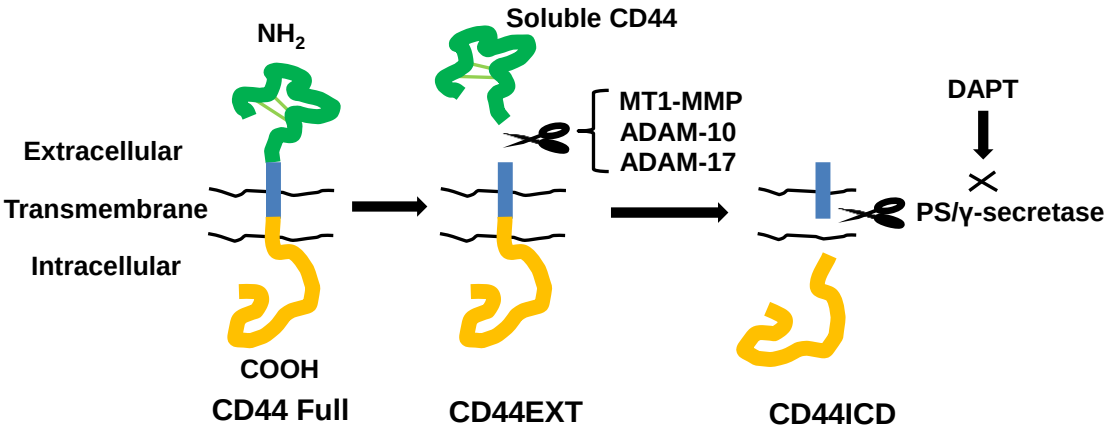

Fig.1.5. Proteolytic processes of CD44 (Nagano and Saya 2004)

The impact of CD44 on platelet activation and apoptosis has been reported utilizing a CD44 deficient mice model (Liu et al. 2016). Compared with wild type mice, the platelets from CD44 deficient mice displayed enhanced activation, PS exposure and caspase-3 activity after treatment with the agonists in vitro. The SOCE of CD44 deficient platelets significantly elevated in comparison with wild type mice. Similarly, thrombus formation of CD44 deficient mice in vitro also significantly increased under the high arterial shear rates.

All these reports point to the potential role of γ-secretase in platelets. Therefore, this study explored whether γ-secretase inhibitor DAPT regulated platelet Ca^{2+} signaling and SOCE as well as DAPT modified the stimulating effect of CRP on platelet activation, apoptosis and oxidative stress.

2. Materials and Methods

2.1 Preparation of mice

The generation of Ano 6 deficient mice (*ano6*$^{-/-}$) and corresponding wild type mice (*ano6*$^{+/+}$) has been described detailed elsewhere (Ehlen et al. 2013), and littermates mice were genotyped utilizing polymerase chain reaction (PCR). Wild type C57BL/6 mice were provided for γ-secretase relative experiments. Before taking blood from the mice, free drinking water and the control of chow were necessary (Ssniff, Soest, Germany). All animal experiments were conducted in line with the animal welfare law of Germanym and were approved by the authorities of the state of Baden-Württemberg.

2.2 Isolation of platelets

Platelets were isolated from the whole blood of 3 month-old mice of either sex. The mice were rapidly anesthetized before 800 µl blood was taken from each mouse and put into a 1.5 ml tube containing 200 µl acid-citrate-dextrose buffer (ACD, 80 mM citrate, 50 mM citric acid, 180 mM D-gluclose). 200 µl Tyrode buffer (pH 7.4, 133 mM NaCl, 12 mM $NaHCO_3$, 10 mM HEPES, 2.8 mM KCl, 5 mM D-glucose, 0.1% Bovine serum albumin) without Ca^{2+} was added into ACD-blood. Then the mixture was centrifuged at 260 g for 5 minutes to obtain platelet rich plasma (PRP). Next, PRP was transferred to another 1.5 ml tube and the platelets were pelleted after a 640 g centrifugation for 5 minutes. During this process, 0.02 U/ml apyrase (Sigma-Aldrich) and 0.5 µM prostaglandin I_2 (Calbiochem) were added to prevent the activation of platelets. Then the platelet pellet was washed twice before it was resuspended in 200 µl Tyrode buffer. The concentration of washed platelets was measured utilizing KX21-N automatic hematology analyzer (Sysmex).

In order to test blood parameter, 100 µl fresh EDTA-anticoagulated whole blood was obtained from Ano 6 defective mice and corresponding wild type

mice. Blood count was performed utilizing automatic hematology analyzer.

2.3 The impact of defective Ano 6 on platelet activation and apoptosis

2.3.1 Quantification of ROS

2',7'- Dichlorofluorescin diacetate (DCFDA, Sigma-Aldrich, Schnelldorf, Germany) was used to determine platelet oxidative stress. 10^8 isolated *ano6*$^{-/-}$ and *ano6*$^{+/+}$ platelets were stimulated by 0.01 U/ml thrombin (Roche, Switzerland) and 2 µg/ml collagen related peptide (CRP, provided by R. Farndale, University of Cambridge, Cambridge, UK) in the presence of 1 mM $CaCl_2$ and then incubated for 15 minutes at 37°C. The platelets of control groups were treated with Tyrode buffer in the same conditions. All the samples were washed twice with the 300 µl Tyrode buffer after agonist stimulation. Next, the treated platelets were stained for 30 minutes in 50 µl buffer containing 10 µM DCFDA, and the loaded platelets were washed once to remove residual dye. After a 760 g centrifugation, samples were resuspended in 200 µl Tyrode buffer and then ROS related fluorescence was measured by Fluorescence activated cell sorting (FACS, Calibur) system (BD, Heidelberg, Germany). DCFDA fluorescence was detected at an excitation wavelength of 488 nm and an emission wavelength of 530 nm (FL1 channel) on FACS machine.

2.3.2 Agonists-induced platelet Ca^{2+} response

For the measurement of $[Ca^{2+}]_i$, platelet pellet was resuspended in 100 µl Tyrode buffer without $CaCl_2$, and 10^6 platelets were transferred into a 1.5 ml tube. All the samples were stained with 3 µM Fluo-3 (Biotinium, USA) and then incubated at 37°C for 30 minutes. The samples were washed once and resuspended in 100 µl Tyrode buffer (1 mM $CaCl_2$). After stimulation with 0.01 U/ml thrombin or 2 µg/ml CRP for 100 seconds, activated Fluo-3 fluorescence was detected immediately in FL1 channel of FACS machine (excitation

wavelength: 488 nm, emission wavelength: 530 nm).

2.3.3 Platelet store-operated calcium entry (SOCE)

Platelets were firstly resuspended in 100 µl Ca^{2+} free Tyrode buffer and the final concentration was adjusted to 10^6 platelets/ml. Afterwards, platelets were treated with 3 µM Fluo-3 (Biotinium, USA) for 30 minutes at 37°C. Then the samples were washed for another time, and the loaded platelets were again suspended in Ca^{2+} free Tyrode buffer containing 1 µM thapsigargin (Invitrogen). After 10 minutes incubation, Ca^{2+} store depletion was measured immediately in FL1 channel of BD FACS. In order to measure store-operated Ca^{2+} entry, 1 mM $CaCl_2$ was added into the thapsigargin treated sample. 5 minutes later, the fluorescence of sample was detected utilizing FACS.

2.3.4 Orai1 protein abundance at the platelet surface

The expression of Orai1 protein at the surface of platelets was measured utilizing fluorescent labeled antibody and flow cytomerty. 10^8 platelets were stimulated by 0.01 U/ml thrombin and 2 µg/ml CRP in 100 µl Tyrode buffer containing 1 mM $CaCl_2$. 15 minutes later, 200 µl Tyrode buffer were added into the samples, which was followed by 760g centrifugation for 5 minutes. Washed platelets were fixed with 1% paraformaldehyde for 10 minutes. Next, all the samples were washed once and incubated with anti-Orai1 primary antibody (ab59330, Abcam; rabbit anti-mouse antibody) for 90 minutes at 37^{o}C. Following another time of wash, the treated platelets were further incubated with 1:250 diluted anti-rabbit secondary antibody (CF™ 488A; Sigma, USA) for 1 hour. Labeled platelets were analyzed immediately in FACS Calibur (FL1).

2.3.5 Expression of total Orai1 protein in platelets

Immunofluorescence and confocal laser scanning microscopy were used to determine the expression of total Orai1 protein in platelets. 3×10^6 platelets were adhered to fibrinogen coated surface on glass slips and fixed with 200 µl 1% paraformaldehyde (PFA) for 15 minutes. Following two times of wash, the

platelets were blocked for 20 minutes by 200 µl Tyrode buffer containing 2% BSA. Platelet membrane was permeabilized by 0.1% Triton-X 100 treatment for 5 minutes and then washed once to remove residual reagent. After that, the platelets were incubated with anti-Orai1 primary antibody (1:200, Abcam) overnight at 4^{o}C. The slips were washed twice and the platelets were incubated with secondary antibody (1:200; CF™ 488A, Sigma) for 2 hours in darkness. Additional F-actin was stained with rhodamine-phalloidin (1:200; Invitrogen) for 30 minutes at the room temperature. Then the samples were mounted with ProLong Gold antifade reagent (Invitrogen), and fluorescent pictures from 63× ocular were taken utilizing confocal laser scanning microscope (Zeiss LSM 5 EXCITER; Carl Zeiss, Germany).

2.3.6 P-selectin abundance and integrin αIIbβ3 activation

Platelet activation was measured utilizing both FITC conjugated P- selectin antibody (Wug.E9-FITC) and PE conjugated integrin αIIbβ3 (JON/A-PE) antibody. 10^6 platelets from *ano6*$^{-/-}$ and *ano6*$^{+/+}$ mice were suspended in 50 µl Tyrode buffer with $CaCl_2$ (1 mM). All the samples were incubated with fluorophore labeled antibodies (1:10 dilution) and then stimulated with 0.01 U/ml thrombin or 2 µg/ml CRP at 37°C. 15 minutes later, 150 µl PBS were added into the sample to stop the reaction. Two-color staining was analyzed immediately on FACS machine following fluorescent compensation setting.

2.3.7 Phosphatidylserine exposure and forward scatter

In order to evaluate the effect of Ano 6 on Ca^{2+} dependent PS exposure, platelets were centrifuged at 640g for 5 minutes, and then the platelet pellet was resuspended in 100 µl modified Tyrode buffer (1 mM Ca^{2+}). Next, the samples were treated with 0.01 U/ml thrombin or 5 µg/ml CRP at 37°C for 15 minutes, and then 200 µl Tyrode buffer was added to the sample to stop the reaction. Then the samples were washed once before they were stained with 1:20 dilution of Annexin-V FITC (Mabtag, Germany) in 50µl Tyrode buffer

containing 2 mM $CaCl_2$. Treated platelets were moved to the incubator and incubated for 20 minutes at 37^oC. The volume of sample was supplemented to 200 µl with Tyrode buffer and fluorescent analysis was performed immediately in FL1 channel of BD FACS. At the same time, platelet size was analyzed by forward scatter (FSC).

2.3.8 Platelet aggregation

Agonist induced platelet aggregation was measured utilizing FACS machine as previously reported (De Cuyper et al. 2013). Platelets, with the concentration no less than 5 × 10^7 platelets/ml, were pre-incubated respectively with CD9-APC and CD9-PE antibodies (Abcam; 1:100 dilution) in Ca^{2+} free Tyrode buffer at the room temperature. After 15 minutes, the samples were washed twice to remove residual antibody, and then the platelet pellet was resuspended in 100 µl modified Tyrode buffer with 1 mM $CaCl_2$. The differently labeled platelets of each group were mixed in 1:1 ratio, and then the mixture was incubated at 37^oC while being shaken at 600 rpm for 10 minutes. Next, the platelets were stimulated with CRP or thrombin under the condition of shaking (1000 rpm). At the indicated time points (0, 2, 4, 6, 8, 10 minutes), labeled-platelets were immediately fixed by 0.5% paraformaldehyde (Carl Roth, Germany) in PBS buffer, and then the samples were analyzed by flow cytometry in FL2 and FL4 channel.

The percentage of double-colored events against total labeled events was used to evaluate platelet aggregation. A quadrant was first set in dot plot model of FL2 and FL4 channels using labeled-resting platelets. Double-colored events appeared in upper right quadrant (Q2) following agonists simulation and the sum of events in the three regions (Q1+Q2+Q4) represents the total labeled events.

2.4 Effect of γ-secretase inhibitor DAPT on platelet activation and apoptosis

2.4.1 CRP-induced platelet Ca^{2+} response

To explore the effect of γ-secretase inhibitor DAPT upon CRP stimulation on $[Ca^{2+}]_i$, the platelets were exposed to 10 μM DAPT while being stained with Fluo-3 (3μM) in Ca^{2+} free Tyrode buffer for 30 minutes. After a wash, the loaded platelets were suspended in 100 μl Tyrode buffer with 1mM $CaCl_2$. Then the samples were stimulated with the agonist in two different ways. The first was to stimulate the platelets with CRP of different concentrations (0.5, 1, 2, and 5 μg/ml) for 100 seconds. In the second way, both the control and DAPT treated platelets were treated with 2 μg/ml CRP for different time durations (50, 100, 150 and 200 seconds). The fluorescence of sample was measured on FACS machine (FL1 channel).

2.4.2 DAPT sensitive platelet SOCE

10^6 platelets were suspended in Ca^{2+} free Tyrode buffer and stained with 3 μM Fluo-3 for 30 minutes in the presence of γ-secretase inhibitor DAPT (10 μM). Following a wash, the loaded platelets were resuspended into 100 μl Ca^{2+} free Tyrode buffer and treated with1 μM thapsigargin for 10 minutes. Platelet Ca^{2+} store depletion was detected immediately by flow cytometry in the absence of extracellular Ca^{2+}. 1 mM $CaCl_2$ was added into the thapsigargin treated sample to trigger platelet SOCE. After 5 minutes of incubation, the fluorescence of sample was detected utilizing FACS.

2.4.3 The analysis of Orai1/STIM1 protein expression using Western blot

Following CRP stimulation, DAPT treated platelets were collected by centrifugation at 1000 rpm for 3 minutes. Then the pellet was resuspended in 100 μl cell lysis buffer (1:10; cell signaling, #9803) containing EDTA-free protease inhibitor cocktail (cOmplete™, Sigma-Aldrich). After a 10 minutes centrifugation at 14000g and 4°C, the supernatant was moved into a 1.5 ml cooled centrifuge tube and then protein concentration was measured utilizing Bradford (Bio-Rad). Afterwards, platelet proteins were separated and

transferred to PVDF membrane by SDS- polyacrylamide gel electrophoresis. The membrane was blocked with 5% BSA for 60 minutes at room temperature. Following two washes, it was incubated with the primary antibody against Orai1(0.5 µg/ml, Abcam), STIM1(1:1000, Cell Signaling) and GAPDH (1:1000, Cell Signaling) overnight at 4°C. Next, the membrane was washed three times with TBS-T buffer, and then incubated with horse radish peroxidase (HRP) conjugated secondary antibody (1:5000, Cell Signaling) for 60 minutes at room temperature. Antibody binding was detected utilizing the Hyperfilm ECL detection system (Amersham, GE healthcare), and the optical density of the bands was quantified by scanning densitometry.

2.4.4 Orai1protein abundance at the platelet surface

The expression of Orai1 protein at the surface of platelet plasma membrane was measured using flow cytometry. The platelets were treated with two ways. In one way, 10^6 isolated platelets were pretreated with γ-secretase inhibitor DAPT (Sigma-Aldrich, Germany) of the indicated concentration (1, 5, 10, 20 µM) at 37^{o}C for 30 minutes. Pretreated-platelets were washed once and stimulated with 2 µg/ml CRP for 100 seconds in 100 µl Tyrode buffer (1mM $CaCl_2$). In the second way, platelets were pretreated with 10 µM DAPT for 30 minutes and then stimulated with 2 µg/ml CRP (100 seconds, 15 minutes). Next, activated-platelets were fixed with 1% paraformaldehyde for 10 minutes. After one wash with Tyrode buffer, all the samples were incubated with primary anti-Orai1 antibody (ab59330, Abcam; rabbit anti-mouse antibody) for 90 minutes at 37^{o}C. Afterwards, the samples were washed again and then incubated with anti-rabbit secondary antibody in 1:250 diluted (Sigma, USA) for 1 hour, which was labeled by CF™ 488A. Antibody related fluorescence was analyzed immediately on FACS Calibur.

2.4.5 Platelet degranulation and integrin αIIbβ3 activation

Platelet P-selectin and integrin αIIbβ3 abundance were measured respectively

utilizing their corresponding fluorophore conjugated antibodies. After a 10 µM DAPT treatment for 30 minutes, 10^6 platelets were incubated with antibodies of P-selectin (Wug.E9-FITC) and αIIbβ3 integrin (JON/A-PE) in the presence of 2 µg/ml CRP. Following 15 minutes stimulation, 150 µl PBS were added into the samples to stop the reaction. Two-color analysis was performed using BD FACS machine.

2.4.6 Reactive oxygen species (ROS) formation

Platelets were first treated with 10 µM γ-secretase inhibitor DAPT at 37^{o}C for 30 minutes. After one wash, both control and DAPT treated-platelets were resuspended in 200 µl Tyrode buffer with 1 mM $CaCl_2$ and loaded with 10 µM 2',7'- dichlorodihydrofluorescein diacetate (DCFDA; Sigma-Aldrich) for 30 minutes. Next, the loaded platelets were stimulated by 2 µg/ml CRP and the ROS relative fluorescence was measured at the interval of one minute within 15 minutes.

2.4.7 Mitochondrial membrane potential

The loss of platelet mitochondrial membrane potential was evaluated using flow cytometry. The isolated platelets were first incubated with 10 µM DAPT for 30 minutes as is described above. 10^8 treated platelets were further stimulated with 5µg/ml CRP for 60 minutes and stained for 30 minutes with 10 µM TMRE (tetramethylrhodamine, ethyl ester perchlorate; Invitrogen, USA) in the dark. The fluorescence of TMRE loaded platelets were determined utilizing FL1 channel of FACS machine.

2.4.8 Platelet PS exposure and cell shrinkage

In order to evaluate the effect of γ-secretase inhibitor DAPT on platelet PS exposure, 10^8 platelets were first incubated for 30 minutes with 10 µM γ-secretase inhibitor DAPT and then stimulated with 5 µg/ml CRP for 10 minutes in the presence of 1 mM $CaCl_2$. Afterwards, 200 µl Tyrode buffer were added into the samples to stop the reaction. Following a wash, the platelets

were stained with 1:20 dilution of Annexin-V FITC (Mabtag, Germany) in 50 µl Tyrode buffer with 2 mM $CaCl_2$. After 20 minutes incubation, Annexin-V binding that reflected PS exposure at the platelet surface was analyzed on FACS machine (FL1 channel). At the same time, platelet shrinkage was analyzed utilizing forward scatter (FSC) of dot plot model.

2.4.9 DAPT sensitive platelet aggregation

DAPT sensitive platelet aggregation was tested utilizing flow cytometry as is aforementioned. To this end, platelets were labeled with 1:100 diluted CD9-APC (Abcam, ab82392; Ex: 645nm, Em: 660nm), while equal amounts of platelets were labeled with CD9-PE antibodies (Abcam, ab82394; Ex: 488nm, Em: 575nm) for 15 minutes. After two times of wash, the two differently labeled platelets were mixed in the ration of 1:1. The mixture was treated with 10 µM DAPT (Sigma-Aldrich, Germany) for 30 minutes and shaken at low frequency (600 rpm) for 10 minutes. Then, the samples were treated with CRP (2 ug/ml) while being shaken at the frequency of 1000 rpm. Following their fixation with 0.5% paraformaldehyde in PBS, the samples were analyzed using flow cytometry. The percentage of double-colored events against the total fluorescent events was used to evaluate platelet aggregation.

2.4.10 In vitro platelet thrombus formation

Glass coverslips were coated with 250 µl Tyrode buffer containing 100µg/ml collagen overnight at 4°C. Whole blood was taken with heparin anticoagulant and then diluted 1:3 with Tyrode buffer (pH 7.4, 2 mM $CaCl_2$). After that, the sample was perfused with high shear rates (1700 s^{-1}) through a transparent parallel-plate flow chamber (slit depth 50 µm) over a collagen coated glass coverslip for 5 minutes. Next, the flow chamber was rinsed with Tyrode buffer for 5 minutes utilizing peristaltic pump. Images of platelet adhesion were captured from 4 or 6 different microscopic fields of CCD camera (Axiovert 200, objective 20x; Carl Zeiss, Germany). The image analysis was performed

utilizing AxioVision software (Carl Zeiss) and the mean value of the covered area was calculated to estimate thrombus formation in vitro.

2.5 Statistical analysis

The statistical analysis of collected-data was performed via one-way ANOVA with Tukey's test using Graphpad Prism 6.1 software, which applies to post-test and unpaired- student's t-test. All the results were reported as arithmetic means value ± SEM (standard error of mean) using Microsoft excel 2010, while n represents the repeated number of independent experiments. The results were considered statistically significant with P-value <0.05.

3. Results

The parts of results in this dissertation have been published as follows:

Liu G, Liu Guilai, Chatterjee M, Umbach A.T, Chen H, Gawaz M, Lang F. Influence of γ-Secretase Inhibitor 24-Diamino-5-Phenylthiazole DAPT on Platelet Activation. Cell Physiol Biochem. 2016;38(2):726-36.

Liu G, Liu Guilai, Chen H, Borst O, Gawaz M, Vortkamp A, Schreiber R, Kunzelmann K, Lang F. Involvement of Ca^{2+} Activated Cl^- Channel Ano 6 in Platelet Activation and Apoptosis. Cell Physiol Biochem. 2015;37(5): 1934-44.

3.1 The role of Ano 6 on platelet activation and apoptosis

This study explored whether Ano 6 affects physiological parameter of platelets in the blood. For this goal, Whole blood was taken from Ano 6 deficient mice (*ano6*$^{-/-}$) and corresponding littermates wild type mice (*ano6*$^{+/+}$). As is listed in Table 3.1.1, Platelet number in the blood of *ano6*$^{-/-}$ mice was significantly higher ($p<0.05$) in comparison with wild-type mice. Moreover, the data showed that others platelet parameters of *ano6*$^{-/-}$ mice such as platelet volume, platelet distribution width and platelet larger cell ratio were similar to that of *ano6*$^{+/+}$ mice. Besides, the physiological parameters of erythrocyte including number, hemoglobin concentration, volume, and so on were also investigated in this research, and all of them were actually identical in Ano 6 deficient mice and wild type mice.

Table 3.1.1: Blood parameter of *ano6*$^{-/-}$ mice and corresponding *ano6*$^{+/+}$ mice. Arithmetic mean (AM) ± SEM (n = 6~9), *(p<0.05) shows significant difference between the two genotypic mice (Liu et al. 2015).

	***ano6*$^{+/+}$**	***ano6*$^{-/-}$**
Platelet number (10^3/μl)	*1086 ± 53.58*	*1252 ± 39.59****
Mean platelet volume (MPV) (fl)	*6.40 ± 0.11*	*6.27 ± 0.10*
Platelet Distribution Width (PDW) (fl)	*7.33 ± 0.17*	*7.11 ± 0.17*

Platelet larger cell ratio (P-LCR) (%)	*4.68 ± 0.51*	*4.21 ± 0.48*
Erythrocyte number (10^6/µl)	*11.25 ± 2.11*	*10.56 ± 1.35*
Hemoglobin (g/dl)	*13.90 ± 0.45*	*14.34 ± 0.33*
Hematocrit (%)	*44.35 ± 1.12*	*46.33 ± 0.97*
Mean erythrocyte volume (MCV) (fl)	*51.13 ± 0.25*	*50.99 ± 0.41*
Erythrocyte hemoglobin concentration (MCHC) (g/dl)	*31.25 ± 0.33*	*32.07 ± 0.97*
Hemoglobin/erythrocyte (MCH) (pg)	*15.98 ± 0.23*	*15.80 ± 0.26*

In order to test the impact of Ano 6 with agonists stimulation on platelet $[Ca^{2+}]_i$, Fluo-3 was employed to measure cytosolic Ca^{2+} activity. As is illustrated in Fig.3.1.1, resting platelets displayed similar $[Ca^{2+}]_i$ in *ano6*$^{+/+}$ platelets and *ano6*$^{-/-}$ platelets (Fig.3.1.1A, D). Following stimulation of 0.01 U/ml thrombin for 100 seconds, $[Ca^{2+}]_i$ significantly ($p<0.001$) increased in both *ano6*$^{+/+}$ and *ano6*$^{-/-}$ platelets. However, the increased magnitude of $[Ca^{2+}]_i$ was significantly ($p<0.05$) less pronounced in Ano 6 deficient platelets in comparison with normal platelets (Fig.3.1.1B, D). Activation of the platelets with 2 µg/ml CRP treatment for 100 seconds was followed by a significant ($p<0.001$) increase of $[Ca^{2+}]_i$ in both Ano 6 deficient and wild type platelets. The effect of CRP and thrombin, however, was remarkably smaller in platelets from Ano 6 deficient mice than in platelets from wild type mice (Fig.3.1.1C, D).

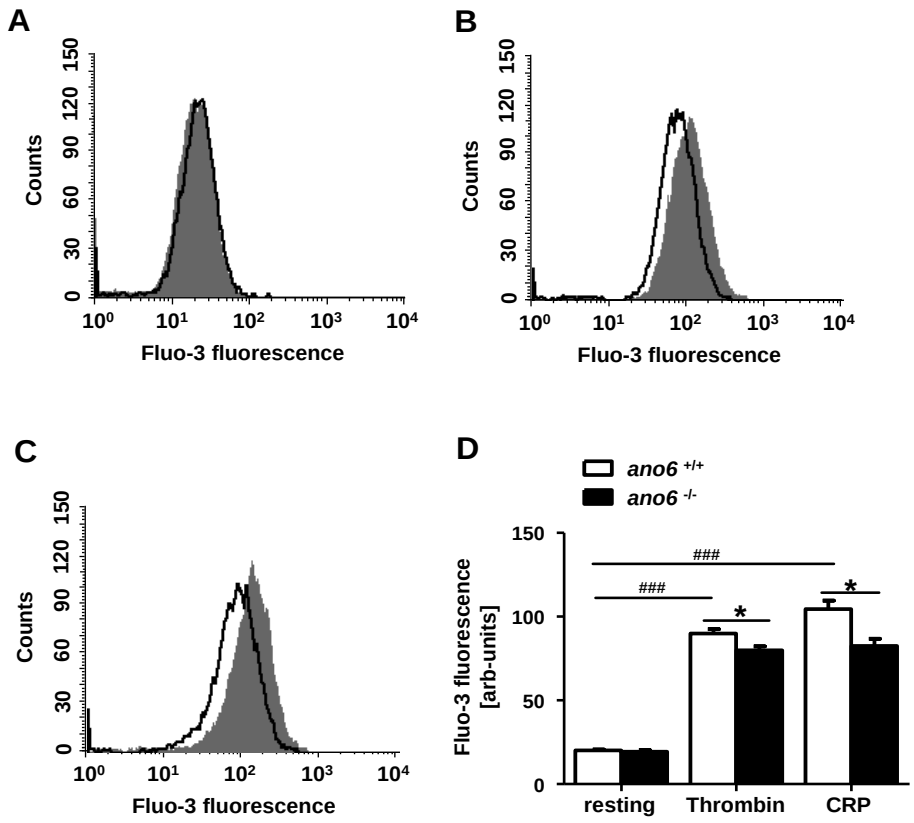

Fig.3.1.1. Ano 6 sensitive agonists induced platelet Ca^{2+} response

A-C. Typical histogram of platelet Fluo-3 fluorescence from FACS assay indicated cytosolic Ca^{2+} activity before (A) and after a 100 sec exposure to (B) thrombin (0.01 U/ml) or (C) CRP (2 µg/ml). Grey shadows: *ano6*$^{+/+}$ platelets, black lines: *ano6*$^{-/-}$ platelets.

D. Arithmetic mean (AM) ± SEM (n = 4) of fluorescence intensity (arb-units) of Fluo-3 in *ano6*$^{+/+}$ platelets (white bars) and *ano6*$^{-/-}$ platelets (black bars).

###(p<0.001) represents significant increase from the stimulation of thrombin or CRP, *(p<0.05) represents significant decrease from defective Ano 6. (Liu et al. 2015)

It is known that the depletion of intracellular Ca^{2+} pool causes extracellular Ca^{2+} entry via store-operated Ca^{2+} channel in platelets. In order to explore the effect of Ano 6 on platelet SOCE, Thapsigargin, sarco/endoplasmic reticulum Ca^{2+} ATPase inhibitor, was used to treat the platelets form Ano 6 deficient mice and corresponding wild type mice. As is illustrated in Fig.3.1.2A, $[Ca^{2+}]_i$ of *ano6*$^{+/+}$ and *ano6*$^{-/-}$ platelets increased remarkably with 1 µM thapsigargin treatment for 10 minutes in the absence of extracellular Ca^{2+}, and the effect of Ano 6 was negligible. After the addition of 1 mM $CaCl_2$, platelet $[Ca^{2+}]_i$ further elevated, but there was no significant difference between the two genotypes.

Agonists induced an impaired Ca^{2+} response in *ano6*$^{-/-}$ platelets. In order to elucidate whether Orai1 channel contributed to this process, the expression of Orai1 protein was measured utilizing flow cytometry and immunofluorescence. As is demonstrated in Fig.3.1.2B, the expression of Orai1 was similarly low at the surface of the resting platelets and significantly increased after thrombin or CRP treatment. But there was no remarkable difference between *ano6*$^{+/+}$ and *ano6*$^{-/-}$ platelets. Besides, the expression of total Orai1 protein in platelets was measured utilizing immunofluorescence and confocal microscopy. As is shown in Fig.3.1.2C, treatment with thrombin and CRP was followed by an increased expression of Orai1 in platelets. However, the expression level in the two genotypic platelets was similarly higher.

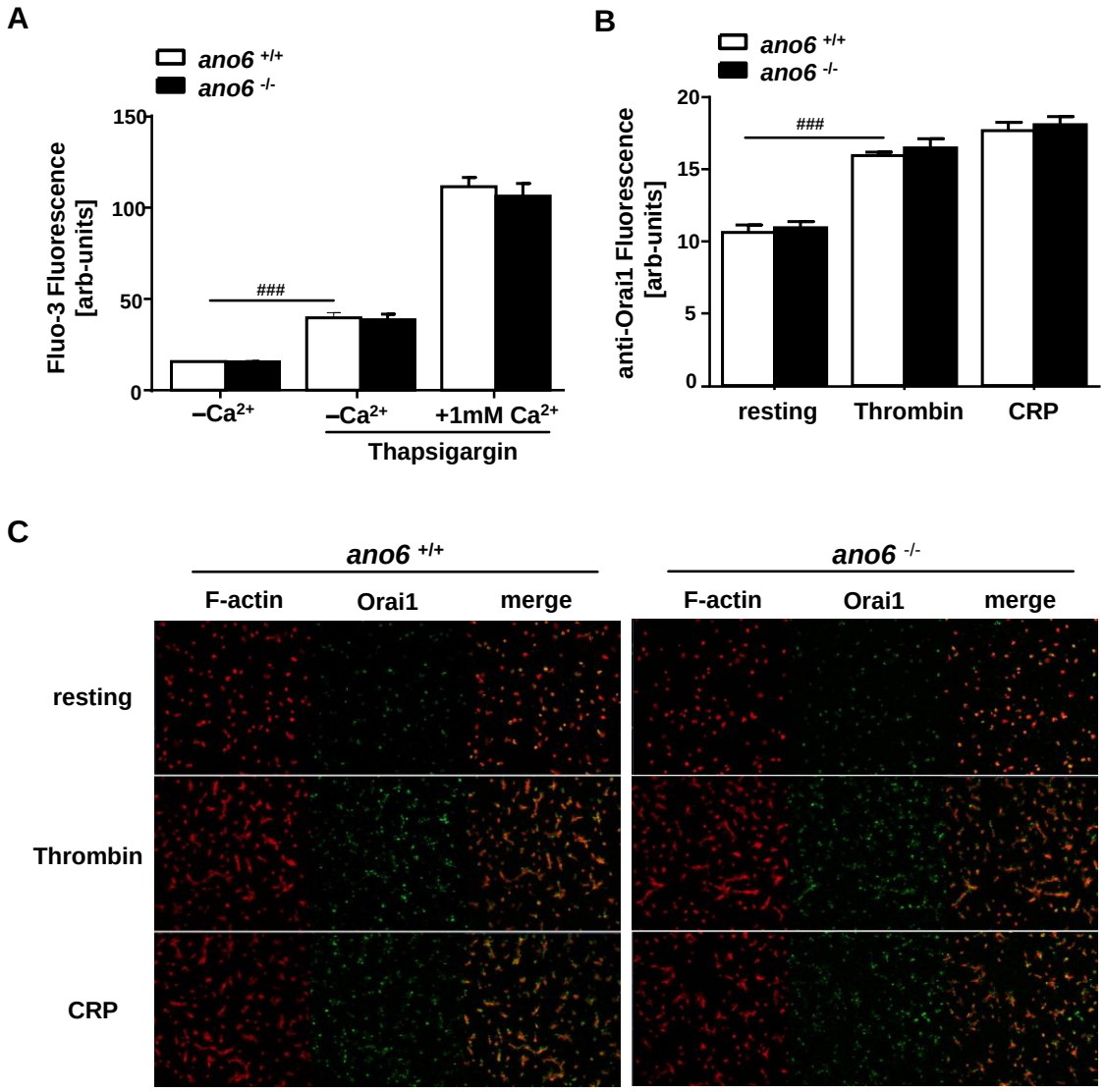

Fig.3.1.2. SOCE and Orai1 expression in *ano6*$^{+/+}$ and *ano6*$^{-/-}$ platelets

A. Arithmetic mean (AM) ± SEM (n = 4) of fluorescence intensity (arb-units) of Fluo-3 in *ano6*$^{+/+}$ platelets (white bars) and *ano6*$^{-/-}$ platelets (black bars). Loaded platelets were incubated in Ca^{2+} free Tyrody buffer (left bars), and then treated with thapsigargin (1 µM) for 10 min to deplete Ca^{2+} store (middle bars). Following re-addition of 1 mM $CaCl_2$, platelet SOCE was triggered and cytosolic Ca^{2+} concentration reached the maximum after 5 min (right bars). ###($p<0.001$) represents significant increase from thapsigargin treatment.

B. Arithmetic mean (AM) ± SEM (n = 4~5) of fluorescence intensity (arb-units) from FACS assay of Orai1 abundance at the plasma membrane surface of *ano6*$^{+/+}$ platelets (white bars) and *ano6*$^{-/-}$ platelets (black bars) prior to (resting) and following a 15 min exposure to thrombin (0.01 U/ml) or CRP (2 µg/ml). ###($p<0.001$) indicates significant increase from stimulation of the agonists.

C. Immunofluorescence analysis of total Orai1 protein in *ano6*$^{+/+}$ platelets (left panels) and *ano6*$^{-/-}$ platelets (right panels) after a 15 min exposure to thrombin (0.01 U/ml) or CRP (2 µg/ml). Red: F-actin; green: Orai1. (unpublished)

The stimulation of agonists triggered ROS formation by regulating cytosolic Ca^{2+} concentration. Further analyses explored the role of Ano 6 in platelet oxidative stress. The abundance of reactive oxygen species (ROS) was measured using FACS machine by testing DCFDA fluorescence. As is described in Fig.3.1.3, the level of ROS was similarly high in resting platelets from both genotypic (*ano6*$^{+/+}$ and *ano6*$^{-/-}$) mice (Fig.3.1.3A, D). After a 15 minutes exposure to 0.01 U/ml thrombin, ROS formation significantly ($p<0.001$) increased in both *ano6*$^{+/+}$ and *ano6*$^{-/-}$ platelets, but the increased magnitude of ROS was significantly ($p<0.05$) less pronounced in Ano 6 deficient platelets than in normal platelets (Fig.3.1.3B, D). 15 minutes treatment with 2 μg/ml CRP again led to significant increase of ROS formation in both Ano 6 deficient and wild type platelets. Unlike the stimulation of thrombin, the effect of CRP on ROS formation was not significantly different between *ano6*$^{-/-}$ platelets and *ano6*$^{+/+}$ platelets (Fig.3.1.3C, D)

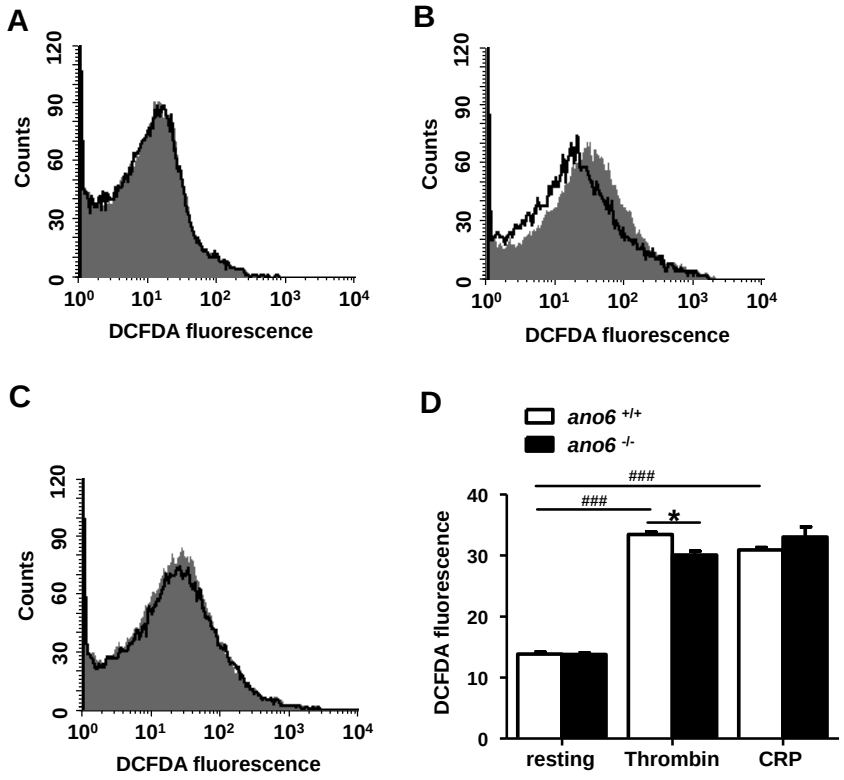

Fig.3.1.3. The effect of Ano 6 on platelet oxidative stress

A-C. Typical histogram of DCFDA related fluorescence from FACS assay reflected platelet

reactive oxidant species (ROS) formation before (A) and after a 15 min exposure to (B) 0.01U/ml thrombin or (C) 2µg/ml CRP. Grey shadows: *ano6*$^{+/+}$ platelets, black lines: *ano6*$^{-/-}$ platelets.
D. Arithmetic mean (AM) ± SEM (n = 3~5) of relative fluorescence unit of ROS abundance in *ano6*$^{+/+}$ platelets (white bars) and *ano6*$^{-/-}$ platelets (black bars).
###(p<0.001) shows significant increase from the stimulation of thrombin or CRP, *(p<0.05) represents significant decrease in *ano6*$^{-/-}$ platelets.(Liu et al. 2015)

The next experiments addressed the impact of Ano 6 on platelet degranulation. The degranulation was quantified using flow cytometry via checking P-selectin abundance at the surface of platelet plasma membrane. As is shown in Fig.3.1.4, P-selectin abundance was similarly low at the surface of untreated platelets, which were isolated respectively from wild type mice and Ano 6 deficient mice (Fig.3.1.4A, D). Following a 15 minutes exposure to 0.01 U/ml thrombin, P-selectin abundance radically increased in both *ano6*$^{+/+}$ and *ano6*$^{-/-}$ platelets. Although there was a slight difference between the growth ranges in the two different platelets, it was not statistically significant (Fig.3.1.4B, D). 2 µg/ml CRP induced a significant (p<0.001) increase of P-selectin abundance in both genotypic (*ano6*$^{+/+}$ and *ano6*$^{-/-}$) platelets, and the increase was significantly blunted in Ano 6 deficient platelets (Fig.3.1.4C, D).

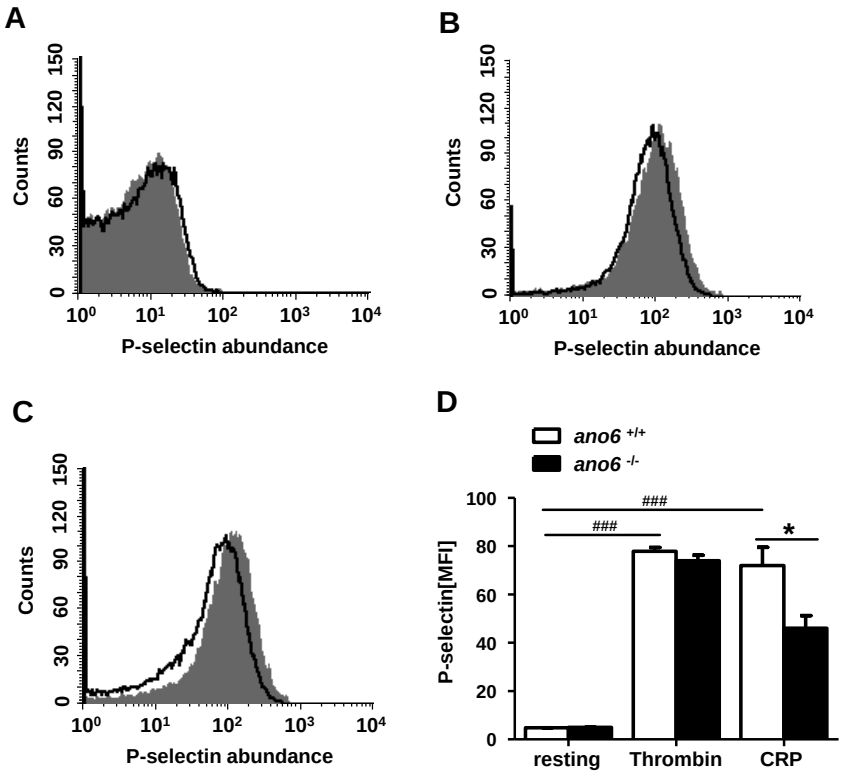

Fig.3.1.4. Agonists induced platelet degranulation in *ano6*$^{+/+}$ and *ano6*$^{-/-}$ platelets

A-C. Original histogram from FACS assay reflected the abundance of degranulation-dependent P-selectin before (A) and after 15 min stimulation with (B) 0.01U/ml thrombin or (C) 2µg/ml CRP in platelets. Grey shadows: *ano6*$^{+/+}$ platelets, black lines: *ano6*$^{-/-}$ platelets.

D. Arithmetic mean (AM) ± SEM (n = 4~7) of fluorescence intensity unit of P-selectin antibody in *ano6*$^{+/+}$ (white bars) and *ano6*$^{-/-}$ (black bars) platelets.

###(p<0.001) indicates significant increase to value from the stimulation of thrombin or CRP, *(p<0.05) shows significant decrease from defective Ano 6. (Liu et al. 2015)

The elevated $[Ca^{2+}]_i$ can induce activation of platelet integrin αIIbβ3 by the mechanism of inside-out signalling pathway. To study the impact of Ano 6 on platelet integrin αIIbβ3 activation, further experiments were conducted by incubating platelets with the specifically fluorescent-labeled antibody. Like P-selectin, the abundance of activated integrin αIIbβ3 at the surface of platelet plasma membrane was similarly low in resting platelets of both genotypes (*ano6*$^{+/+}$ and *ano6*$^{-/-}$) (Fig.3.1.5A, D). The related fluorescence of activated integrin αIIbβ3 significantly (p<0.001) increased following 0.01 U/ml thrombin

treatment for 15 minutes in both *ano6*$^{+/+}$ and *ano6*$^{-/-}$ platelets. Although there was a slight difference between the increase ranges in the two different platelets, it was not statistically significant (Fig.3.1.5B, D). After a 15 minutes stimulation with CRP (2 µg/ml), integrin αIIbβ3 activation remarkably increased in both *ano6*$^{-/-}$ and *ano6*$^{+/+}$ platelets. The impact of CRP was again significantly ($p<0.05$) attenuated in *ano6*$^{-/-}$ platelets than in *ano6*$^{+/+}$ platelets (Fig.3.1.5C, D).

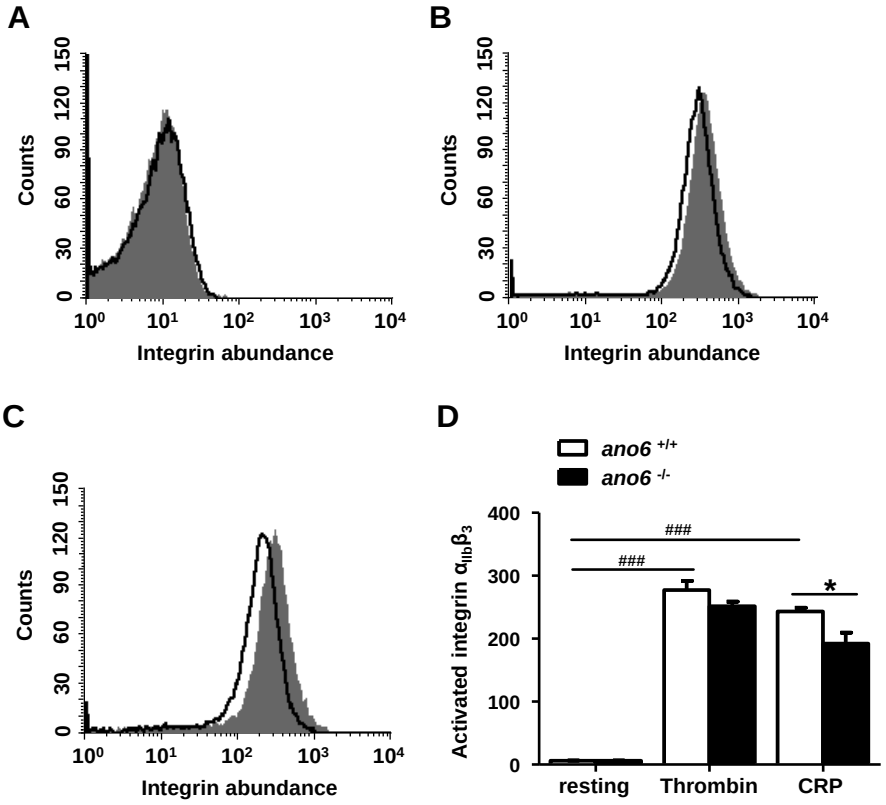

Fig.3.1.5. The effect of Ano 6 on platelet integrin αIIbβ3 activation

A-C. Original histogram of antibody related fluorescence from flow cytometric assay reflected the activation of platelet integrin αIIbβ3 without stimulation (A) and with a 15 min exposure to (B) 0.01U/ml thrombin or (C) 2µg/ml CRP. Grey shadows: *ano6*$^{+/+}$ platelets, black lines: *ano6*$^{-/-}$ platelets.

D. Arithmetic mean (AM) ± SEM (n = 4~6) of relative fluorescence intensity (arb-units) of activated integrin αIIbβ3 in responds to a 15 min stimulation with thrombin (0.01 U/ml) or CRP (2 µg/ml). White bars: *ano6*$^{+/+}$ platelets, black bars: *ano6*$^{-/-}$ platelets.

###($p<0.001$) shows significant increase from the treatment of thrombin or CRP, *($p<0.05$) represents significant attenuation from defective Ano 6. (Liu et al. 2015)

Platelet apoptosis is characterized by volume shrinkage and plasma membrane scrambling with the translocation of phosphatidylserine (PS) from the inner leaflet to the outer leaflet. In order to elucidate the impact of transmembrane protein Ano 6 on platelet apoptosis, PS abundance of the platelets was detected by flow cytometry utilizing annexin-V-binding. At the same time, platelet volume was quantified via the analysis of forward scatter. As is shown in Fig.3.1.6, the percentage of annexin-V-binding (marked area) was low in resting platelets in vitro and there was no significant difference between the two genotypes (Fig.3.1.6A, D). After a 15 minutes simulation with 0.01 U/ml thrombin or 5 µg/ml CRP, the percentage of annexin-V labeled platelets significantly ($p<0.001$) rose in both *ano6*$^{+/+}$ and *ano6*$^{-/-}$ genotype. The effect of agonists, however, significantly attenuated in *ano6*$^{-/-}$ platelets in comparison with *ano6*$^{+/+}$ platelets (Fig.3.1.6B, C, D).

Fig.3.1.7 shows the platelet volume shrinkage. The volumes of the two types of untreated platelets (*ano6*$^{+/+}$ and *ano6*$^{-/-}$) were almost the same in vitro. Incubation with 0.01 U/ml thrombin (15 minutes) was followed by a significant ($p<0.001$) contraction of forward scatter in both Ano 6 deficient platelets and wild type platelets. But the effect of thrombin significantly ($p<0.01$) weakened in Ano6 deficient platelets. The exposure to 5 µg/ml CRP also resulted in a significant ($p<0.001$) contraction of forward scatter in both genotypic platelets. However, the defective Ano 6 significantly ($p<0.05$) reduced the effect of CRP in platelets.

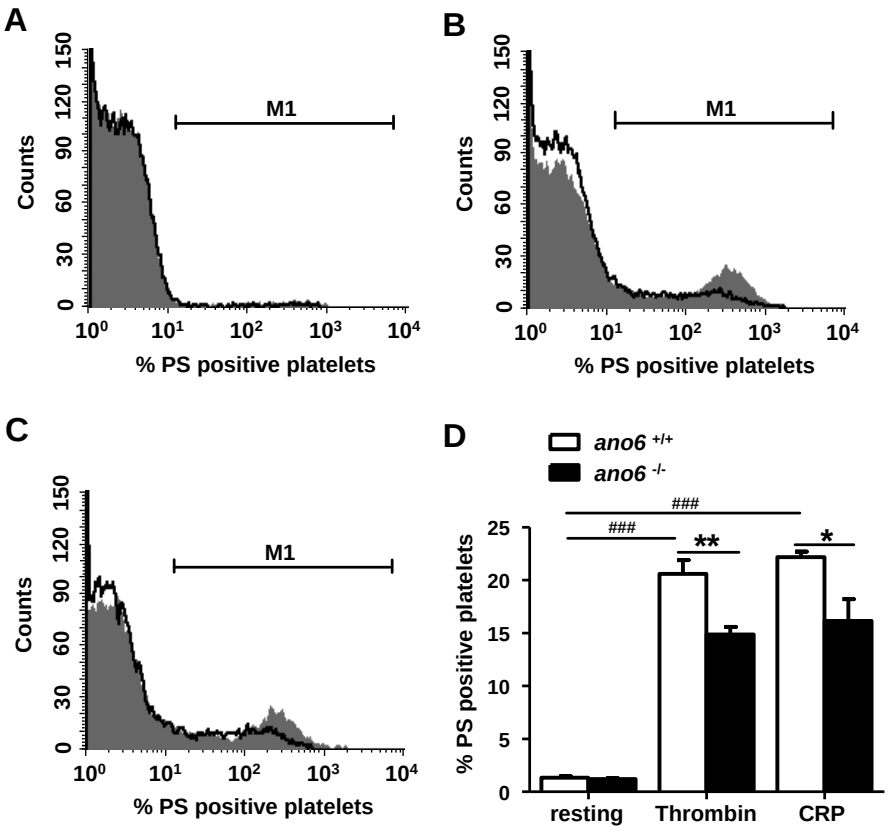

Fig.3.1.6. Ano 6 sensitive PS exposure at the surface of platelets

A-C. The marked area of overlaid annexin-V binding histogram from FACS assay reflected platelet PS exposure in platelets before (A) and after (B) 0.01U/ml thrombin or (C) 5µg/ml CRP treatment for 15 min. Grey shadows: *ano6*$^{+/+}$ platelets, black lines: *ano6*$^{-/-}$ platelets.

D. Arithmetic mean (AM) ± SEM (n = 4~6) of % annexin-V-binding to *ano6*$^{+/+}$ (white bars) and *ano6*$^{-/-}$ (black bars) platelets in resting and following a 15 min exposure to thrombin or CRP.

###($p<0.001$) indicates significant increase from the stimulation of thrombin or CRP, *($p<0.05$) and ** ($p<0.01$) represents significant decrease from defective Ano 6. (Liu et al. 2015)

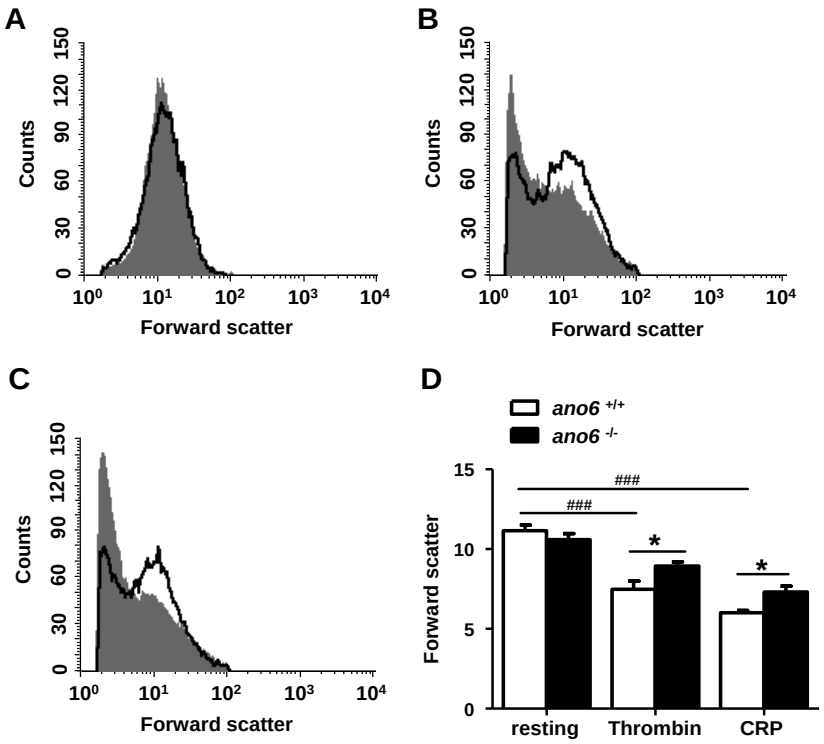

Fig.3.1.7. The impact of Ano 6 on agonist induced cell shrinkage

A-C. Original histogram of forward scatter from flow cytometric assay reflected the shrinkage of cell volume of *ano6*$^{+/+}$ platelets (grey shadows) and *ano6*$^{-/-}$ platelets (black lines) before (A) and after a 15 min stimulation with (B) 0.01U/ml thrombin or (C) 5 µg/ml CRP.

D. Arithmetic mean (AM) ± SEM (n = 4~6) of relative light intensity unit of forward scatter following a 15 min exposure to thrombin or CRP. White bars: *ano6*$^{+/+}$ platelets, black bars: *ano6*$^{-/-}$ platelets.

###($p<0.001$) represents significant decrease from the treatment of thrombin or CRP, *($p<0.05$) shows significant difference between *ano6*$^{+/+}$ and *ano6*$^{-/-}$ platelets. (Liu et al. 2015)

To study the influence of Ano 6 with the stimulation of agonists on platelet aggregation, the platelets were incubated with PE and APC conjugated CD9 antibody. Two color analysis of aggregation was performed by flow cytometry. As is shown in Fig.3.1.8, the percentage of double-colored events reflecting aggregation was similarly low in both genotypic (*ano6*$^{+/+}$ and *ano6*$^{-/-}$) resting platelets, and significantly increased following a few minutes stimulation with thrombin (0.005 U/ml) or CRP (2 µg/ml). There was no notable difference of the effect of the agonists in *ano6*$^{+/+}$ and *ano6*$^{-/-}$ platelets.

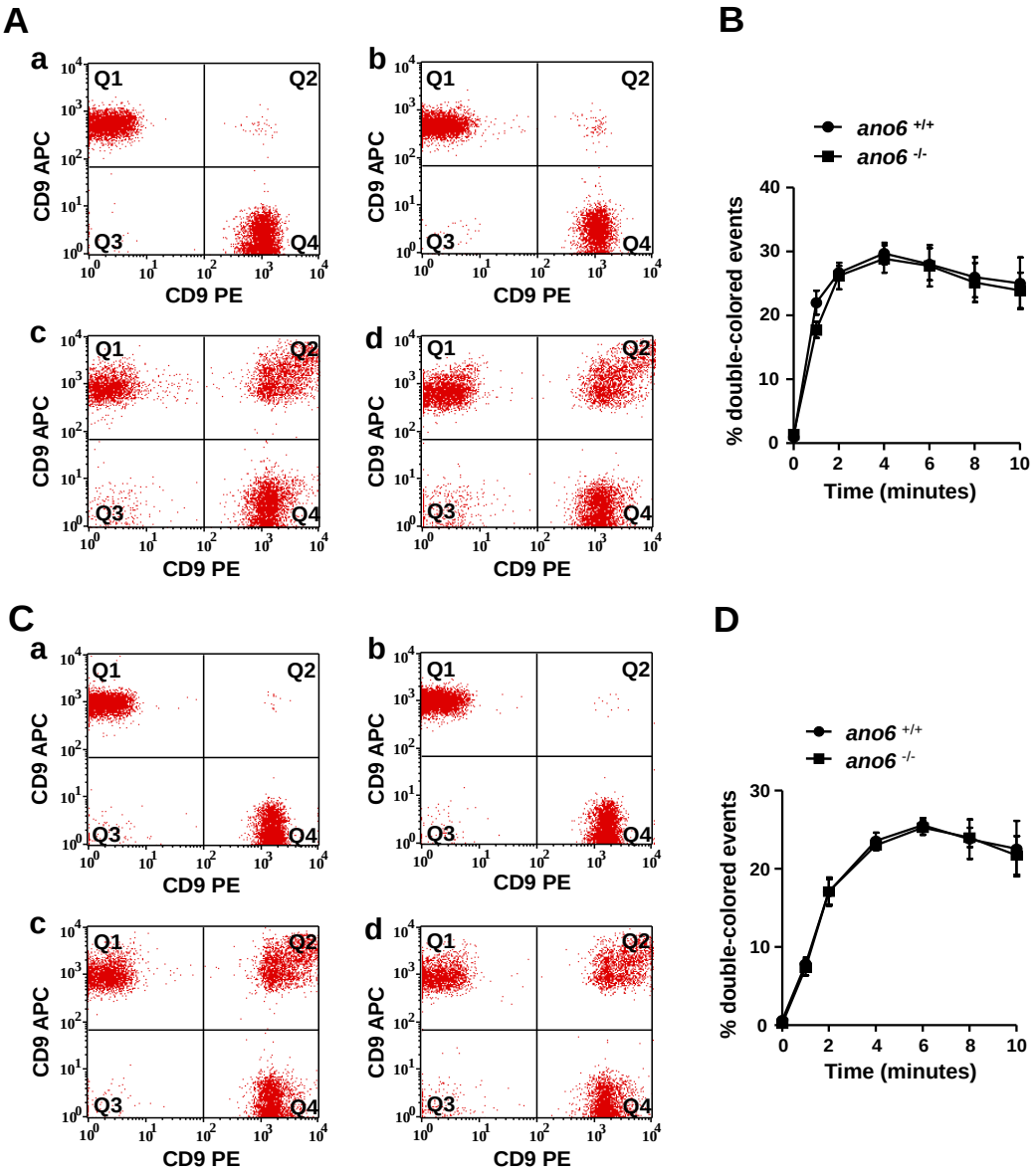

Fig.3.1.8. Activation-dependent platelet aggregation in vitro

A. Representative dot blots from FACS assay reflected the aggregation of *ano6*$^{+/+}$ platelets (a, c) and *ano6*$^{-/-}$ platelets (b, d) in responds to the stimulation of 0.005 U/ml thrombin in 0 min (a, b) and 10 min (c, d).

B. Arithmetic mean (AM) ± SEM (n = 4) of % double-colored events (Q2) reflected platelet aggregation in indicated time point after stimulation with thrombin (0.005 U/ml). Black circles: *ano6*$^{+/+}$ platelets, black square: *ano6*$^{-/-}$ platelets.

C. Representative dot blots from FACS assay reflected the aggregation of *ano6*$^{+/+}$ platelets (a, c) and *ano6*$^{-/-}$ platelets (b, d) in responds to stimulation of 2 µg/ml collagen related peptide CRP in 0 min (a, b) and 10 min (c, d).

D. Arithmetic mean (AM) ± SEM (n = 4) of % double-colored events (Q2) reflected platelet aggregation in indicated time point after stimulation with CRP (2 µg/ml). Black circles: *ano6*$^{+/+}$ platelets, black square: *ano6*$^{-/-}$ platelets.(Liu et al. 2015)

3.2 γ-secretase inhibitor DAPT sensitive platelet activation and apoptosis

DAPT, a potent inhibitor of γ-secretase, was employed to block γ-secretase activity in platelets isolated from wild type mice. This study explored the effects of DAPT on platelet Ca^{2+} signalling, activation and apoptosis.

In order to elucidate whether the treatment of γ-secretase inhibitor DAPT modify the stimulating effect of CRP on platelet Ca^{2+} signalling, a series of experiments were conducted utilizing FACS machine and Fluo-3 fluorescence. As is depicted in Fig.3.2.1A and C, prior to CRP stimulation, the cytosolic Ca^{2+} concentration was similar in DAPT treated platelets and untreated platelets. Following exposure to 2 μg/ml CRP, platelet $[Ca^{2+}]_i$ significantly increased. But the stimulating effect of CRP significantly attenuated after ≥100 seconds stimulation in the presence of DAPT (Fig.3.2.1B, C). Further experiment explored the effect of DAPT on platelet Ca^{2+} signaling following stimulation of CRP at the different concentrations. As is shown in Fig.3.2.1D, the elevation of platelet $[Ca^{2+}]_i$ was significantly blunted after 100 seconds' stimulation with ≥2 μg/ml CRP in the DAPT treated platelets.

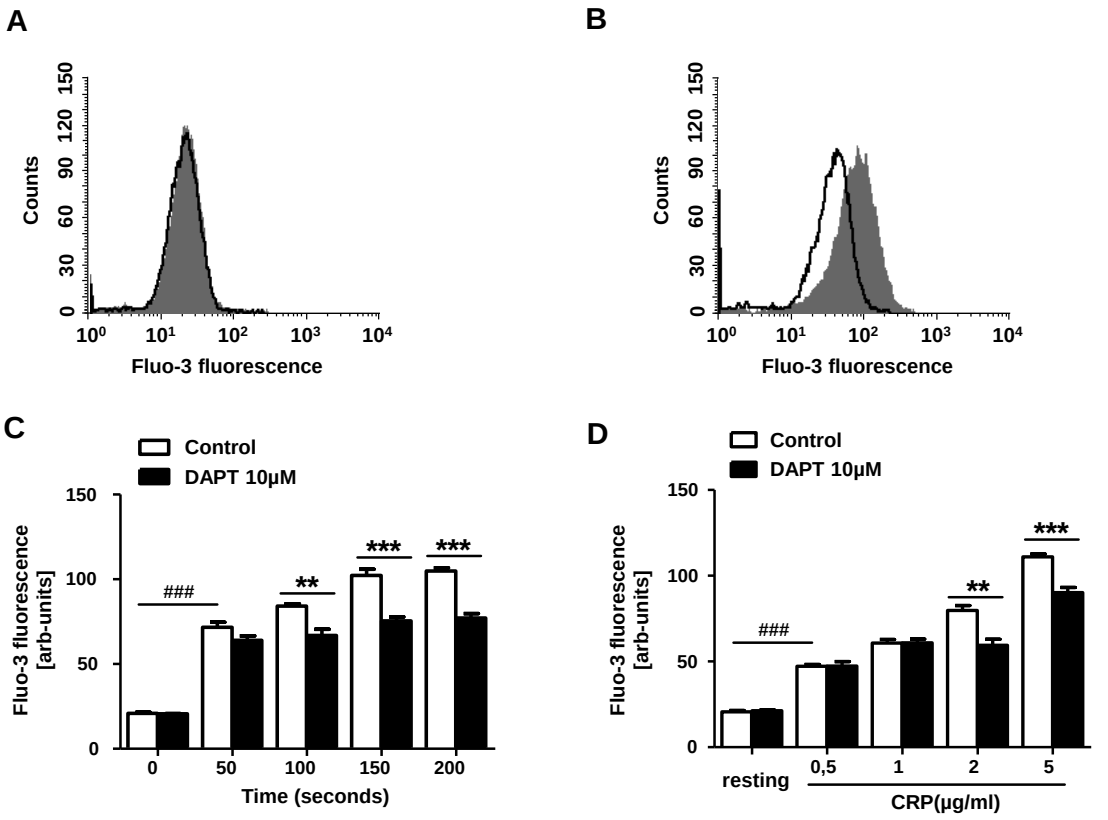

Fig.3.2.1. DAPT sensitive CRP-induced platelet Ca^{2+} response

A,B. Typical histogram of Fluo-3 fluorescence from flow cytometric assay indicated cytosolic Ca^{2+} activity in the control (grey shadows) and DAPT treated (black lines) platelets before stimulation (A) and after (B) a 100 sec exposure to CRP (2 µg/ml).

C,D. Arithmetic mean (AM) ± SEM (n = 4) of fluorescence intensity (arb-units) of activated Fluo-3 reflected (C) the influence of CRP (2 µg/ml) at different stimulation times and (D) the impact of CRP at different concentrations following a 100 seconds stimulation.

White bars: control platelets, black bars: 10 µM DAPT treated platelets.

###(p<0.001) denotes significant increase from CRP stimulation, **(p<0.01) and *** (p<0.001) denotes significant decrease from the treatment of DAPT.(Liu et al. 2016)

In response to CRP stimulation, the elevation of $[Ca^{2+}]_i$ significantly decreased in DAPT treated platelets. This indicated that when γ-secretase activity was inhibited in platelets, store-operated Ca^{2+} entry (SOCE) might also be impaired. Thus, platelet $[Ca^{2+}]_i$ was measured prior to treatment and after a 10 minutes exposure to 1 µM thapsigargin. As is shown in Fig.3.2.2A, following thapsigargin treatment, platelet $[Ca^{2+}]_i$ significantly increased in the absence of extracellular Ca^{2+}, and the effect of γ-secretase inhibitor DAPT was negligible. 5 minutes from

the re-adding of 1 mM $CaCl_2$, platelet $[Ca^{2+}]_i$ further increased, and the effect of thapsigargin was significantly blunted in DAPT treated platelets.

To explore whether Orai1/STIM1 was required for the impaired CRP induced Ca^{2+} response in DAPT treated platelets, Western blot was performed to measure the expression of Orai1 and STIM1 in platelets. As is shown in Fig.3.2.2B and C, the expression of STIM1 was similar before and after CRP stimulation in the absence and presence of DAPT. Fig.3.2.2B and D showed that the expression of Orai1 significantly increased after a 15 minutes treatment with 2 μg/ml CRP treatment. However, the effect of CRP remarkably attenuated in the presence of 10 μM γ-secretase inhibitor DAPT.

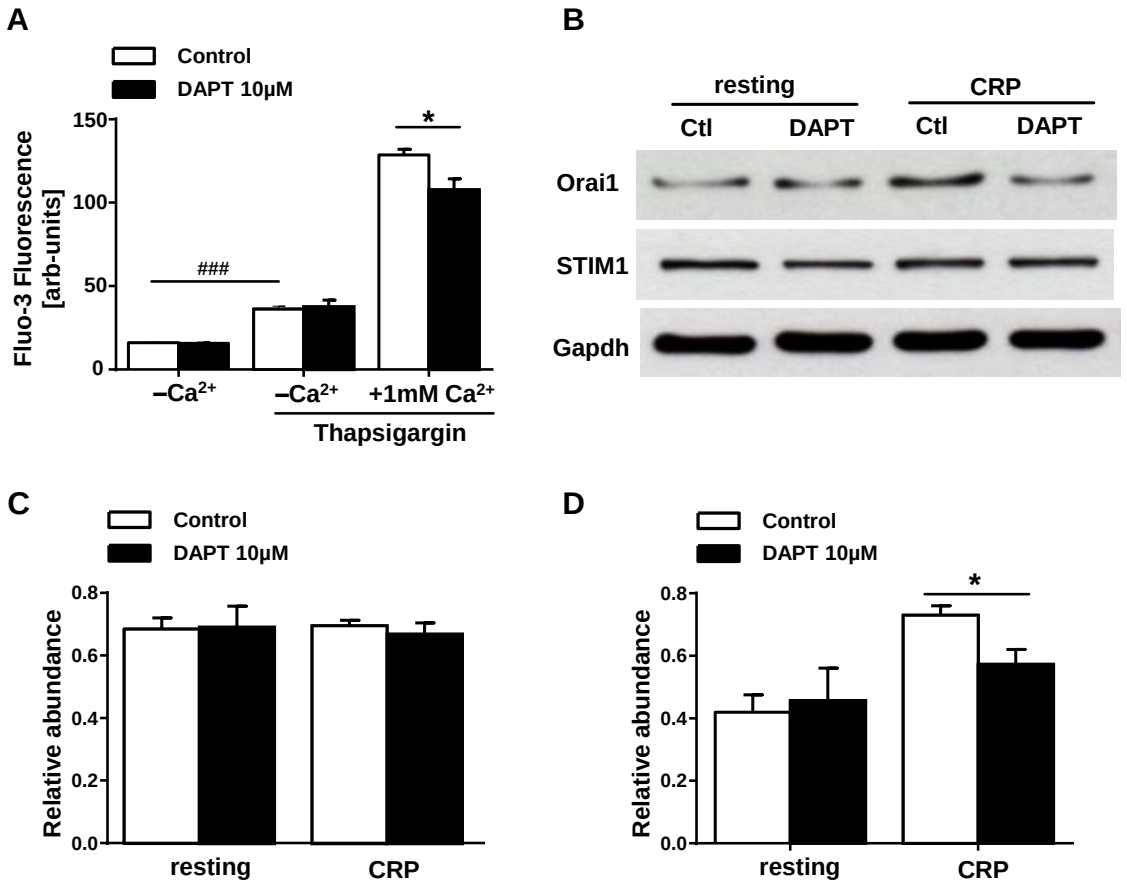

Fig.3.2.2. SOCE and CRP induced Orai1/STIM1 expression in DAPT sensitive platelets

A. Arithmetic mean (AM) ± SEM (n = 4~5) of fluorescence unit (arb-units) of activated Fluo-3 reflected $[Ca^{2+}]_i$ in the control platelets (white bars) and 10μM DAPT treated platelets (black bars). Fluo-3 loaded platelets were incubated in Ca^{2+} free Tyrody buffer (left bars), and then

treated with thapsigargin (1 μM) for 10 min to deplete Ca^{2+} store (middle bars). Following re-addition of 1 mM $CaCl_2$, platelet SOCE was triggered and cytosolic Ca^{2+} concentration reached the maximum after 5 min (right bars).
B. The expression of total Orai1/STIM1 protein before and after exposure to CRP (2μg/ml) for 15 min was analyzed by Western blots in the presence and absence of DAPT.
C,D. Arithmetic mean (AM) ± SEM (n = 4) of STIM1 (C) and Orai1 (D) protein abundance in the control platelets (white bars) and 10 μM DAPT treated platelets (black bars) before and after a 15 min exposure to CRP (2μg/ml).
###($p<0.001$) represents significant increase from thapsigargin treatment, *($p<0.05$) represents significant decrease from DAPT treatment. (unpublished)

The expression of Orai1 protein at the surface of platelet plasma membrane was quantified utilizing fluorescence conjugated antibody and flow cytomerty. As is shown in Fig.3.2.3A and D, the Orai1 abundance at the surface of resting platelets was similar in the absence and presence of DAPT. Upon the stimulation of CRP (2 μg/ml), Orai1 abundance significantly ($p<0.001$) increased in both DAPT treated platelets and untreated platelets. After a 100 seconds treatment, although the stimulating effect of CRP was slightly blunted in 10 μM DAPT treated platelets, it was not significantly different in comparison with the control platelets (Fig.3.2.3B, D). After 15 minutes treatment, the increase of Orai1 protein abundance significantly ($p<0.01$) decreased in DAPT treated platelets (Fig.3.2.3C, D). Fig.3.2.3E showed the impact of DAPT under different concentrations on Orai1 abundance. The expression level of Orai1 protein at the surface of resting platelets was almost the same in the presence of 1~ 20 μM DAPT. The increase of Orai1 abundance following a 100 seconds exposure to 2 μg/ml CRP was also similar in the presence of ≤10 μM DAPT. The stimulating effect of CRP on platelets, however, was significantly ($p<0.05$) blunted in the presence of 20 μM DAPT.

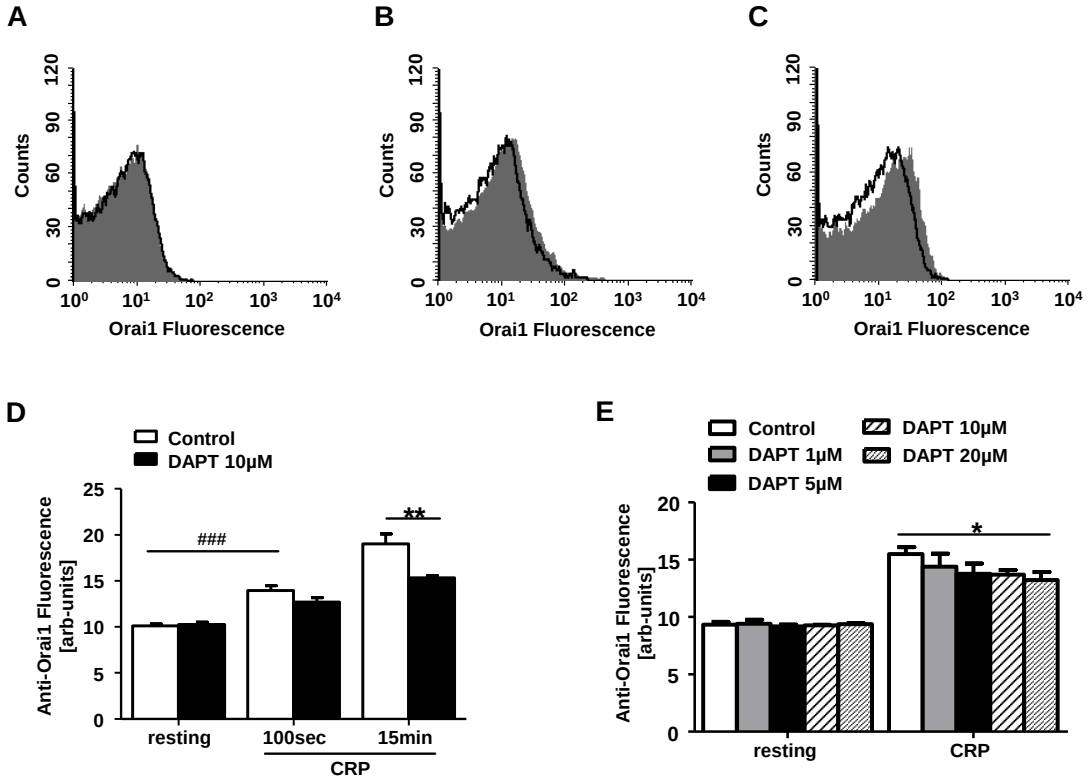

Fig.3.2.3. Orai1 protein abundance at the surface of platelets

A,B,C. Typical histogram overlays of antibody fluorescence from FACS assay reflected Orai1 protein abundance at the platelet surface before (A) and after a (B)100 sec or (C)15 min stimulation with CRP (2 µg/ml). Grey shadows: control platelets, black lines: 10 µM DAPT treated platelets.

D. Arithmetic mean (AM) ± SEM (n = 4) of the fluorescence unit of Orai1 abundance at the surface of platelets before (left bars) and after a (middle bars) 100 sec or (right bars) 15 min stimulation with 2µg/ml CRP. White bars: control platelets, black bars: 10 µM DAPT treated platelets.

E. Arithmetic mean (AM) ± SEM (n = 5) of the fluorescence unit of Orai1 abundance in the control platelets (white bar) and the different concentrations (1, 5, 10 or 20 µM) DAPT treated platelets (filled bar) before (left bars) and after a 100 sec (right bars) stimulation with CRP (2 µg/ml).

###(p<0.001) indicates significant increase from CRP stimulation, *(p<0.05) and ** (p<0.01) represents significant decrease from DAPT treatment. (Liu et al. 2016)

The elevation of $[Ca^{2+}]_i$ lead to platelet degranulation, which is evaluated effectively by detecting the expression level of P-selectin at the platelet surface. In order to study the effect of DAPT on platelet degranulation, P-selectin abundance was detected utilizing flow cytometry and fluorescence labeled

antibody. As is illustrated in Fig.3.2.4A and C, P-selectin abundance at the surface of resting platelets was nearly the same in the absence and presence of 10 μM DAPT. After stimulation with CRP (2 μg/ml), P-selectin abundance significantly ($p<0.001$) increased in DAPT treated and untreated platelets. But the stimulating effect of CRP significantly ($p<0.05$) abated in the presence of DAPT (Fig.3.2.4B, C)

Likewise, the effect of DAPT on platelet activation was evaluated by detecting related-fluorescence of integrin αIIbβ3 antibody. Fig.3.2.4D and F showed the activation of integrin αIIbβ3 in resting platelets was negligible, and there was no remarkable distinction between DAPT treated and untreated platelets. The stimulation of platelets with CRP significantly increased the activation of integrin αIIbβ3. However, the preincubation of DAPT remarkably inhibited the increase of integrin activation (Fig.3.2.4E, F).

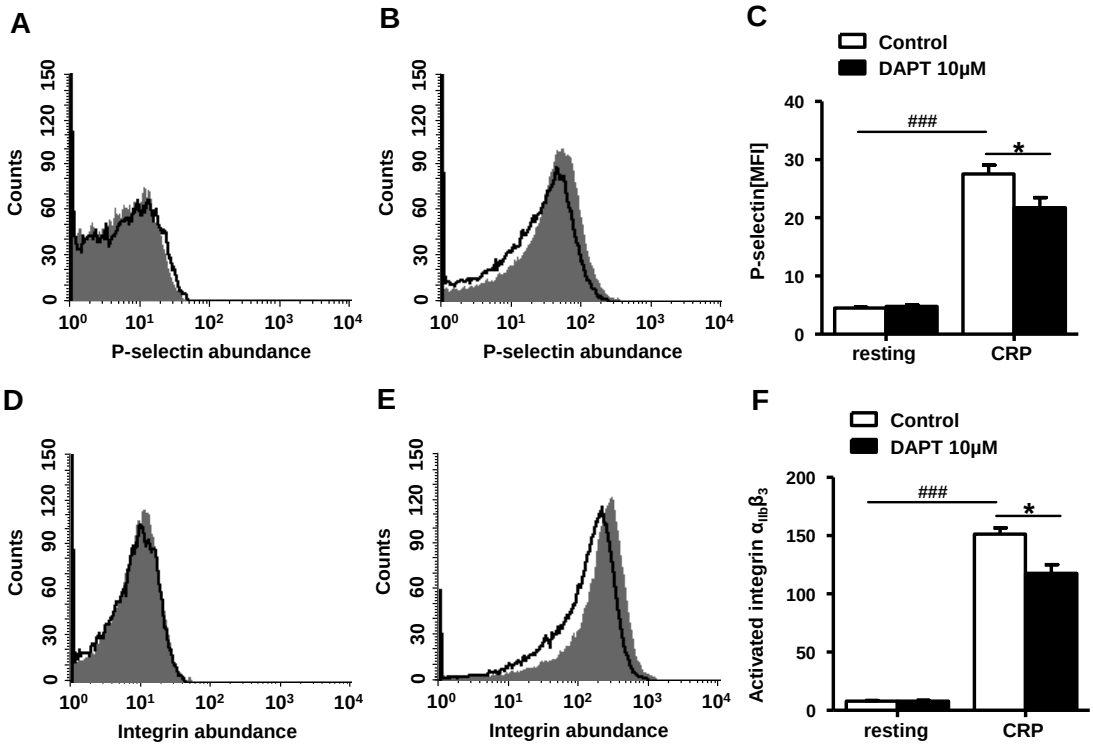

Fig.3.2.4. DAPT sensitive platelet degranulation and integrin αIIbβ3 activation

A,B. Original histogram of fluorescence from FACS assay reflected the abundance of degranulation-dependent P-selectin before (A) and after a (B) 15 min stimulation with 2

µg/ml CRP in platelets. Grey shadows: control platelets, black lines: 10 µM DAPT treated platelets.
C. Arithmetic mean (AM) ± SEM (n = 4) of fluorescence intensity unit of anti-P-selectin antibody in platelets. White bars: control platelets, black bars: 10 µM DAPT treated platelets.
D,E. Typical histogram of fluorescence from FACS assay reflected the activation of integrin αIIbβ3 before(D) and after a (E) 15 minutes stimulation with 2 µg/ml CRP in platelets. Grey shadows: control platelets, black lines: 10 µM DAPT treated platelets.
F. Arithmetic mean (AM) ± SEM (n = 4) of relative fluorescence (arb-units) of the activated integrin αIIbβ3 in platelets. White bars: control platelets, black bars: 10 µM DAPT treated platelets
###(p<0.001) represents significant increase from CRP stimulation, *(p<0.05) represents significant decrease from DAPT treatment. (Liu et al. 2016)

The stimulation of CRP inducted ROS generation by regulating platelet cytosolic Ca^{2+} concentration. Further experiments investigated the effect of γ-secretase inhibitor DAPT on platelet oxidative stress utilizing DCFDA fluorescence. As is revealed by flow cytometry (Fig.3.2.5), following the stimulation of CRP (2 µg/ml), ROS formation gradually increased and reached a steady level after 9 minutes. However, the increase of ROS in DAPT treated platelets was significantly inhibited after 7 minutes stimulation.

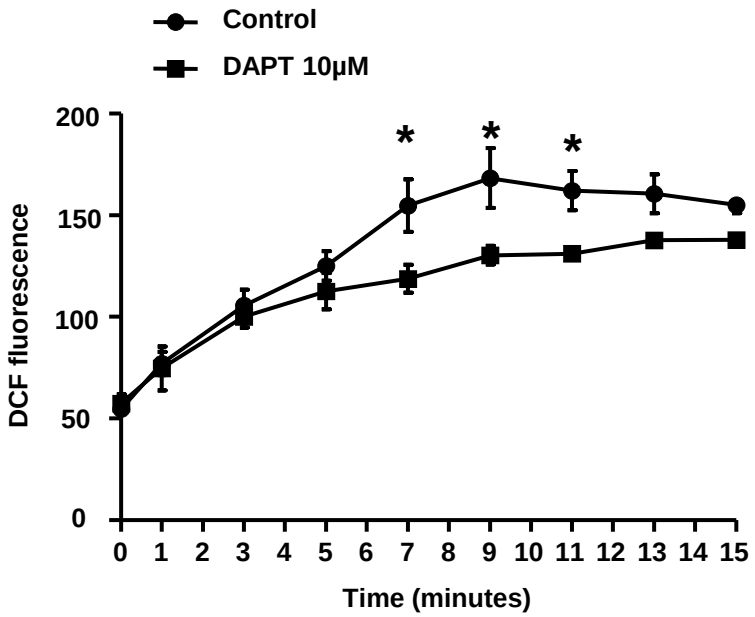

Fig.3.2.5. DAPT sensitive CRP-induced ROS formation
Arithmetic mean (AM) ± SEM (n = 4) of ROS abundance related fluorescence (arb-units) in platelets following 2 µg/ml CRP treatment.

Black circles: control platelets, black square: 10 μM DAPT treated platelets
*(p<0.05) indicates significant decrease in the presence of DAPT. (Liu et al. 2016)

The loss of mitochondrial membrane potential ($\Delta\psi_m$) is a very important marker for apoptosis of various kinds of cells. To further understand the effect of DAPT on platelet apoptosis, $\Delta\psi_m$ was tested following CRP treatment using flow cytometry and cationic dye TMRE (tetramethylrhodamine, ethyl ester perchlorate). As the result, $\Delta\psi_m$ was similar in the resting platelets with and without DAPT treatment (Fig.3.2.6A, C). TMRE fluorescence analysis showed that platelet $\Delta\psi_m$ significantly declined following 5 μg/ml CRP treatment. However, the stimulating effect of CRP again pronouncedly abated in the presence of DAPT (Fig.3.2.6B, C).

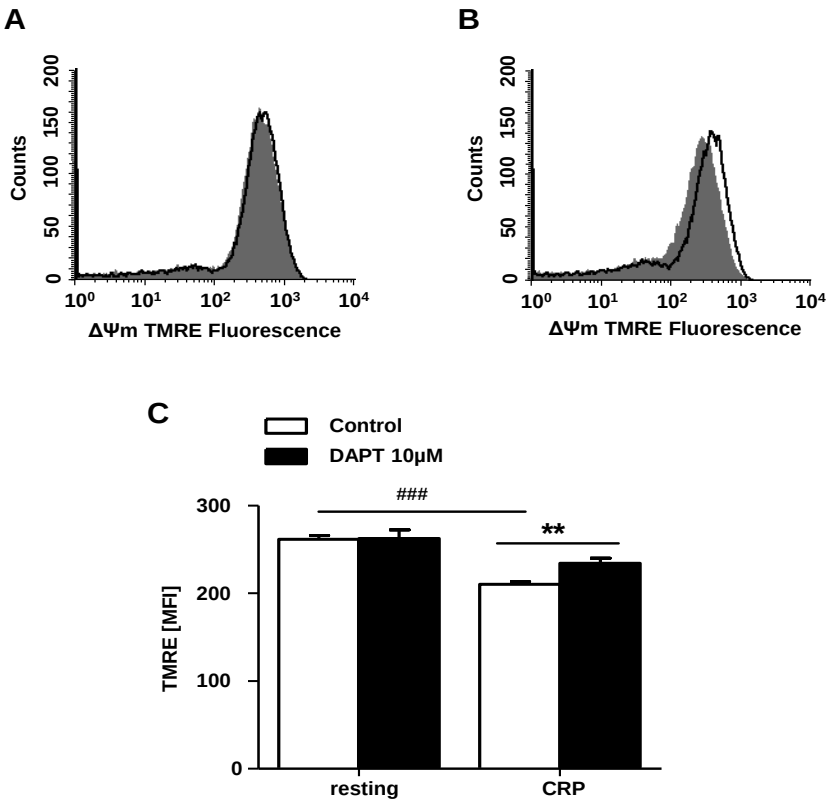

Fig.3.2.6. The effect of DAPT on platelet mitochondrial depolarization

A,B. Original histogram of TMRE fluorescence from FACS assay reflected the loss of platelet mitochondrial membrane potential (Δψm) before (A) and after CRP (5 μg/ml) stimulation (B). Grey shadows: control platelets, black lines: 10 μM DAPT treated platelets.

C. Arithmetic mean (AM) ± SEM (n = 4) of TMRE fluorescence (arb-units) of Δψm before (left bars) and after (right bars) 5µg/ml CRP stimulation in the control (white bars) and DAPT (black bars) treated platelets.
###(p<0.001) represents significant decrease from CRP stimulation, **(p<0.01) represents significant difference from DAPT treatment. (Liu et al. 2016)

Ca^{2+}-dependent phospholipid scrambling contributes to both platelet activation and apoptosis. Thus, a series of experiments were conducted to test the effect of DAPT on platelet PS exposure and cell shrinkage utilizing flow cytometry. As is shown in Fig.3.2.7A and C, the percentage of annexin-V-binding (marked area) was negligible in resting platelets, irrespective of the preincubation of 10 µM DAPT. The stimulation of CRP (5 µg/ml) for 10 minutes significantly enhanced platelet PS exposure. However, the increased percentage of annexin-V-binding was significantly downregulated in the presence of DAPT (Fig.3.2.7B, C).

The shrinkage of platelet volume was evaluated via the analysis of forward scatter. As is illustrated in Fig.3.2.7D and F, the size of resting platelets was similar in the absence and presence of γ-secretase inhibitor DAPT. The exposure to CRP (5 µg/ml) for 10 minutes caused significant platelet shrinkage, but the reduction of platelet volume was again significantly ($p<0.05$) attenuated by DAPT (Fig.3.2.7E, F).

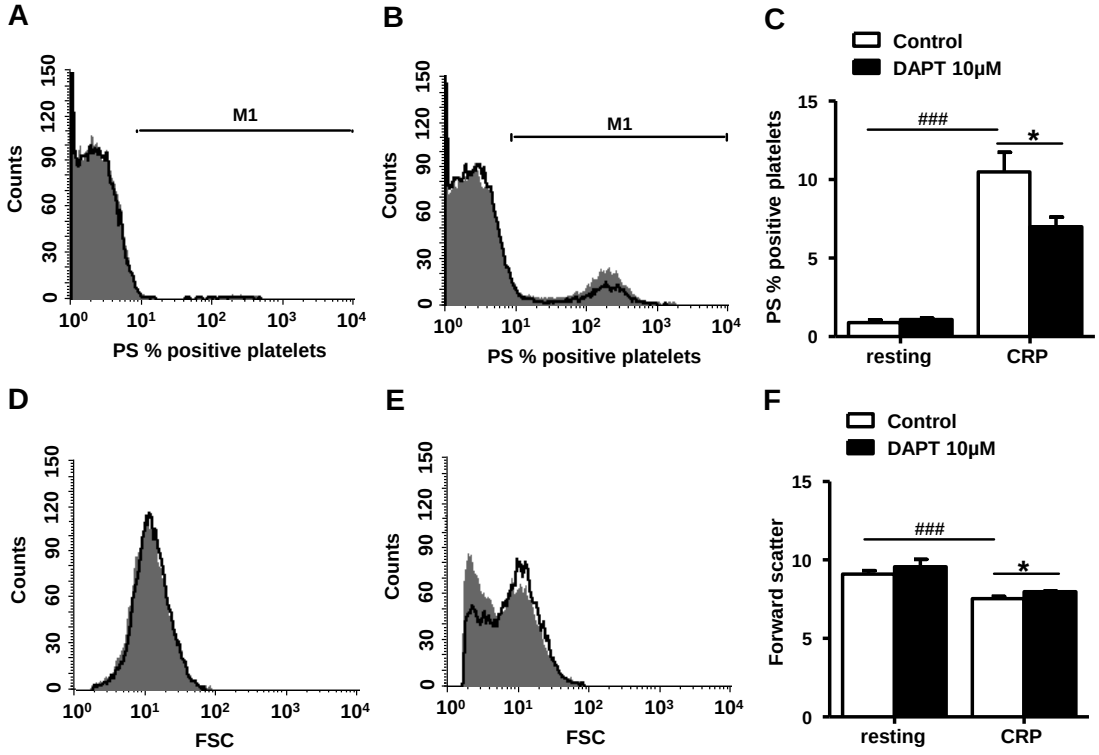

Fig.3.2.7. DAPT sensitive platelet membrane scrambling and forward scatter

A,B. Typical histogram of platelet annexin-V-binding from FACS assay reflected PS exposure before (A) and after (B) a 10 minutes exposure to 5 μg/ml CRP.

Grey shadows: control platelets, black lines: 10 μM DAPT treated platelets.

C. Arithmetic mean (AM) ± SEM (n = 4) of % annexin-V binding (marked area) of the control (white bars) and DAPT (black bars) treated platelets before (left bars) and after (right bars) a 10 min exposure to 5 μg/ml CRP.

D,E. Original histogram of platelet forward scatter from flow cytometric assay reflected shrinkage of cell volume in the resting (D) and following (E) a 10 min exposure to 5 μg/ml CRP.

Grey shadows: control platelets, black lines: 10 μM DAPT treated platelets.

F. Arithmetic mean (AM) ± SEM (n = 4) of light intensity related unit of forward scatter before (left bars) and after (right bars) stimulation with 5 μg/ml CRP for 10 min in the control (white bars) and DAPT (black bars) treated platelets.

###($p<0.001$) indicates significant difference from CRP stimulation, *($p<0.05$) represents significant difference from DAPT treatment. (Liu et al. 2016)

Further experiment was performed to explore the influence of DAPT on platelet aggregation. To this end, platelets were stained with CD9-APC and CD9-PE, and then the fluorescence was detected on FACS machine. As is demonstrated in Fig.3.2.8, the stimulation of CRP (2 μg/ml) led to the rapid aggregation of

platelets, which reached a steady level after 4 minutes. The increased percentage of double-colored events significantly decreased as the result of DAPT treatment.

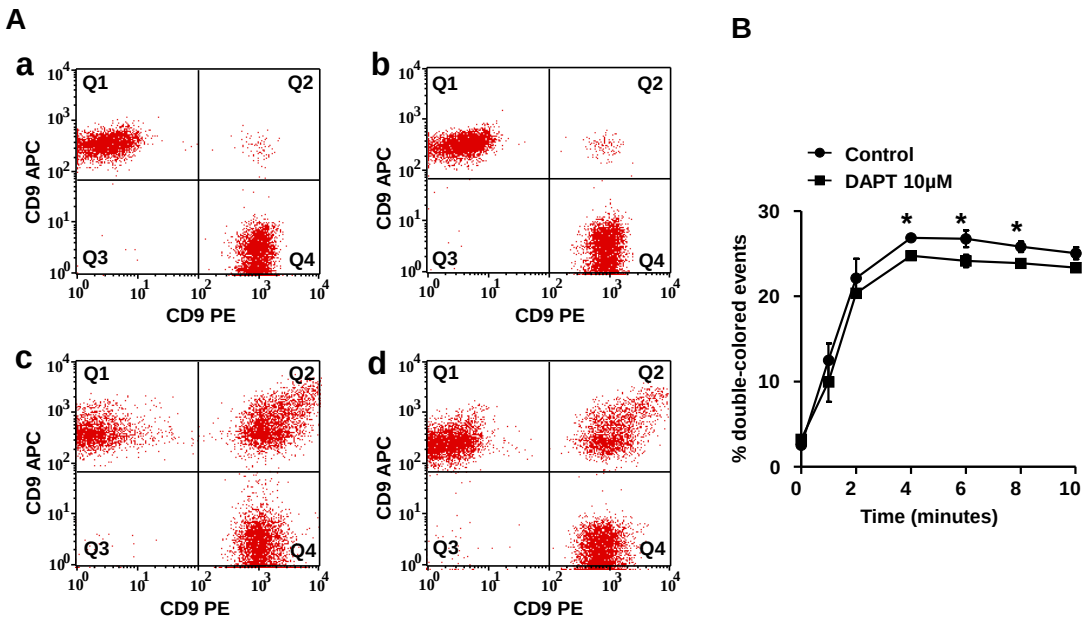

Fig.3.2.8. Activation dependent platelet aggregation in the presence of DAPT

A. Representative dot blots from FACS assay reflected the platelet aggregation of the control group (a, c) and DAPT preincubated group (b, d) in responds to the stimulation of 2 μg/ml CRP in 0 min (a, b) and 4 min (c, d).

B. Arithmetic mean (AM) ± SEM (n = 4) of % double-colored evens (Q2) reflecting platelet aggregation following stimulation with CRP in indicated time point. Black circles: control platelets, black square: DAPT treated platelets.

*($p<0.05$) represents significant decrease from DAPT treatment. (Liu et al. 2016)

To explore whether the impaired platelet activation upon CRP treatment led to the reduce of thrombus formation in the presence of DAPT, further experiments were conducted to test thrombus formation on collagen coated glass surfaces under the condition of high shear rates. As is illustrated in Fig.3.2.9, the thrombus formation slightly decreased in the presence of 10 μM DAPT and 25 μM DAPT. However, the difference between the control group and DAPT treated groups was not statistically significant difference.

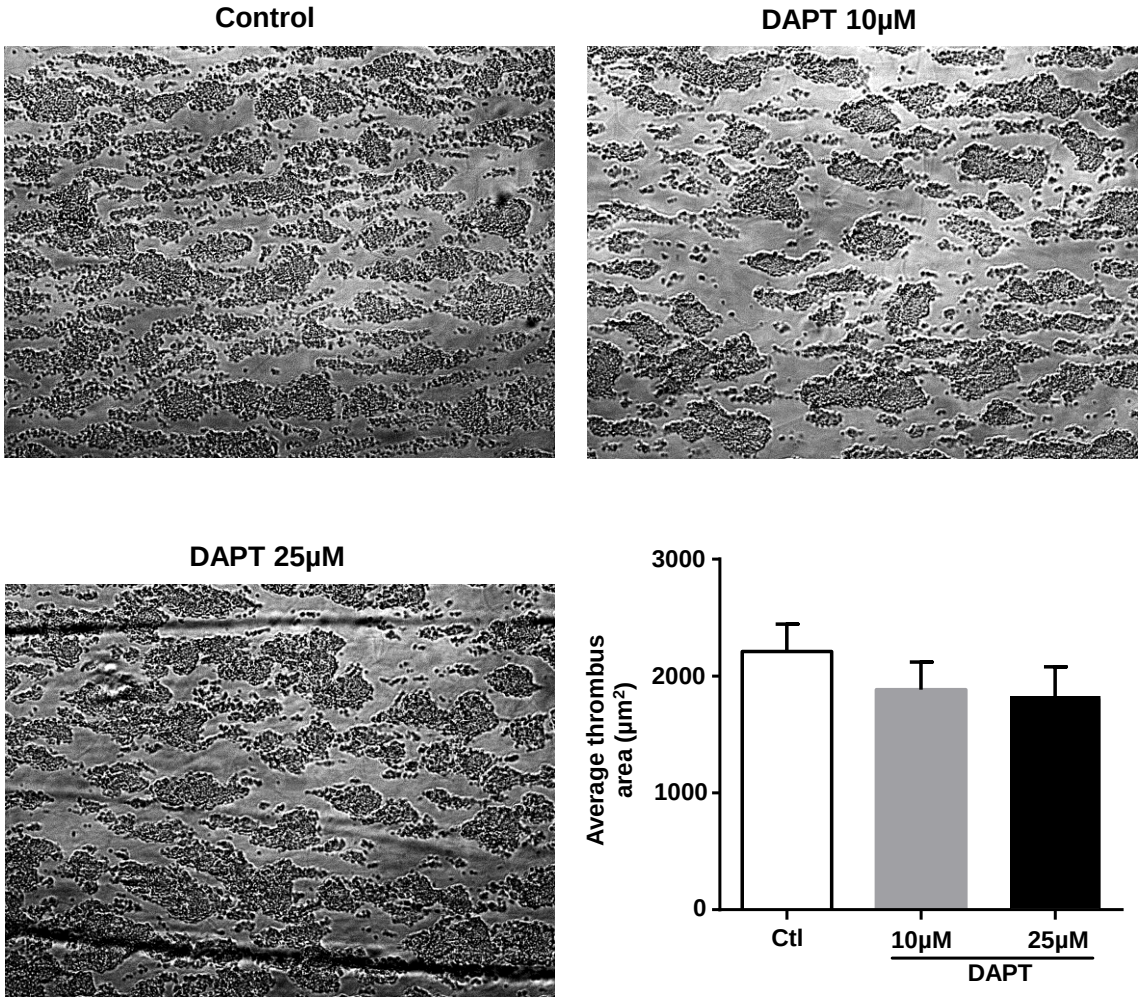

Fig.3.2.9. Platelet thrombus formation with DAPT treatment in vitro

Whole Blood was perfused over a collagen-coated glass surface before (upper left) and after a 30 min pretreatment with 10 µM DAPT (upper right) and 25 µM DAPT (lower left) under the high wall shear rates (1700s^{-1}).

Data shows arithmetic mean (AM) ± SEM (n=5, lower right) of thrombus area. (unpublished)

4. Discussion

It is well known that anucleate platelets participate in a variety of pathophysiological processes including atherosclerosis, thrombosis and hemostasis, while platelet activation is essential for achieving these processes (Harrison 2005). Cytosolic Ca^{2+} plays a vital role in the complex activation mechanism of platelets, which contributes to platelet degranulation, integrin activation, PS exposure and subsequent platelet aggregation as well as thrombus formation (Bergmeier and Stefanini 2009). Besides, the increase of intracellular Ca^{2+} concentration can trigger apoptotic process of platelets and regulate platelet oxidative stress (Rakesh et al. 2014). According to recent researches, the entry of extracellular Ca^{2+} mainly results from Orai1/STIM1 mediated store-operated Ca^{2+} entry (SOCE) in platelets (Lang et al. 2013). This study explored the role of Anoctamin 6 (Ano 6) and γ-secretase in regulating platelet Ca^{2+} signaling, relative platelet activation and apoptosis, which were accomplished respectively by using an Ano 6 deficient mice model and a γ-secretase specific inhibitor DAPT.

4.1 The effect of defective Ano 6 on platelet activation and apoptosis

The membrane protein Ano 6 (Tmem16F) is a member of the Anoctamin protein family, which plays a variety of roles in different cells and was described as Ca^{2+}-regulated nonselective Ca^{2+} permeable cation channel or Ca^{2+}-dependent and a volume-regulated Cl^- channel (Kunzelmann et al. 2014). Defective Ano 6 is strongly associated with Scott syndrome, which is a rare inherited bleeding disorder resulting from impaired platelet phospholipid scrambling and subsequent decreased generation of thrombin (Picollo et al. 2015). The present observations unravel a subtle but remarkable influence of Ano 6 on platelet activation and apoptosis in the wake of thrombin or collagen related peptide (CRP) treatment. Prior to activation, Intracellular Ca^{2+}

concentration ($[Ca^{2+}]_i$), platelet degranulation (P-selectin abundance), reactive oxygen species (ROS), phosphatidylserine (PS) exposure, αIIbβ3 integrin activation, and cell volume were similar in platelets isolated from Ano 6 deficient mice (*ano6*$^{-/-}$) and corresponding wild-type mice (*ano6*$^{+/+}$). The stimulation of thrombin and CRP resulted in the significant increase of $[Ca^{2+}]_i$ and platelet oxidative stress, and triggered integrin αIIbβ3 activation and platelet degranulation. However, the effects of these agonists were less pronounced in *ano6*$^{-/-}$ platelets than in *ano6*$^{+/+}$ platelets. The increase of $[Ca^{2+}]_i$ is a key event during the platelet activation (Varga-Szabo et al. 2011), which further triggers platelet degranulation, adhesion and aggregation, thus supporting the development of thrombosis (Bergmeier and Stefanini 2009). Orai1/STIM1 mediated store-operated Ca^{2+} entry (SOCE) is considered as the primary pathway for agonist induced Ca^{2+} influx (Prakriya and Lewis 2015). However, platelet SOCE was similar in platelets from *ano6*$^{-/-}$ than in *ano6*$^{+/+}$ mice. The increased Orai1 expression after thrombin and CRP stimulation at the surface of plasma membrane and in whole cells was not significantly different between both genotypic platelets. These data indicate that the impaired Ca^{2+} response in Ano 6 deficient platelets does not result from the activation of STIM1 mediated Orai1 channel. According to Viitanen's report (Viitanen et al. 2013), Ano 1, another member of the Anoctamin protein family, functionally coupled with transient receptor potential channel 2 (TRPC2) channel in thyroid cells. TRPC2 is an important Ca^{2+}-permeable cation channel and mediate Ca^{2+} influx in many types of cells (Pedersen et al. 2005). Whether Ano 6 blunting thrombin and CRP evoked Ca^{2+} influx by interacting with other ion channels in platelets calls for further study.

The treatment of thrombin and CRP further led to platelet PS translocation and cell shrinkage, which are key events in apoptosis that limit the life span of circulating platelets (Kile 2014).The stimulation of platelet apoptosis may similarly be secondary to the increase of $[Ca^{2+}]_i$ (Varga-Szabo et al. 2011), which is known to stimulate cell membrane phospholipid scrambling with PS

translocation (Borst et al. 2012), (Mahaut-Smith 2013), (Harper and Poole 2011), (Mushtaq et al. 2011). The present research shows that PS exposure of platelets depends partly on the presence of membrane protein Ano 6. Besides, the agonists (thrombin or CRP) induced platelet shrinkage also relies in part on the activity of Ano 6 protein. It is conceivable that Ano 6 mediates Cl^- exit as a Ca^{2+} dependent Cl^- channel in platelets (Kunzelmann et al. 2014) and thus supports the loss of ions and osmotically obliged water (Lang and Hoffmann 2012).

Upon thrombin and CRP stimulation, the increase of $[Ca^{2+}]_i$ was significantly blunted in platelets from *ano6*$^{-/-}$ mice. It is important to note that the role of Ano6 has been described as a nonselective and Ca^{2+} permeable channel in platelets, which could be relevant to the present results (Jin et al. 2013), (Yang et al. 2012), (Yu et al. 2015). However, It should be pointed out that the defect of phospholipid scrambling in *ano6*$^{-/-}$ platelets was not caused by impaired Ca^{2+} influx through Ano 6 protein (Kunzelmann et al. 2014). It is possible that Ano 6 protein indirectly regulates platelet Ca^{2+} signaling, similar to the case of Ano 1 (Tian et al. 2012).

PS exposure has double effects on platelets. On the one hand, PS exposing platelets can bind to macrophages and then be eliminated through engulfment (Badlou et al. 2006). On the other hand, PS at the platelet surface stimulates blood coagulation and thus contributes to the hemostasis of injured blood vessel (Lhermusier et al. 2011). Besides, PS exposure also stimulates the generation of thrombin and platelet pro-coagulant activity (Harper and Poole 2011), (Mushtaq et al. 2011), (Wolfs et al. 2005), (Mahaut-Smith 2013).

An early clinical study investigated the hemostasis parameters of several Scott patients and the platelet number was normal in the blood of the patients (Toti et al. 1996). According to this research, however, the platelet number was higher in the blood of *ano6*$^{-/-}$ mice than that of *ano6*$^{+/+}$ mice. It is tempting to speculate that the reduced sensitivity of PS translocation to the stimulation of agonists is followed by reduced clearance of PS exposing platelets from circulating blood.

In conclusion, the present study shows that Ano 6 contributes to both platelet activation and apoptosis (Fig 4.1.1). Ano 6 deficiency attenuates the effect of thrombin and CRP on Ca^{2+} influx, integrin activation, platelet degranulation, as well as PS exposure and platelet shrinkage. Thus, Ano 6 is a novel element in the regulation of platelet function and survival.

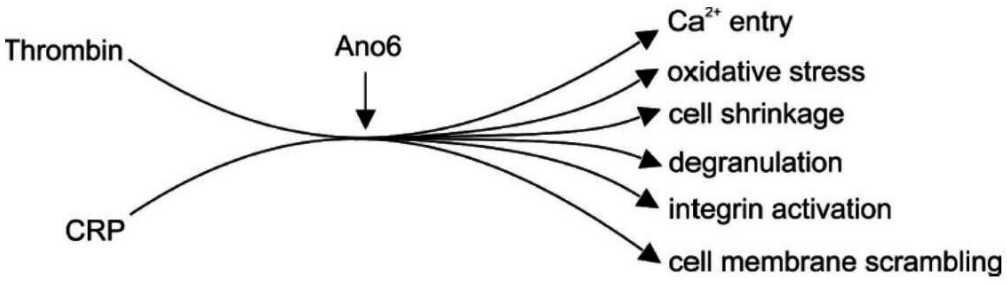

Fig 4.1.1 Synopsis of Ano6 sensitive platelet functions (Liu et al. 2015)

4.2 DAPT sensitive platelet activation and apoptosis

γ-secretase is a complex composed of multiple subunits, which cleaves many type I membrane proteins, such as Notch 1-4, CD44, APP, and so on, as an intramembrane-cleaving proteases (i-CLiPs) in various kinds of cells (Zhang et al. 2014), (Kopan and Ilagan 2004), (Nagano and Saya 2004). DAPT, N-[N-(3,5-difluorophenacetyl)-Lalanyl]-S-phenylglycinet-butyl ester, was reported as a γ-secretase specific inhibitor and wildly used in the related researches of functions and signaling of γ-secretase and its target proteins (Hosaka et al. 2014), (Su et al. 2016), (Sigounas et al. 2017), (Terabe et al. 2016).

The present study uncovers a novel effect of the γ-secretase inhibitor DAPT, i.e. the attenuation of platelet activation in responding to CRP stimulation. Prior to CRP stimulation, the impact of DAPT on the properties of the tested platelet was negligible. In contrast, DAPT treatment significantly weakens the effect of CRP on integrin activation, platelet degranulation, cell membrane scrambling as well as cell shrinkage. PS translocation to the surface of platelet plasma

membrane upon membrane phospholipid scrambling is expected to foster the procoagulant function of platelets, which is a key event in hemostasis (Lhermusier et al. 2011).

According to Terabe's report (Terabe et al. 2016), γ-secretase inhibitor DAPT effectively inhibited the fragmentation of CD44 in bovine articular chondrocytes. The effects of DAPT in platelets could be explained as follows: the inhibition of γ-secretase is expected to enhance the CD44 protein abundance and thus strengthen the inhibitory effects of CD44 on platelet activation and apoptosis (Fig 4.2.1) (Liu et al. 2016).

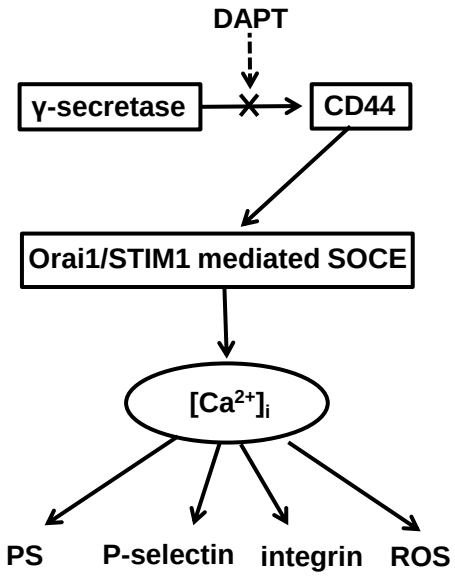

Fig 4.2.1 A potential mechanism of DAPT sensitive platelet activation and apoptosis

Platelet activation, apoptosis and thrombus formation is in large part secondary to the increase of $[Ca^{2+}]_i$ (Lang et al. 2013), and the negative regulations of DAPT on platelet activation and plasma membrane scrambling is paralleled by a significantly attenuated increase of $[Ca^{2+}]_i$. CRP evoked Ca^{2+} influx mainly derived from Orai1/STIM1 mediated SOCE in platelets (Prakriya and Lewis 2015), (Lang et al. 2013). In rat neurons, the expression of mutated presenilin-1 not only inhibited γ-secretase activity, but also caused prolonged

SOCE upon the stimulation of cyclopiazonic acid. Further experiments showed that the neurons treated with γ-secretase inhibitor also displayed slightly prolonged SOCE (Shideman et al. 2009). This study shows that γ-secretase inhibitor DAPT treated platelets display impaired SOCE. Besides, the expression of Orai1 protein with CRP stimulation in the whole cells and at the platelet surface is significantly blunted by DAPT. Correspondingly, platelet SOCE is strengthened in CD44 deficient platelets (Liu et al. 2016). This study enlightens that the effect of DAPT on Ca^{2+} signaling in platelets is likely to be achieved via the γ-secretase/CD44 pathway.

Oxidative stress could be partly due to the increase of $[Ca^{2+}]_i$ upon CRP treatment. This study shows that the treatment of γ-secretase inhibitor DAPT blunts the increase of platelet reactive oxygen species (ROS) formation upon CRP treatment. The oxidative stress of platelets is paralleled by mitochondrial depolarization. Following this thought, CD44 counteracts oxidative stress (Yoshida and Saya 2014) and could thus contribute to or even account for the attenuation of ROS formation by DAPT. However, amyloid-β (Aβ) peptide could be another factor for ROS formation in platelets. It is derived from APP, which is cleaved by γ-secretase (Haass et al. 2012). Gowert's research showed that Aβ stimulation could induce platelet ROS generation in vitro (Gowert et al. 2014).

The increased cytosolic Ca^{2+} triggers platelet activation, which supports the development of arterial thrombosis (Bergmeier and Stefanini 2009). The increase of $[Ca^{2+}]_i$ further leads to platelet phospholipid scrambling with the translocation of PS to the surface of cell plasma membrane (Borst et al. 2012), (Mushtaq et al. 2011). The attenuation of CRP-induced PS exposure may thus be due to the decrease of Ca^{2+} influx in DAPT treated platelets. As is described before, PS exposure at the platelet surface contributes to the formation of clotting factor complex and thus the generation of thrombin, which in turn augments the activation of platelets (Harper and Poole 2011), (Wolfs et al. 2005), (Mushtaq et al. 2011). Besides, the exposed PS is further bound to the

receptors on the surface of macrophages, which leads to platelets' eventual engulfment by macrophages (Badlou et al. 2006). Both platelet activation and apoptosis contribute to the stimulation of platelet aggregation, which is again slightly, but significantly inhibited by γ-secretase inhibitor DAPT.

Following stimulation, platelets release the CD44 activating ligand macrophage migration inhibitory factor (MIF) (Strussmann et al. 2013), which inhibits platelet activation and plasma membrane scrambling as part of an autocrine negative feedback loop. Chatterjee's study shows that MIF effectively limits activation-induced apoptosis of platelets through interaction with CXCR7 (Chatterjee et al. 2014). CD44 contributes to inflammatory disease via MIF signaling, and is deemed as a target for the treatment of such diseases (Sanchez-Nino et al. 2013). To the extent that γ-secretase degrades CD44 via activity of intramembrane-cleaving proteases (McManus et al. 2014), (Nagase et al. 2011), (Nagase and Nakayama 2013), pharmacological inhibition of γ-secretase activity could enhance the negative feedback loop and thus attenuate platelet activation and membrane phospholipid scrambling. Nonetheless, although CD44 participates in the regulation of MIF signaling (Merk et al. 2012), (Sanchez-Nino et al. 2013), and the activation of platelets by several agonists such as CRP is augmented in CD44 deficent platelets (Liu et al. 2016), the observed blunting effect of DAPT on platelet activation and cell membrane scrambling is not necessarily caused by increased CD44 abundance and activity.

In conclusion, the γ-secretase inhibitor DAPT blunts platelet SOCE, the CRP-induced increase of Orai1 expression, cytosolic Ca^{2+} activity, ROS generation, integrin activation, platelet degranulation, the translocation of PS to the platelet surface and cell shrinkage, and thus attenuates platelet activation and apoptosis.

5. Summary

It is well known that Ca^{2+} contributes to various steps of platelet activation and apoptosis. The increased plasma Ca^{2+} mainly derives from store release and Orai1/STIM1 mediated store-operated Ca^{2+} entry (SOCE). This study explores the effects of Anoctamin 6 (Ano 6) and γ-secretase inhibitor DAPT on platelet Ca^{2+} signaling, activation and apoptosis.

Ano 6 was described as a Ca^{2+} activated Cl^- channel in many kinds of cells. Defective Ano 6 underlies Scott syndrome, which is a rare bleeding disorder resulting from impaired platelet phospholipid scrambling. The present study shows that platelet number was remarkably higher in the blood from *ano6*$^{-/-}$ mice than that from *ano6*$^{+/+}$ mice. There was no significant difference in platelet SOCE and Orai1 abundance between the two genotypes. Besides, phosphatidylserine (PS) exposure, ROS abundance, platelet degranulation, integrin αIIbβ3 activation and intracellular Ca^{2+} concentration ($[Ca^{2+}]_i$) were similar in resting platelets from *ano6*$^{+/+}$ mice and *ano6*$^{-/-}$ mice. The stimulation of CRP or thrombin resulted in the significant increase of $[Ca^{2+}]_i$, ROS formation, integrin αIIbβ3 activation and P-selectin abundance, and triggered PS exposure as well as cell shrinkage in both genotypes. However, all effects were significantly attenuated in *ano6*$^{-/-}$ platelets compared with that in ano6$^{+/+}$ platelets. In conclusion, defective Ano 6 attenuates CRP or thrombin induced platelet activation and apoptosis.

DAPT inhibits γ-secretase complex, which cleaves membrane protein CD44, a negative regulator of platelet activation and apoptosis. The present research showed that platelet SOCE was significantly attenuated in the presence of DAPT. In addition, the exposure of platelets to CRP was followed by significant increase of $[Ca^{2+}]_i$, Orai1 abundance, integrin αIIbβ3 activation, platelet degranulation, mitochondrial depolarization, cell shrinkage, annexin-V-binding, ROS formation and aggregation. However, all effects of CRP were inhibited by DAPT. In conclusion, the γ-secretase inhibitor DAPT counteracts the CRP induced platelet activation, apoptosis and aggregation.

6. Zusammenfassung

Es ist wohlbekannt, dass Ca^{2+} vielfältig zu zahlreichen Schritten der Thrombozytenaktivierung und -apoptose beiträgt. Das erhöhte Plasma-Ca^{2+} ist hauptsächlich durch Speicherfreisetzung und Orai1/STIM1-vermittelten speicherabhängigen Ca^{2+}-Einstrom (SOCE) bedingt. Diese Studie untersucht die effekte von Anoctamin 6 (Ano 6) und dem γ-Sekretase-Inhibitor DAPT auf den Ca^{2+}-Signalweg, Aktivierung und Apoptose von Thrombozyten.

Ano 6 wurde in vielen Zellarten als Ca^{2+}-gesteuerter Cl^--Kanal beschrieben. Defektes Ano 6 liegt dem Scott Syndrom, einer seltenen Blutgerinnungsstörung, die aus einer gestörten Umlagerung der Phospholipide an der Thrombozyten-Zellmembran hervorgeht, zugrunde. Die vorliegende Arbeit zeigt, dass die Anzahl der Thrombozyten auffallend höher im Blut von *ano6*$^{-/-}$-Mäusen als von *ano6*$^{+/+}$-Mäusen war. SOCE und Orai1-Menge der Thrombozyten waren in beiden Genotypen nicht signifikant verschieden. Außerdem waren die Phosphatidylserin (PS)-Exposition, ROS-Menge, Plättchendegranulation, Integrin αIIbβ3-Aktivierung und intrazelluläre Ca^{2+}-Konzentration ($[Ca^{2+}]_i$) in ruhenden Thrombozyten von *ano6*$^{+/+}$- and *ano6*$^{-/-}$-Mäusen ähnlich. Die Stimulation durch CRP oder Thrombin erhöhte signifikant die $[Ca^{2+}]_i$, P-Selektin-Menge, Integrin αIIbβ3-Aktivierung und Bildung von ROS und triggerte die PS-Exposition sowie Zellschrumpfung in beiden Genotypen. Jedoch verminderten sich alle Effekte deutlich in *ano6*$^{-/-}$-gegenüber *ano6*$^{+/+}$-Thrombozyten. Schlussfolgernd vermindert defektes Ano 6 die durch CRP oder Thrombin induzierte Aktivierung und Apoptose von Thrombozyten.

DAPT inhibiert den γ-Sekretase-Komplex, welches CD44, einen negativen Regulator der Thrombozytenaktivierung und -apoptose, spaltet. Die vorliegende Arbeit zeigt, dass SOCE in Thrombozyten in Anwesenheit von DAPT signifikant gesenkt wurde. Zusätzlich führte die Exposition der Thrombozyten gegenüber CRP zu einem beachtlichen Zuwachs an $[Ca^{2+}]_i$,

Integrin αIIbβ3-Aktivierung, Thrombozyten-Degranulation, mitochondrialer Depolarisation, Orai1 Menge, ROS-Bildung, Annexin-V-Bindung, Zellschrumpfung und -aggregation. Alle Effekte von CRP wurden jedoch von DAPT inhibiert. Schlussfolgernd wirkt der γ-Sekretase-Inhibitor DAPT einer CRP-induzierten Thrombozytenaktivierung, -apoptose und -aggregation entgegen.

7. Reference

Alansary D, Schmidt B, Dorr K, Bogeski I, Rieger H, Kless A and Niemeyer BA (2016) Thiol dependent intramolecular locking of Orai1 channels. Sci Rep 6: 33347.

Andre P (2004) P-selectin in haemostasis. Br J Haematol 1263: 298-306.

Androutsellis-Theotokis A, Leker RR, Soldner F, Hoeppner DJ, Ravin R, Poser SW, Rueger MA, Bae SK, Kittappa R and McKay RD (2006) Notch signalling regulates stem cell numbers in vitro and in vivo. Nature 4427104: 823-826.

Arachiche A, Kerbiriou-Nabias D, Garcin I, Letellier T and Dachary-Prigent J (2009) Rapid procoagulant phosphatidylserine exposure relies on high cytosolic calcium rather than on mitochondrial depolarization. Arterioscler Thromb Vasc Biol 2911: 1883-1889.

Aslan JE (2017) Platelet Shape Change. 321-336.

Aster RH (1966) Pooling of platelets in the spleen: role in the pathogenesis of "hypersplenic" thrombocytopenia. J Clin Invest 455: 645-657.

Badlou BA, Wu YP, Smid WM and Akkerman JW (2006) Platelet binding and phagocytosis by macrophages. Transfusion 468: 1432-1443.

Baig AA, Haining EJ, Geuss E, Beck S, Swieringa F, Wanitchakool P, Schuhmann MK, Stegner D, Kunzelmann K and Kleinschnitz C (2016) TMEM16F-mediated platelet membrane phospholipid scrambling is critical for hemostasis and thrombosis but not thromboinflammation in mice. Arteriosclerosis, thrombosis, and vascular biology: ATVBAHA. 116.307727.

Banno A and Ginsberg MH (2008) Integrin activation. Biochem Soc Trans 36Pt 2: 229-234.

Bauer M, Retzer M, Wilde JI, Maschberger P, Essler M, Aepfelbacher M, Watson SP and Siess W (1999) Dichotomous regulation of myosin phosphorylation and shape change by Rho-kinase and calcium in intact human platelets. Blood 945: 1665-1672.

Begonja AJ, Gambaryan S, Geiger J, Aktas B, Pozgajova M, Nieswandt B and Walter U (2005) Platelet NAD(P)H-oxidase-generated ROS production regulates alphaIIbbeta3-integrin activation independent of the NO/cGMP pathway. Blood 1068: 2757-2760.

Bergmeier W, Oh-Hora M, McCarl C-A, Roden RC, Bray PF and Feske S (2009) R93W mutation in Orai1 causes impaired calcium influx in platelets. Blood 1133: 675-678.

Bergmeier W and Stefanini L (2009) Novel molecules in calcium signaling in platelets. J Thromb Haemost 7 Suppl 1: 187-190.

Bergmeier W and Stefanini L (2009) Novel molecules in calcium signaling in platelets. J Thromb Haemost 7 Suppl 1: 187-190.

Bergmeier W and Stefanini L (2013) Platelet ITAM signaling. Current opinion in

hematology 205: 445-450.

Berna-Erro A, Galan C, Dionisio N, Gomez LJ, Salido GM and Rosado JA (2012) Capacitative and non-capacitative signaling complexes in human platelets. Biochim Biophys Acta 18238: 1242-1251.

Blair P and Flaumenhaft R (2009) Platelet alpha-granules: basic biology and clinical correlates. Blood Rev 234: 177-189.

Bogeski I, Kummerow C, Al-Ansary D, Schwarz EC, Koehler R, Kozai D, Takahashi N, Peinelt C, Griesemer D, Bozem M, Mori Y, Hoth M and Niemeyer BA (2010) Differential redox regulation of ORAI ion channels: a mechanism to tune cellular calcium signaling. Sci Signal 3115: ra24.

Boisseau P, Bene MC, Besnard T, Pachchek S, Giraud M, Talarmain P, Robillard N, Gourlaouen MA, Bezieau S and Fouassier M (2016) A new mutation of ANO6 in two familial cases of Scott syndrome. Br J Haematol.

Borst O, Munzer P, Gatidis S, Schmidt EM, Schonberger T, Schmid E, Towhid ST, Stellos K, Seizer P, May AE, Lang F and Gawaz M (2012) The inflammatory chemokine CXC motif ligand 16 triggers platelet activation and adhesion via CXC motif receptor 6-dependent phosphatidylinositide 3-kinase/Akt signaling. Circ Res 11110: 1297-1307.

Borst O, Munzer P, Gatidis S, Schmidt EM, Schonberger T, Schmid E, Towhid ST, Stellos K, Seizer P, May AE, Lang F and Gawaz M (2012) The inflammatory chemokine CXC motif ligand 16 triggers platelet activation and adhesion via CXC motif receptor 6-dependent phosphatidylinositide 3-kinase/Akt signaling. Circ Res 11110: 1297-1307.

Borst O, Schmidt EM, Munzer P, Schonberger T, Towhid ST, Elvers M, Leibrock C, Schmid E, Eylenstein A, Kuhl D, May AE, Gawaz M and Lang F (2012) The serum- and glucocorticoid-inducible kinase 1 (SGK1) influences platelet calcium signaling and function by regulation of Orai1 expression in megakaryocytes. Blood 1191: 251-261.

Braun A, Varga-Szabo D, Kleinschnitz C, Pleines I, Bender M, Austinat M, Bosl M, Stoll G and Nieswandt B (2009) Orai1 (CRACM1) is the platelet SOC channel and essential for pathological thrombus formation. Blood 1139: 2056-2063.

Brewer DB (2006) Max Schultze (1865), G. Bizzozero (1882) and the discovery of the platelet. Br J Haematol 1333: 251-258.

Broos K, Feys HB, De Meyer SF, Vanhoorelbeke K and Deckmyn H (2011) Platelets at work in primary hemostasis. Blood Reviews 254: 155-167.

Calaminus SD, Thomas S, McCarty OJ, Machesky LM and Watson SP (2008) Identification of a novel, actin-rich structure, the actin nodule, in the early stages of platelet spreading. J Thromb Haemost 611: 1944-1952.

Caputo A, Caci E, Ferrera L, Pedemonte N, Barsanti C, Sondo E, Pfeffer U, Ravazzolo R, Zegarra-Moran O and Galietta LJ (2008) TMEM16A, a membrane protein associated with calcium-dependent chloride channel activity. Science 3225901: 590-594.

Carrim N, Arthur JF, Hamilton JR, Gardiner EE, Andrews RK, Moran N, Berndt MC and Metharom P (2015) Thrombin-induced reactive oxygen species generation in platelets: A novel role for protease-activated receptor 4 and GPIbalpha. Redox Biol 6: 640-647.

Castoldi E, Collins PW, Williamson PL and Bevers EM (2011) Compound heterozygosity for 2 novel TMEM16F mutations in a patient with Scott syndrome. Blood 11716: 4399-4400.

Chatterjee M, Borst O, Walker B, Fotinos A, Vogel S, Seizer P, Mack A, Alampour-Rajabi S, Rath D, Geisler T, Lang F, Langer HF, Bernhagen J and Gawaz M (2014) Macrophage migration inhibitory factor limits activation-induced apoptosis of platelets via CXCR7-dependent Akt signaling. Circ Res 11511: 939-949.

Chen J, De S, Damron DS, Chen WS, Hay N and Byzova TV (2004) Impaired platelet responses to thrombin and collagen in AKT-1-deficient mice. Blood 1046: 1703-1710.

Cheng KT, Ong HL, Liu X and Ambudkar IS (2013) Contribution and regulation of TRPC channels in store-operated Ca2+ entry. Curr Top Membr 71: 149-179.

Chicka MC, Ren Q, Richards D, Hellman LM, Zhang J, Fried MG and Whiteheart SW (2016) Role of Munc13-4 as a Ca2+-dependent tether during platelet secretion. Biochem J 4735: 627-639.

Choi YH, Gwon AR, Jeong HY, Park JS, Baik SH, Arumugam TV and Jo DG (2010) Contribution of gamma-secretase to calcium-mediated cell death. Neurosci Lett 4693: 425-428.

Chung SH, Polgar J and Reed GL (2000) Protein kinase C phosphorylation of syntaxin 4 in thrombin-activated human platelets. J Biol Chem 27533: 25286-25291.

Cifuni SM, Wagner DD and Bergmeier W (2008) CalDAG-GEFI and protein kinase C represent alternative pathways leading to activation of integrin alphaIIbbeta3 in platelets. Blood 1125: 1696-1703.

Coller BS and Shattil SJ (2008) The GPIIb/IIIa (integrin alphaIIbbeta3) odyssey: a technology-driven saga of a receptor with twists, turns, and even a bend. Blood 1128: 3011-3025.

Coxon CH, Lewis AM, Sadler AJ, Vasudevan SR, Thomas A, Dundas KA, Taylor L, Campbell RD, Gibbins JM, Churchill GC and Tucker KL (2012) NAADP regulates human platelet function. Biochem J 4411: 435-442.

Crittenden JR, Bergmeier W, Zhang Y, Piffath CL, Liang Y, Wagner DD, Housman DE and Graybiel AM (2004) CalDAG-GEFI integrates signaling for platelet aggregation and thrombus formation. Nature medicine 109: 982-986.

De Cuyper IM, Meinders M, van de Vijver E, de Korte D, Porcelijn L, de Haas M, Eble JA, Seeger K, Rutella S, Pagliara D, Kuijpers TW, Verhoeven AJ, van den Berg TK and Gutierrez L (2013) A novel flow cytometry-based platelet aggregation assay. Blood 12110: e70-80.

De Gaetano G (2001) A new blood corpuscle: an impossible interview with Giulio Bizzozero. Thromb Haemost 864: 973-979.

De Strooper B, Iwatsubo T and Wolfe MS (2012) Presenilins and gamma-secretase: structure, function, and role in Alzheimer Disease. Cold Spring Harb Perspect Med 21: a006304.

Dobrydneva Y, Williams RL and Blackmore PF (2010) Diethylstilbestrol and other nonsteroidal estrogens: novel class of store-operated calcium channel modulators. J Cardiovasc Pharmacol 555: 522-530.

Dransfield I, Zagorska A, Lew ED, Michail K and Lemke G (2015) Mer receptor tyrosine kinase mediates both tethering and phagocytosis of apoptotic cells. Cell Death & Disease 6.

Duran C and Hartzell HC (2011) Physiological roles and diseases of Tmem16/Anoctamin proteins: are they all chloride channels? Acta Pharmacol Sin 326: 685-692.

Ehlen HW, Chinenkova M, Moser M, Munter HM, Krause Y, Gross S, Brachvogel B, Wuelling M, Kornak U and Vortkamp A (2013) Inactivation of anoctamin-6/Tmem16f, a regulator of phosphatidylserine scrambling in osteoblasts, leads to decreased mineral deposition in skeletal tissues. J Bone Miner Res 282: 246-259.

Elzagallaai A, Rosé SD and Trifaró J-Ma (2000) Platelet secretion induced by phorbol esters stimulation is mediated through phosphorylation of MARCKS: a MARCKS-derived peptide blocks MARCKS phosphorylation and serotonin release without affecting pleckstrin phosphorylation. Blood 953: 894-902.

Evin G and Li QX (2012) Platelets and Alzheimer's disease: Potential of APP as a biomarker. World J Psychiatry 26: 102-113.

Eyre L and Gamlin F (2010) Haemostasis, blood platelets and coagulation. Anaesthesia & Intensive Care Medicine 116: 244-246.

Falet H (2017). Anatomy of the Platelet Cytoskeleton. Platelets in Thrombotic and Non-Thrombotic Disorders, Springer**:** 139-156.

Falet H, Barkalow KL, Pivniouk VI, Barnes MJ, Geha RS and Hartwig JH (2000) Roles of SLP-76, phosphoinositide 3-kinase, and gelsolin in the platelet shape changes initiated by the collagen receptor GPVI/FcR gamma-chain complex. Blood 9612: 3786-3792.

Flaumenhaft R (2016) SERCAmnavigating calcium signaling in platelets. Blood 1288: 1034-1035.

Flaumenhaft R (2017) Platelet Secretion. 353-366.

Frischauf I, Schindl R, Derler I, Bergsmann J, Fahrner M and Romanin C (2008) The STIM/Orai coupling machinery. Channels (Austin) 24: 261-268.

Fujii T, Sakata A, Nishimura S, Eto K and Nagata S (2015) TMEM16F is required for phosphatidylserine exposure and microparticle release in activated mouse platelets. Proc

Natl Acad Sci U S A 11241: 12800-12805.

Galan C, Zbidi H, Bartegi A, Salido GM and Rosado JA (2009) STIM1, Orai1 and hTRPC1 are important for thrombin- and ADP-induced aggregation in human platelets. Arch Biochem Biophys 4902: 137-144.

Garcia-Martinez MC, Labios M, Hermenegildo C, Tarin JJ, O'Connor E and Cano A (2004) The effect of hormone replacement therapy on Ca2+ mobilization and P-selectin (CD62P) expression in platelets examined under flow cytometry. Blood Coagul Fibrinolysis 151: 1-8.

Ge S, White JG and Haynes CL (2012) Cytoskeletal F-actin, not the circumferential coil of microtubules, regulates platelet dense-body granule secretion. Platelets 234: 259-263.

Gehrmann G, Elbers C and Berninger FS (1972) Pooling and destruction of platelets in the spleen in hypersplenism. Klin Wochenschr 507: 379-382.

George JN (2000) Platelets. The Lancet 3559214: 1531-1539.

Gerrard JM, White JG and Peterson DA (1978) The platelet dense tubular system: its relationship to prostaglandin synthesis and calcium flux. Thromb Haemost 402: 224-231.

Gilio K, Munnix IC, Mangin P, Cosemans JM, Feijge MA, van der Meijden PE, Olieslagers S, Chrzanowska-Wodnicka MB, Lillian R, Schoenwaelder S, Koyasu S, Sage SO, Jackson SP and Heemskerk JW (2009) Non-redundant roles of phosphoinositide 3-kinase isoforms alpha and beta in glycoprotein VI-induced platelet signaling and thrombus formation. J Biol Chem 28449: 33750-33762.

Gilio K, van Kruchten R, Braun A, Berna-Erro A, Feijge MA, Stegner D, van der Meijden PE, Kuijpers MJ, Varga-Szabo D, Heemskerk JW and Nieswandt B (2010) Roles of platelet STIM1 and Orai1 in glycoprotein VI- and thrombin-dependent procoagulant activity and thrombus formation. J Biol Chem 28531: 23629-23638.

Ginsberg MH, Partridge A and Shattil SJ (2005) Integrin regulation. Curr Opin Cell Biol 175: 509-516.

Girish KS, Paul M, Thushara RM, Hemshekhar M, Shanmuga Sundaram M, Rangappa KS and Kemparaju K (2013) Melatonin elevates apoptosis in human platelets via ROS mediated mitochondrial damage. Biochem Biophys Res Commun 4381: 198-204.

Goggs R and Poole AW (2012) Platelet signaling-a primer. J Vet Emerg Crit Care (San Antonio) 221: 5-29.

Gowert NS, Donner L, Chatterjee M, Eisele YS, Towhid ST, Munzer P, Walker B, Ogorek I, Borst O, Grandoch M, Schaller M, Fischer JW, Gawaz M, Weggen S, Lang F, Jucker M and Elvers M (2014) Blood platelets in the progression of Alzheimer's disease. PLoS One 92: e90523.

Gremmel T, Frelinger AL, 3rd and Michelson AD (2016) Platelet Physiology. Semin Thromb Hemost 423: 191-204.

Guidetti GF, Manganaro D, Consonni A, Canobbio I, Balduini C and Torti M (2013) Phosphorylation of the guanine-nucleotide-exchange factor CalDAG-GEFI by protein kinase A regulates Ca(2+)-dependent activation of platelet Rap1b GTPase. Biochem J 4531: 115-123.

Guidetti GF and Torti M (2012) The Small GTPase Rap1b: A Bidirectional Regulator of Platelet Adhesion Receptors. J Signal Transduct 2012: 412089.

Gyulkhandanyan AV, Allen DJ, Mykhaylov S, Lyubimov E, Ni H, Freedman J and Leytin V (2017) Mitochondrial Inner Membrane Depolarization as a Marker of Platelet Apoptosis : Disclosure of Nonapoptotic Membrane Depolarization. Clin Appl Thromb Hemost 232: 139-147.

Gyulkhandanyan AV, Mutlu A, Freedman J and Leytin V (2012) Markers of platelet apoptosis: methodology and applications. J Thromb Thrombolysis 334: 397-411.

Gyulkhandanyan AV, Mutlu A, Freedman J and Leytin V (2013) Selective triggering of platelet apoptosis, platelet activation or both. Br J Haematol 1612: 245-254.

Haass C, Kaether C, Thinakaran G and Sisodia S (2012) Trafficking and proteolytic processing of APP. Cold Spring Harb Perspect Med 25: a006270.

Hakii H, Fujiki H, Suganuma M, Nakayasu M, Tahira T, Sugimura T, Scheuer PJ and Christensen SB (1986) Thapsigargin, a histamine secretagogue, is a non-12-O-tetradecanoylphorbol-13-acetate (TPA) type tumor promoter in two-stage mouse skin carcinogenesis. J Cancer Res Clin Oncol 1113: 177-181.

Han J, Lim CJ, Watanabe N, Soriani A, Ratnikov B, Calderwood DA, Puzon-McLaughlin W, Lafuente EM, Boussiotis VA, Shattil SJ and Ginsberg MH (2006) Reconstructing and deconstructing agonist-induced activation of integrin alphaIIbbeta3. Curr Biol 1618: 1796-1806.

Hankins HM, Baldridge RD, Xu P and Graham TR (2015) Role of flippases, scramblases and transfer proteins in phosphatidylserine subcellular distribution. Traffic 161: 35-47.

Harper AG and Sage SO (2007) A key role for reverse Na+/Ca2+ exchange influenced by the actin cytoskeleton in store-operated Ca2+ entry in human platelets: evidence against the de novo conformational coupling hypothesis. Cell Calcium 426: 606-617.

Harper MT and Poole AW (2010) Diverse functions of protein kinase C isoforms in platelet activation and thrombus formation. J Thromb Haemost 83: 454-462.

Harper MT and Poole AW (2011) Store-operated calcium entry and non-capacitative calcium entry have distinct roles in thrombin-induced calcium signalling in human platelets. Cell Calcium 504: 351-358.

Harrison P (2005) Platelet function analysis. Blood Rev 192: 111-123.

Harrison P and Goodall AH (2008) "Message in the platelet"--more than just vestigial mRNA! Platelets 196: 395-404.

Hoffman M and Monroe DM (2007) Coagulation 2006: a modern view of hemostasis. Hematol Oncol Clin North Am 211: 1-11.

Hoffman M and Monroe DM, 3rd (2001) A cell-based model of hemostasis. Thromb Haemost 856: 958-965.

Hosaka Y, Sugita S, Okada K, Tanaka S, Kawaguchi H and Saito T (2014) γ-secretase inhibitor dapt prevents osteoarthritis progression in mouse experimental model by inhibition of notch signaling. Osteoarthritis and Cartilage 22: S159-S160.

Hou Y, Carrim N, Wang Y, Gallant RC, Marshall A and Ni H (2015) Platelets in hemostasis and thrombosis: Novel mechanisms of fibrinogen-independent platelet aggregation and fibronectin-mediated protein wave of hemostasis. J Biomed Res 29.

Huang Y and Whiteheart SW (2015) Platelet secretion paves the way. Blood 1264: 433-434.

Italiano J (2008) The structure and production of blood platelets. Platelets in Hematolojic and Cardiovasculer Disorders. eBook. Chambridge University 1: 1-21.

Jackson SP (2007) The growing complexity of platelet aggregation. Blood 10912: 5087-5095.

Jackson SP, Nesbitt WS and Kulkarni S (2003) Signaling events underlying thrombus formation. J Thromb Haemost 17: 1602-1612.

Jackson SP and Schoenwaelder SM (2010) Procoagulant platelets: are they necrotic? Blood 11612: 2011-2018.

Jardin I, Gomez LJ, Salido GM and Rosado JA (2009) Dynamic interaction of hTRPC6 with the Orai1-STIM1 complex or hTRPC3 mediates its role in capacitative or non-capacitative Ca2+ entry pathways. Biochemical Journal 420: 267-276.

Jardin I, Lopez JJ, Pariente JA, Salido GM and Rosado JA (2008) Intracellular calcium release from human platelets: different messengers for multiple stores. Trends Cardiovasc Med 182: 57-61.

Jardin I, Lopez JJ, Salido GM and Rosado JA (2008) Orai1 mediates the interaction between STIM1 and hTRPC1 and regulates the mode of activation of hTRPC1-forming Ca2+ channels. Journal of Biological Chemistry 28337: 25296-25304.

Jin X, Shah S, Liu Y, Zhang H, Lees M, Fu Z, Lippiat JD, Beech DJ, Sivaprasadarao A, Baldwin SA, Zhang H and Gamper N (2013) Activation of the Cl- channel ANO1 by localized calcium signals in nociceptive sensory neurons requires coupling with the IP3 receptor. Sci Signal 6290: ra73.

Johansson E, Grassi ES, Pantazopoulou V, Tong B, Lindgren D, Berg TJ, Pietras EJ, Axelson H and Pietras A (2017) CD44 Interacts with HIF-2alpha to Modulate the Hypoxic Phenotype of Perinecrotic and Perivascular Glioma Cells. Cell Rep 207: 1641-1653.

Jones S, Evans RJ and Mahaut-Smith MP (2011) Extracellular Ca2+ modulates

ADP-evoked aggregation through altered agonist degradation: implications for conditions used to study P2Y receptor activation. British Journal of Haematology 1531: 83-91.

Katoh M (2004a) GDD1 is identical to TMEM16E, a member of the TMEM16 family. American journal of human genetics 755: 927-928; author reply 928-929.

Kaushansky K (2008) Historical review: megakaryopoiesis and thrombopoiesis. Blood 1113: 981-986.

Kile BT (2009) The role of the intrinsic apoptosis pathway in platelet life and death. J Thromb Haemost 7 Suppl 1: 214-217.

Kile BT (2014) The role of apoptosis in megakaryocytes and platelets. Br J Haematol 1652: 217-226.

Kimberly WT, LaVoie MJ, Ostaszewski BL, Ye W, Wolfe MS and Selkoe DJ (2003) Gamma-secretase is a membrane protein complex comprised of presenilin, nicastrin, Aph-1, and Pen-2. Proc Natl Acad Sci U S A 10011: 6382-6387.

King SM and Reed GL (2002) Development of platelet secretory granules. Semin Cell Dev Biol 134: 293-302.

Konopatskaya O, Matthews SA, Harper MT, Gilio K, Cosemans JM, Williams CM, Navarro MN, Carter DA, Heemskerk JW, Leitges M, Cantrell D and Poole AW (2011) Protein kinase C mediates platelet secretion and thrombus formation through protein kinase D2. Blood 1182: 416-424.

Kopan R and Ilagan MX (2004) Gamma-secretase: proteasome of the membrane? Nat Rev Mol Cell Biol 56: 499-504.

Koseoglu S, Peters CG, Fitch-Tewfik JL, Aisiku O, Danglot L, Galli T and Flaumenhaft R (2015) VAMP-7 links granule exocytosis to actin reorganization during platelet activation. Blood 1265: 651-660.

Kuchay S, Wieschhaus A, Marinkovic M, Herman I and Chishti A (2012) Targeted gene inactivation reveals a functional role of calpain‐1 in platelet spreading. Journal of Thrombosis and Haemostasis 106: 1120-1132.

Kunzelmann K, Nilius B, Owsianik G, Schreiber R, Ousingsawat J, Sirianant L, Wanitchakool P, Bevers EM and Heemskerk JW (2014) Molecular functions of anoctamin 6 (TMEM16F): a chloride channel, cation channel, or phospholipid scramblase? Pflugers Arch 4663: 407-414.

Lang F, Gawaz M and Borst O (2015) The serum- & glucocorticoid-inducible kinase in the regulation of platelet function. Acta Physiol (Oxf) 2131: 181-190.

Lang F and Hoffmann EK (2012) Role of ion transport in control of apoptotic cell death. Compr Physiol 23: 2037-2061.

Lang F, Munzer P, Gawaz M and Borst O (2013) Regulation of STIM1/Orai1-dependent Ca2+ signalling in platelets. Thromb Haemost 1105: 925-930.

Lang F and Shumilina E (2013) Regulation of ion channels by the serum- and glucocorticoid-inducible kinase SGK1. FASEB J 271: 3-12.

Lefort CT, Rossaint J, Moser M, Petrich BG, Zarbock A, Monkley SJ, Critchley DR, Ginsberg MH, Fassler R and Ley K (2012) Distinct roles for talin-1 and kindlin-3 in LFA-1 extension and affinity regulation. Blood 11918: 4275-4282.

Lentz BR (2003) Exposure of platelet membrane phosphatidylserine regulates blood coagulation. Prog Lipid Res 425: 423-438.

Leytin V (2012) Apoptosis in the anucleate platelet. Blood Rev 262: 51-63.

Leytin V, Allen DJ, Lyubimov E and Freedman J (2007) Higher thrombin concentrations are required to induce platelet apoptosis than to induce platelet activation. Br J Haematol 1365: 762-764.

Leytin V, Allen DJ, Mykhaylov S, Mis L, Lyubimov EV, Garvey B and Freedman J (2004) Pathologic high shear stress induces apoptosis events in human platelets. Biochem Biophys Res Commun 3202: 303-310.

Lhermusier T, Chap H and Payrastre B (2011) Platelet membrane phospholipid asymmetry: from the characterization of a scramblase activity to the identification of an essential protein mutated in Scott syndrome. Journal of Thrombosis and Haemostasis 910: 1883-1891.

Lhermusier T, Chap H and Payrastre B (2011) Platelet membrane phospholipid asymmetry: from the characterization of a scramblase activity to the identification of an essential protein mutated in Scott syndrome. J Thromb Haemost 910: 1883-1891.

Li S, Wang Z, Liao Y, Zhang W, Shi Q, Yan R, Ruan C and Dai K (2010) The glycoprotein Ibalpha-von Willebrand factor interaction induces platelet apoptosis. J Thromb Haemost 82: 341-350.

Li Z, Delaney MK, O'Brien KA and Du X (2010) Signaling during platelet adhesion and activation. Arterioscler Thromb Vasc Biol 3012: 2341-2349.

Lian L, Wang Y, Draznin J, Eslin D, Bennett JS, Poncz M, Wu D and Abrams CS (2005) The relative role of PLCbeta and PI3Kgamma in platelet activation. Blood 1061: 110-117.

Lin KH, Chang HC, Lu WJ, Jayakumar T, Chou HC, Fong TH, Hsiao G and Sheu JR (2009) Comparison of the relative activities of inducing platelet apoptosis stimulated by various platelet-activating agents. Platelets 208: 575-581.

Liu G, Liu G, Alzoubi K, Chatterjee M, Walker B, Munzer P, Luo D, Umbach AT, Elvira B, Chen H, Voelkl J, Foller M, Mak TW, Borst O, Gawaz M and Lang F (2016) CD44 sensitivity of platelet activation, membrane scrambling and adhesion under high arterial shear rates. Thromb Haemost 1151: 99-108.

Liu G, Liu G, Chatterjee M, Umbach AT, Chen H, Gawaz M and Lang F (2016) Influence of gamma-Secretase Inhibitor 24-Diamino-5-Phenylthiazole DAPT on Platelet Activation. Cell Physiol Biochem 382: 726-736.

Liu G, Liu G, Chen H, Borst O, Gawaz M, Vortkamp A, Schreiber R, Kunzelmann K and Lang F (2015) Involvement of Ca2+ Activated Cl- Channel Ano6 in Platelet Activation and Apoptosis. Cell Physiol Biochem 375: 1934-1944.

Loiko EN, Samal AB and Shulyakovskaya SM (2003) H2O2-induced platelet aggregation and increase in intracellular Ca2+ concentration are blocked by inhibitors of intracellular signaling. Biochemistry (Mosc) 6811: 1210-1216.

Lopez JJ, Salido GM, Gomez-Arteta E, Rosado JA and Pariente JA (2007) Thrombin induces apoptotic events through the generation of reactive oxygen species in human platelets. Journal of Thrombosis and Haemostasis 56: 1283-1291.

Lopez JJ, Salido GM, Pariente JA and Rosado JA (2008) Thrombin induces activation and translocation of Bid, Bax and Bak to the mitochondria in human platelets. J Thromb Haemost 610: 1780-1788.

Mahaut-Smith MP (2013) A role for platelet TRPC channels in the Ca2+ response that induces procoagulant activity. Sci Signal 6281: pe23.

Mahaut-Smith MP (2013) A role for platelet TRPC channels in the Ca2+ response that induces procoagulant activity. Sci. Signal. 6281: pe23-pe23.

Mahaut-Smith MP, Jones S and Evans RJ (2011) The P2X1 receptor and platelet function. Purinergic Signal 73: 341-356.

McManus MM, Weiss KR and Hughes DP (2014) Understanding the role of Notch in osteosarcoma. Adv Exp Med Biol 804: 67-92.

Merk M, Mitchell RA, Endres S and Bucala R (2012) D-dopachrome tautomerase (D-DT or MIF-2): doubling the MIF cytokine family. Cytokine 591: 10-17.

Merten M and Thiagarajan P (2004) P-selectin in arterial thrombosis. Z Kardiol 9311: 855-863.

Mirinics ZK, Calafat J, Udby L, Lovelock J, Kjeldsen L, Rothermund K, Sisodia SS, Borregaard N and Corey SJ (2002) Identification of the presenilins in hematopoietic cells with localization of presenilin 1 to neutrophil and platelet granules. Blood Cells Mol Dis 281: 28-38.

Mittal K and Kaur R (2015) Platelet storage lesion: An update. Asian J Transfus Sci 91: 1-3.

Monroe DM (2002) Platelets and Thrombin Generation. Arteriosclerosis, Thrombosis, and Vascular Biology 229: 1381-1389.

Morimoto T, Ogihara S and Takisawa H (1990) Anchorage of secretion-competent dense granules on the plasma membrane of bovine platelets in the absence of secretory stimulation. J Cell Biol 1111: 79-86.

Morohashi Y, Kan T, Tominari Y, Fuwa H, Okamura Y, Watanabe N, Sato C, Natsugari H, Fukuyama T, Iwatsubo T and Tomita T (2006) C-terminal fragment of presenilin is the

molecular target of a dipeptidic gamma-secretase-specific inhibitor DAPT (N-[N-(3,5-difluorophenacetyl)-L-alanyl]-S-phenylglycine t-butyl ester). J Biol Chem 28121: 14670-14676.

Munzer P, Tolios A, Pelzl L, Schmid E, Schmidt EM, Walker B, Frohlich H, Borst O, Gawaz M and Lang F (2013) Thrombin-sensitive expression of the store operated Ca(2+) channel Orai1 in platelets. Biochem Biophys Res Commun 4361: 25-30.

Mushtaq M, Nam TS and Kim UH (2011) Critical role for CD38-mediated Ca2+ signaling in thrombin-induced procoagulant activity of mouse platelets and hemostasis. J Biol Chem 28615: 12952-12958.

Nagano O and Saya H (2004) Mechanism and biological significance of CD44 cleavage. Cancer Sci 9512: 930-935.

Nagase H, Koh C-S and Nakayama K (2011) γ-Secretase-regulated signaling pathways, such as notch signaling, mediate the differentiation of hematopoietic stem cells, development of the immune system, and peripheral immune responses. Current stem cell research & therapy 62: 131-141.

Nagase H and Nakayama K (2013) γ-Secretase-regulated signaling typified by Notch signaling in the immune system. Current stem cell research & therapy 85: 341-356.

Ngo JC, Huang M, Roth DA, Furie BC and Furie B (2008) Crystal structure of human factor VIII: implications for the formation of the factor IXa-factor VIIIa complex. Structure 164: 597-606.

Ni H and Freedman J (2003) Platelets in hemostasis and thrombosis: role of integrins and their ligands. Transfus Apher Sci 283: 257-264.

Nurden AT (2014) Platelet membrane glycoproteins: a historical review. Semin Thromb Hemost 405: 577-584.

Offermanns S (2006) Activation of platelet function through G protein-coupled receptors. Circ Res 9912: 1293-1304.

Ogawa A, Firth AL, Smith KA, Maliakal MV and Yuan JX (2012) PDGF enhances store-operated Ca2+ entry by upregulating STIM1/Orai1 via activation of Akt/mTOR in human pulmonary arterial smooth muscle cells. Am J Physiol Cell Physiol 3022: C405-411.

Ohkubo YZ and Tajkhorshid E (2008) Distinct structural and adhesive roles of Ca2+ in membrane binding of blood coagulation factors. Structure 161: 72-81.

Okamoto I, Kawano Y, Murakami D, Sasayama T, Araki N, Miki T, Wong AJ and Saya H (2001) Proteolytic release of CD44 intracellular domain and its role in the CD44 signaling pathway. J Cell Biol 1555: 755-762.

Pedemonte N and Galietta LJ (2014) Structure and function of TMEM16 proteins (anoctamins). Physiol Rev 942: 419-459.

Pedersen SF, Owsianik G and Nilius B (2005) TRP channels: an overview. Cell Calcium 383-4: 233-252.

Picollo A, Malvezzi M and Accardi A (2015) TMEM16 proteins: unknown structure and confusing functions. J Mol Biol 4271: 94-105.

Polgar J, Lane WS, Chung SH, Houng AK and Reed GL (2003) Phosphorylation of SNAP-23 in activated human platelets. J Biol Chem 27845: 44369-44376.

Prakriya M and Lewis RS (2015) Store-Operated Calcium Channels. Physiol Rev 954: 1383-1436.

Putney JW, Jr. (1986) A model for receptor-regulated calcium entry. Cell Calcium 71: 1-12.

Rakesh KS, Jagadish S, Vinayaka AC, Hemshekhar M, Paul M, Thushara RM, Sundaram MS, Swaroop TR, Mohan CD, Basappa, Sadashiva MP, Kemparaju K, Girish KS and Rangappa KS (2014) A new ibuprofen derivative inhibits platelet aggregation and ROS mediated platelet apoptosis. PLoS One 99: e107182.

Redondo PC, Salido GM, Rosado JA and Pariente JA (2004) Effect of hydrogen peroxide on Ca2+ mobilisation in human platelets through sulphydryl oxidation dependent and independent mechanisms. Biochem Pharmacol 673: 491-502.

Reed GL (2004) Platelet secretory mechanisms. Semin Thromb Hemost 304: 441-450.

Rendu F and Brohard-Bohn B (2001) The platelet release reaction: granules' constituents, secretion and functions. Platelets 125: 261-273.

Roberts HL, Schneider BL and Brown DR (2017) alpha-Synuclein increases beta-amyloid secretion by promoting beta-/gamma-secretase processing of APP. PLoS One 122: e0171925.

Rosado JA (2011) Acidic Ca(2+) stores in platelets. Cell Calcium 502: 168-174.

Rosado JA, Brownlow SL and Sage SO (2002) Endogenously expressed Trp1 is involved in store-mediated Ca2+ entry by conformational coupling in human platelets. Journal of Biological Chemistry 27744: 42157-42163.

Rosado JA, Redondo PC, Salido GM, Gomez-Arteta E, Sage SO and Pariente JA (2004) Hydrogen peroxide generation induces pp60(src) activation in human platelets - Evidence for the involvement of this pathway in store-mediated calcium entry. Journal of Biological Chemistry 2793: 1665-1675.

Rosing J, Bevers EM, Comfurius P, Hemker HC, van Dieijen G, Weiss HJ and Zwaal RF (1985) Impaired factor X and prothrombin activation associated with decreased phospholipid exposure in platelets from a patient with a bleeding disorder. Blood 656: 1557-1561.

Rowley JW, Schwertz H and Weyrich AS (2012) Platelet mRNA: the meaning behind the message. Curr Opin Hematol 195: 385-391.

Sabrkhany S, Griffioen AW and Oude Egbrink MG (2011) The role of blood platelets in

tumor angiogenesis. Biochim Biophys Acta 18152: 189-196.

Sage SO, Brownlow SL and Rosado JA (2002) TRP channels and calcium entry in human platelets. Blood 10012: 4245-4246; author reply 4246-4247.

Sanchez-Nino MD, Sanz AB, Ruiz-Andres O, Poveda J, Izquierdo MC, Selgas R, Egido J and Ortiz A (2013) MIF, CD74 and other partners in kidney disease: tales of a promiscuous couple. Cytokine Growth Factor Rev 241: 23-40.

Sargeant P, Clarkson WD, Sage SO and Heemskerk JW (1992) Calcium influx evoked by Ca2+ store depletion in human platelets is more susceptible to cytochrome P-450 inhibitors than receptor-mediated calcium entry. Cell Calcium 139: 553-564.

Satta N, Toti F, Fressinaud E, Meyer D and Freyssinet JM (1997) Scott syndrome: an inherited defect of the procoagulant activity of platelets. Platelets 82-3: 117-124.

Schraw TD, Lemons PP, Dean WL and Whiteheart SW (2003) A role for Sec1/Munc18 proteins in platelet exocytosis. Biochem J 374Pt 1: 207-217.

Schroeder BC, Cheng T, Jan YN and Jan LY (2008) Expression cloning of TMEM16A as a calcium-activated chloride channel subunit. Cell 1346: 1019-1029.

Shideman CR, Reinardy JL and Thayer SA (2009) gamma-Secretase activity modulates store-operated Ca2+ entry into rat sensory neurons. Neurosci Lett 4512: 124-128.

Shirakawa R, Higashi T, Tabuchi A, Yoshioka A, Nishioka H, Fukuda M, Kita T and Horiuchi H (2004) Munc13-4 is a GTP-Rab27-binding protein regulating dense core granule secretion in platelets. J Biol Chem 27911: 10730-10737.

Shrivastava M (2009) The platelet storage lesion. Transfus Apher Sci 412: 105-113.

Sigma-Aldrich (PubChem Substance ID 24893987). from http://www.sigmaaldrich.com/catalog/product/sigma/d5942?lang=de&region=DE&gclid=EAIaIQobChMIxevNxeHX1gIVuDLTCh2MjgRqEAAYASAAEgJXpPD_BwE.

Sigounas G, Bertrand FE, Weidner DA, Vinson KE, Clark AG and Khan A (2017) Notch-1 promotes a mesenchymal phenotype in colon cancer cells via Notch-3 and Smad-3 activation, AACR.

Smyth SS, McEver RP, Weyrich AS, Morrell CN, Hoffman MR, Arepally GM, French PA, Dauerman HL, Becker RC and Platelet Colloquium P (2009) Platelet functions beyond hemostasis. J Thromb Haemost 711: 1759-1766.

Stegner D and Nieswandt B (2011) Platelet receptor signaling in thrombus formation. J Mol Med (Berl) 892: 109-121.

Strussmann T, Tillmann S, Wirtz T, Bucala R, von Hundelshausen P and Bernhagen J (2013) Platelets are a previously unrecognised source of MIF. Thromb Haemost 1105: 1004-1013.

Su F, Zhu S, Ruan J, Muftuoglu Y, Zhang L and Yuan Q (2016) Combination therapy of RY10-4 with the γ-secretase inhibitor DAPT shows promise in treating HER2-amplified

breast cancer. Oncotarget 74: 4142.

Subramanian H, Zahedi RP, Sickmann A, Walter U and Gambaryan S (2013) Phosphorylation of CalDAG-GEFI by protein kinase A prevents Rap1b activation. J Thromb Haemost 118: 1574-1582.

Sugahara KN, Murai T, Nishinakamura H, Kawashima H, Saya H and Miyasaka M (2003) Hyaluronan oligosaccharides induce CD44 cleavage and promote cell migration in CD44-expressing tumor cells. J Biol Chem 27834: 32259-32265.

Sun L, Zhao L, Yang G, Yan C, Zhou R, Zhou X, Xie T, Zhao Y, Wu S, Li X and Shi Y (2015) Structural basis of human gamma-secretase assembly. Proc Natl Acad Sci U S A 11219: 6003-6008.

Suzuki J, Denning DP, Imanishi E, Horvitz HR and Nagata S (2013) Xk-related protein 8 and CED-8 promote phosphatidylserine exposure in apoptotic cells. Science 3416144: 403-406.

Suzuki J, Imanishi E and Nagata S (2016) Xkr8 phospholipid scrambling complex in apoptotic phosphatidylserine exposure. Proc Natl Acad Sci U S A 11334: 9509-9514.

Suzuki J, Umeda M, Sims PJ and Nagata S (2010) Calcium-dependent phospholipid scrambling by TMEM16F. Nature 4687325: 834-838.

Sveshnikova AN, Ataullakhanov FI and Panteleev MA (2015) Compartmentalized calcium signaling triggers subpopulation formation upon platelet activation through PAR1. Mol Biosyst 114: 1052-1060.

Terabe K, Takahashi N, Takemoto T, Knudson W, Ishiguro N and Kojima T (2016) Simvastatin inhibits CD44 fragmentation in chondrocytes. Arch Biochem Biophys 604: 1-10.

Terabe K, Takahashi N, Takemoto T, Knudson W, Ishiguro N and Kojima T (2016) Simvastatin inhibits CD44 fragmentation in chondrocytes. Archives of biochemistry and biophysics 604: 1-10.

Thushara RM, Hemshekhar M, Basappa, Kemparaju K, Rangappa KS and Girish KS (2015) Biologicals, platelet apoptosis and human diseases: An outlook. Crit Rev Oncol Hematol 933: 149-158.

Tian Y, Schreiber R and Kunzelmann K (2012) Anoctamins are a family of Ca2+-activated Cl- channels. J Cell Sci 125Pt 21: 4991-4998.

Toda S, Hanayama R and Nagata S (2012) Two-step engulfment of apoptotic cells. Mol Cell Biol 321: 118-125.

Tonon G, Luo X, Greco NJ, Chen W, Shi Y and Jamieson GA (2002) Weak platelet agonists and U46619 induce apoptosis-like events in platelets, in the absence of phosphatidylserine exposure. Thrombosis Research 1076: 345-350.

Toti F, Satta N, Fressinaud E, Meyer D and Freyssinet JM (1996) Scott syndrome,

characterized by impaired transmembrane migration of procoagulant phosphatidylserine and hemorrhagic complications, is an inherited disorder. Blood 874: 1409-1415.

Towhid ST, Schmidt EM, Schmid E, Munzer P, Qadri SM, Borst O and Lang F (2011) Thymoquinone-induced platelet apoptosis. J Cell Biochem 11211: 3112-3121.

Towhid ST, Schmidt EM, Tolios A, Munzer P, Schmid E, Borst O, Gawaz M, Stegmann E and Lang F (2013) Stimulation of platelet death by vancomycin. Cell Physiol Biochem 311: 102-112.

van Kruchten R, Braun A, Feijge MA, Kuijpers MJ, Rivera-Galdos R, Kraft P, Stoll G, Kleinschnitz C, Bevers EM, Nieswandt B and Heemskerk JW (2012) Antithrombotic potential of blockers of store-operated calcium channels in platelets. Arterioscler Thromb Vasc Biol 327: 1717-1723.

van Kruchten R, Mattheij NJ, Saunders C, Feijge MA, Swieringa F, Wolfs JL, Collins PW, Heemskerk JW and Bevers EM (2013) Both TMEM16F-dependent and TMEM16F-independent pathways contribute to phosphatidylserine exposure in platelet apoptosis and platelet activation. Blood 12110: 1850-1857.

Varga-Szabo D, Authi KS, Braun A, Bender M, Ambily A, Hassock SR, Gudermann T, Dietrich A and Nieswandt B (2008) Store-operated Ca2+ entry in platelets occurs independently of transient receptor potential (TRP) C1. Pflugers Archiv-European Journal of Physiology 4572: 377-387.

Varga-Szabo D, Braun A and Nieswandt B (2011) STIM and Orai in platelet function. Cell Calcium 503: 270-278.

Viitanen TM, Sukumaran P, Lof C and Tornquist K (2013) Functional coupling of TRPC2 cation channels and the calcium-activated anion channels in rat thyroid cells: implications for iodide homeostasis. J Cell Physiol 2284: 814-823.

Vogler M, Hamali HA, Sun XM, Bampton ETW, Dinsdale D, Snowden RT, Dyer MJS, Goodall AH and Cohen GM (2011) BCL2/BCL-X-L inhibition induces apoptosis, disrupts cellular calcium homeostasis, and prevents platelet activation. Blood 11726: 7145-7154.

Wachowicz B, Olas B, Zbikowska HM and Buczynski A (2002) Generation of reactive oxygen species in blood platelets. Platelets 133: 175-182.

Wang Z, Cai F, Chen X, Luo M, Hu L and Lu Y (2013) The role of mitochondria-derived reactive oxygen species in hyperthermia-induced platelet apoptosis. PLoS One 89: e75044.

Watson SP, Auger JM, McCarty OJ and Pearce AC (2005) GPVI and integrin alphaIIb beta3 signaling in platelets. J Thromb Haemost 38: 1752-1762.

Watson SP, Herbert JM and Pollitt AY (2010) GPVI and CLEC-2 in hemostasis and vascular integrity. J Thromb Haemost 87: 1456-1467.

Weiss HJ, Vicic WJ, Lages BA and Rogers J (1979) Isolated deficiency of platelet procoagulant activity. Am J Med 672: 206-213.

Williamson DR, Lesur O, Tetrault JP and Pilon D (2014) Drug-induced thrombocytopenia in the critically ill: a case-control study. Ann Pharmacother 486: 697-704.

Wolfs JL, Comfurius P, Rasmussen JT, Keuren JF, Lindhout T, Zwaal RF and Bevers EM (2005) Activated scramblase and inhibited aminophospholipid translocase cause phosphatidylserine exposure in a distinct platelet fraction. Cell Mol Life Sci 6213: 1514-1525.

Woronowicz K, Dilks JR, Rozenvayn N, Dowal L, Blair PS, Peters CG, Woronowicz L and Flaumenhaft R (2010) The platelet actin cytoskeleton associates with SNAREs and participates in alpha-granule secretion. Biochemistry 4921: 4533-4542.

Xu XR, Zhang D, Oswald BE, Carrim N, Wang XZ, Hou Y, Zhang Q, Lavalle C, McKeown T, Marshall AH and Ni HY (2016) Platelets are versatile cells: New discoveries in hemostasis, thrombosis, immune responses, tumor metastasis and beyond. Critical Reviews in Clinical Laboratory Sciences 536: 409-430.

Yang H, Kim A, David T, Palmer D, Jin T, Tien J, Huang F, Cheng T, Coughlin SR, Jan YN and Jan LY (2012) TMEM16F forms a Ca2+-activated cation channel required for lipid scrambling in platelets during blood coagulation. Cell 1511: 111-122.

Yang YD, Cho H, Koo JY, Tak MH, Cho Y, Shim WS, Park SP, Lee J, Lee B, Kim BM, Raouf R, Shin YK and Oh U (2008) TMEM16A confers receptor-activated calcium-dependent chloride conductance. Nature 4557217: 1210-1215.

Yeaman MR (2014) Platelets: at the nexus of antimicrobial defence. Nature Reviews Microbiology 126: 426-437.

Yin H, Stojanovic A, Hay N and Du X (2008) The role of Akt in the signaling pathway of the glycoprotein Ib-IX induced platelet activation. Blood 1112: 658-665.

Yoshida GJ and Saya H (2014) Inversed relationship between CD44 variant and c-Myc due to oxidative stress-induced canonical Wnt activation. Biochem Biophys Res Commun 4432: 622-627.

Yu K, Whitlock JM, Lee K, Ortlund EA, Cui YY and Hartzell HC (2015) Identification of a lipid scrambling domain in ANO6/TMEM16F. Elife 4: e06901.

Zhang G, Xiang B, Ye S, Chrzanowska-Wodnicka M, Morris AJ, Gartner TK, Whiteheart SW, White GC, 2nd, Smyth SS and Li Z (2011) Distinct roles for Rap1b protein in platelet secretion and integrin alphaIIbbeta3 outside-in signaling. J Biol Chem 28645: 39466-39477.

Zhang W, Liu J, Sun R, Zhao L, Du J, Ruan C and Dai K (2011) Calpain activator dibucaine induces platelet apoptosis. Int J Mol Sci 124: 2125-2137.

Zhang X, Li Y, Xu H and Zhang YW (2014) The gamma-secretase complex: from structure to function. Front Cell Neurosci 8: 427.

Zwaal RF (1978) Membrane and lipid involvement in blood coagulation. Biochim Biophys Acta 5152: 163-205.

8. Contributions

In this study, I have designed and performed all the experiments as well as data analysis. In addition to my own contribution, the completion of this dissertation has benefited from the support and assistance of the following people:

- Prof. Dr. Florian Lang, for painstaking guidance and suggestions during the design and implementation of the project.
- Prof. Dr. Meinrad Gawaz and Dr. Oliver Borst, for advice and guidance of the papers and dissertation.
- Dr. Hong Chen, Dr. Anja T. Umbach, Dr. Madhumita Chatterjee, Dr. Michael Föller, for overall experimental support.
- Prof. Dr. Karl Kunzelman and Prof. Dr. Rainer Schreiber, for valuable suggestions.
- Dr. Guilai Liu, Dr. Alexander Tolios, Dr. Syeda Tasneem Towhid, Dr. Wenting Yang, Dr. Patrick Münzer, Dr. Kousi Alzoubi for guidance in experimental techniques.
- Mr. Uwe Schüler, Ms. Elfrieda Faber, Mr. Farooq Subasik, Ms. Lejla Subasic for excellent technical support.

9. Publications

1. **Liu G**, Liu Guilai, Chatterjee M, Umbach A.T, Chen H, Gawaz M, Lang F. Influence of γ-Secretase Inhibitor 24-Diamino-5-Phenylthiazole DAPT on Platelet Activation. Cell Physiol Biochem. 2016;38(2):726-36
2. **Liu G**, Liu Guilai, Chen H, Borst O, Gawaz M, Vortkamp A, Schreiber R, Kunzelmann K, Lang F. Involvement of Ca^{2+} Activated Cl^- Channel Ano 6 in Platelet Activation and Apoptosis. Cell Physiol Biochem. 2015;37(5): 1934-44
3. Liu Guilai*, **Liu G***, Alzoubi K, Chatterjee M, Walker B, Münzer P, Luo D, Umbach AT, Elvira B, Chen H, Voelkl J, Föller M, Mak TW, Borst O, Gawaz M, Lang F. CD44 sensitivity of platelet activation, membrane scrambling and adhesion under high arterial shear rates. Thromb Haemost. 2016 Jan;115(1):99-108

Acknowledgements

I would like to use this opportunity to thank all the people who have helped me throughout my PhD. Accompanied with their support and care, I have enjoyed a wonderful and memorable time in Germany.

First of all, I would like to extend my heartfelt gratitude to Prof. Florian Lang for offering me the chance to carry out my work at the Physiology Institute of Tübingen University. His high efficiency and diligence has impressed and inspired me in my academic life. During my PhD work, he has provided patient guidance and plenty of constructive advices on the design and implementation of the project, which is also valuable and beneficial for my future scientific research.

Secondly, I am grateful to Prof. Meinrad Gawaz for his supportive work to present this dissertation to the medical faculty of Tübingen University.

Thirdly, I am thankful to my colleagues at the physiology department: Alexander Tolios, Syeda Tasneem Towhid, Wenting Yang, Jing Yan, Guilai Liu, Hong Chen, Anja T. Umbach, Hang Cao, Michael Föller, just to name a few. Their assistance and cooperation have been an important contribution to my work. Besides, I also appreciate Ms. Waltraud Hartl for her grandmother-like care of my everyday life.

Last but not least, plenty of thanks and love are owed to Cao Qingqing and my parents for their understanding and support. They have been the greatest motivation driving me progressing towards the final completion.